1996

Photophysics and Photochemistry of Carbocations

Maria R. Valentino
Loyola University Chicago

PHOTOPHYSICS AND PHOTOCHEMISTRY OF CARBOCATIONS

A DISSERTATION SUBMITTED TO

THE FACULTY OF THE GRADUATE SCHOOL OF

LOYOLA UNIVERSITY OF CHICAGO

IN PARTIAL FULFILLMENT OF THE REQUIREMENTS FOR THE DEGREE OF

DOCTOR OF PHILOSOPHY

DEPARTMENT OF CHEMISTRY

BY

MARIA R. VALENTINO

CHICAGO, ILLINOIS

JANUARY, 1996

ACKNOWLEDGEMENT

My sincere thanks to my research advisor, Professor Mary K. Boyd, for all her help and patience. She has helped me mature as a scientist and a person.

I would also like to thank all the members of my research group for their help and constant support. In particular, I am grateful to Joanne M. Bedlek for her hard work in preparing and characterizing the thio alcohols and cations and measuring the fluorescent quantum yields of the cations. I am also grateful to Professor Steve Anderson for his preliminary work on the fluorescence quenching of the thio cations.

The financial support of the Petroleum Research Fund, the Arthur J. Schmitt Foundation and Loyola University is gratefully acknowledged.

Finally, I thank my husband, Charles, and my parents for their constant support.

TABLE OF CONTENTS

LIST OF TABLES

Table

LIST OF FIGURES

Figure

LIST OF FIGURES (Continued)

LIST OF ABBREVIATIONS

Bu	butyl
c	cyclo
C	Celsius
$E^{ox}_{1/2}$	oxidation potential
$E^{red}_{1/2}$	reduction potential
E_s	singlet energy
Et	ethyl
i	iso
K	Kelvin
kcal/mol	kilocalories per mole
m	meta
Me	methyl
M	Molarity
nm	nanometer
ns	nanosecond
o	ortho
p	para

Pr	propyl
s	seconds
t	tertiary
TFA/TFE	trifluoroacetic acid/trifluoroethanol
TFE	trifluoroethanol
UV	ultraviolet
V	volts
Vis	visible

ABSTRACT

Several 9-arylxanthyl and 9-arylthioxanthyl tetrafluoroborate salts (Ar = H, *p,m*-F, *p,m*-Me, *m*-OMe) have been synthesized by reaction of the corresponding 9-arylxanthen-9-ol or 9-arylthioxanthen-9-ol with fluoroboric acid in propionic anhydride.

Fluorescence from the 9-arylxanthyl cations was quenched by the addition of H_2O, alcohols and ethers. Stern-Volmer analysis of the fluorescence quenching gave excited-state bimolecular rate constants ranging from 10^7-10^{10} $M^{-1}s^{-1}$. The larger rate constants were associated with the electron donating substituents. Hammett plots of $\log[k_q(X)/k_q(H)]$ versus σ^{hv} gave negative ρ values for each quencher. This substituent dependence is opposite to that observed for the corresponding ground-state reaction. The relative alcohol quenching order (*i*-PrOH>MeOH>*t*-BuOH>H_2O) also differs from the order observed for ground-state cation reactivity.

Preparative photolysis of the 9-phenylxanthyl cation in the presence of *i*-Pr_2O resulted in the formation of unique photoproducts not produced in the corresponding dark reaction. The photoproducts suggest the intermediacy of the 9-phenylxanthyl radical. An electron-transfer mechanism to form the 9-phenylxanthyl radical was ruled out based on the reduction potentials of the 9-arylxanthyl cations and quenching rate constants. Instead, the excited-state mechanism is proposed to proceed via

nucleophilic attack of the ether on the 9-phenylxanthyl cation to form an oxonium ion intermediate. Homolytic cleavage generates the resonance-stabilized 9-phenylxanthyl radical and the corresponding ether radical cation.

Fluorescence from the 9-arylthioxanthyl cations was also quenched by H_2O and alcohols. In contrast to the 9-arylxanthyl cations, no substituent dependence is observed in the rate constants for quenching of the 9-arylthioxanthyl cations by H_2O and MeOH.

Photophysical properties of the 9-arylxanthyl cations exhibit a substantial substituent dependence in the lifetimes, fluorescence quantum yields, total decay rate constants and non-radiative rate constants. In contrast, no substituent effect was observed on the same photophysical properties in the 9-arylthioxanthyl cations. No substituent dependence was observed on the position of the absorbance or fluorescence maxima for either the 9-arylxanthyl or 9-arylthioxanthyl cations.

CHAPTER I

INTRODUCTION

Carbocations are organic molecules containing a positive charge centered on a carbon atom. The positive charge makes these species inherently reactive, and therefore particularly interesting from both fundamental and practical viewpoints. While ground-state carbocations have been extensively investigated (Olah, 1970), much less is known about the photochemistry of these species. Excited-state cations possess different electronic distributions and higher energies compared to ground-state species. The excited-state reactivity of carbocations may lead to the formation of unique products formed only through an excited state.

Early studies on carbocation photochemistry focused primarily on photoproduct determination following irradiation of cations thermally generated in acidic media (Cabell-Whiting, 1973 and Childs, 1991). The first carbocation photolysis to be investigated was that of the tropylium ion (van Tamelen, 1968). In 5% aqueous sulfuric acid solution, the tropylium ion **1** rearranged to bicyclo[3.2.0]-hepta-3,6-dien-2-ol **3** and the corresponding ether **4** shown in Scheme 1.

Scheme 1

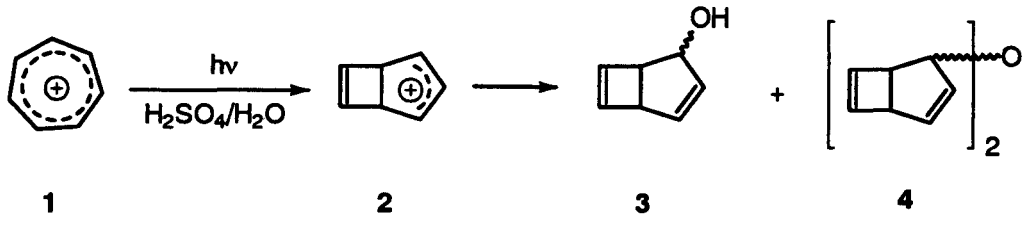

These photoproducts were proposed to have formed via a reactive valence-bond isomer, the "Dewar tropylium ion" **2** (van Tamelen, 1968 and van Tamelen, 1971b). Irradiation of the tropylium ion in ethanol in the absence of acid gave tropyl ethyl ether. With additional irradiation, tropyl ethyl ether continued to react with formation of ditropyl and its photoisomer, hexaene (van Tamelen, 1968 and 1971b). Upon irradiation in stronger acid ($FHSO_3$) the tropylium and methyltropylium ions isomerized to form the 7-norbornadienyl and 2-methyl-7-norbornadienyl cations, respectively (Child, 1970 and Hogeveen, 1970). The phenyltropylium ion is photochemically stable when irradiated in $FHSO_3$ (Childs, 1970) or aqueous sulfuric acid (van Tamelen, 1971b) under anaerobic conditions. When irradiated in aqueous sulfuric acid in the presence of oxygen, the phenyltropylium ion was converted to biphenyl, known to form by the action of hydrogen peroxide (Jutz, 1964). Photolysis of the phenyltropylium ion in acetonitrile gives *ortho*- and *para*-phenylbenzaldehydes as well as the coupling products *cis*- and *trans*-diphenylstilbenes (van Tamelen, 1971b). The mechanism by which these compounds are produced is not clear, but may involve a norcaradiene valence isomer as a precursor.

Irradiation of azulene in 50% aqueous sulfuric acid resulted in formation of dimeric and trimeric azulene-type products in addition to polymeric material. It was proposed that the isopropylidene unit in these products was derived from the azulene moiety, however, a mechanism was not proposed (van Tamelen, 1971b).

The stable triphenylcyclopropenyl cation undergoes an electron-transfer reaction when irradiated in aqueous acid solution, giving hexaphenylbenzene. The reaction is proposed to proceed via an initial charge transfer from an unspecified donor to produce the cyclopropenyl radical which then coupled to give hexaphenylbenzene (van Tamelen, 1968 and 1971b).

Irradiation of the cation produced by the protonation of 1,1-di-*p*-anisylethylene **5** in equilibrium with the alkene in benzene/trifluoroacetic acid solution resulted in a single electron transfer (SET) from the neutral alkene to the electronically excited cation. The electron transfer product pair of radical **6** and radical cation **7** leads to the formation of **8-11** shown in Scheme 2 (Al-Ekabi, 1988).

Scheme 2

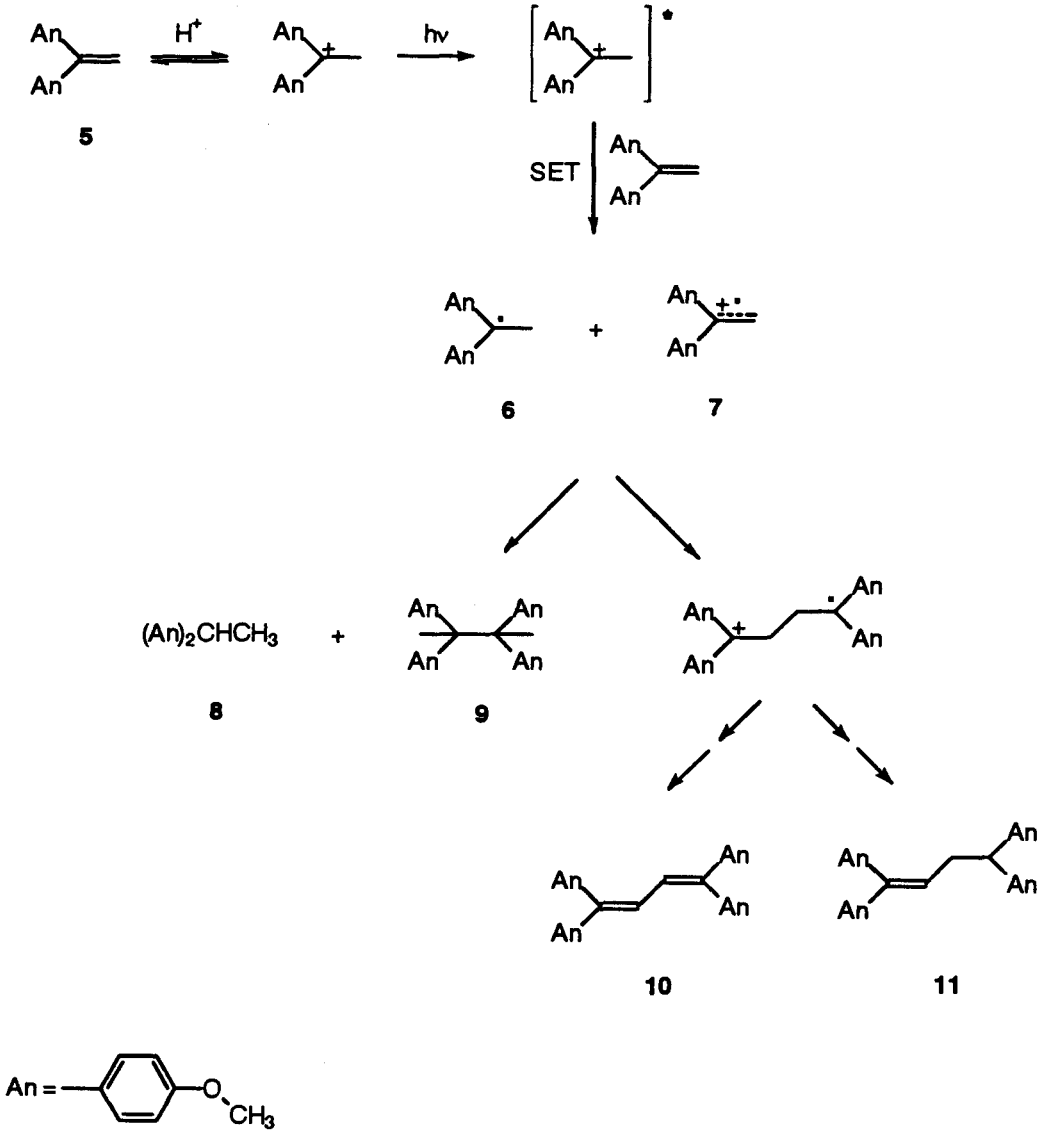

Photoproducts formed following irradiation of the extensively delocalized triphenylmethyl cation have also been investigated. Product formation depended on numerous variables including solvent, pH of the medium and the presence or absence of oxygen. Initial work involved irradiation of the triphenylmethyl cation in

concentrated aqueous H_2SO_4 solution (96%) with the formation of 9-phenylfluoren-9-ol (van Tamelen, 1968). At lower H_2SO_4 concentrations (72%) and the absence of oxygen, irradiation of the triphenylmethyl cation **12** yielded dimeric products **13, 14,** and **15** which are shown in Scheme 3, formed by the interaction of an excited triplet triphenylmethyl cation with a ground-state triphenylmethyl cation.

Scheme 3

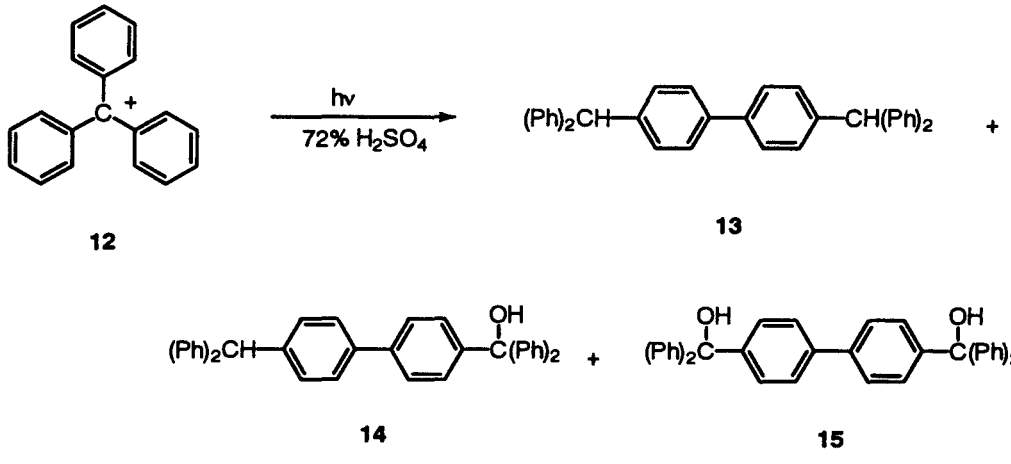

12 **13** **14** **15**

In weaker acid systems and with the addition of benzene or toluene, irradiation of the triphenylmethyl cation produced 9-phenylfluorenyl type compounds such as triphenylmethane, 9-phenylfluorene, *bis*-9-phenylfluorenylperoxide and tetraphenylmethane. The mechanism was proposed to procede via a radical intermediate (van Tamelen, 1971a).

In the presence of oxygen and weakly acidic media, irradiation of a 10^{-3} M solution of the triphenylmethyl cation yielded benzophenone and 2,2-diphenylmethylenedioxybenzene as major photoproducts. It was proposed that direct

combination of an excited triplet triphenylmethyl cation and ground-state molecular oxygen were involved in the mechanism. Irradiation of a 10^{-5} M solution of triphenylmethyl cation in 99% H_2SO_4 yielded 9-phenylfluoren-9-ol as the major photoproduct and upon addition of oxygen, fluoren-9-one was detected (Allen, 1971 and Owen, 1973). An excited triplet cation was again proposed to be involved in the mechanism.

Irradiation of xanthydryl **16**, triphenylmethyl **12** or 5H-dibenzosuberenyl **17** cation in the presence of triphenylmethane in trifluoroacetic acid solution led to the quantitative formation of the triphenylmethyl cation. Results indicated that the triplet excited cation, acting as a sensitizer, was responsible for the photo-oxidation of the hydrocarbon (Bethell, 1972).

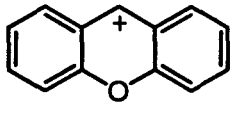

16

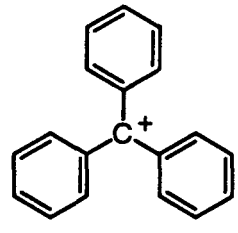

12

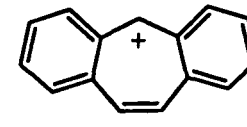

17

There has been considerable recent attention given to the characterization, properties and reactivity of excited-state carbocations (Das, 1993). The photophysical properties of resonance-stabilized carbocations have been characterized by UV/Vis and fluorescence emission spectroscopies. Spectral data for carbocations are usually

obtained on stabilized species in strongly acidic solutions and are only slightly red-shifted compared to those observed by laser flash photolysis in neutral solvents.

Diarylmethyl and trityl cations have been characterized and show absorption bands in the 400-500 nm region with molar extinction coefficients generally greater than 40,000 (Das, 1993 and Azarani, 1991). The trityl cation has been reported to give a fluorescence band in acidified solvents centered at 530 nm (Samanta, 1993) and 475 nm (Azarani, 1991). The diarylmethyl cations $(4\text{-MeO-Ph})_2C(CH_3)^+$ and $(4\text{-MeO-Ph})_2CH^+$ fluoresce at 535 nm and 600 nm, respectively. The singlet lifetimes of these compounds have been measured by a number of groups. Samanta and co-workers and Azarani and co-workers report a fluorescence lifetime for the trityl cation in acidified solvents of <1.0 ns. Singlet lifetimes for $(4\text{-MeO-Ph})_2C(CH_3)^+$ and $(4\text{-MeO-Ph})_2CH^+$ were reported as 6 ns and 3 ns, respectively (Azarani, 1991). A fluoresence quantum yield of 0.001 has been reported for the trityl cation (Samanta, 1993).

Cations containing the xanthyl backbone have a strong absorption maximum around 370 nm and a weaker absorption in the visible range at about 450 nm. In comparison, thioxanthyl cations have absorbance maxima in the 380 nm (strong) and 480 nm (weak) regions (Samanta, 1993). The fluorescence emission of the xanthyl and thioxanthyl cations show broad emission bands with maxima between 500 and 600 nm (Azarani, 1991; Boyd, 1985 and 1991; Samanta, 1990 and 1993). The singlet lifetimes of a variety of xanthyl compounds have been measured, with the 9-phenylxanthyl cation being the most widely studied. The singlet lifetime of the 9-

phenylxanthyl cation has been reported as 24.2 to 36 ns, depending upon the solvent system (Azarani, 1991; Boyd, 1991; Das, 1993; Johnston, 1993; Minto, 1989; Samanta, 1990 and 1993). A lifetime of 37 ns has also been reported for the 9-phenylxanthyl cation generated on silica-gel surfaces (Berger, 1990). Fluorescence quantum yields have also been reported for this cation in acidified solvents and range from 0.33 to 0.48 (Azarani, 1991; Samanta, 1990 and 1993; Minto, 1989). Fluorescence quantum yields of 0.80 for the 9-phenylxanthyl cation and 0.55 for the 9-(4-fluorophenyl)xanthyl cation generated by laser flash photolysis in 1% TFA/TFE solution have been reported (Johnston, 1993). The higher values obtained in primarily TFE solvent were attributed to the absence of water, which is known to quench the singlet excited state of these cations (Boyd, 1991; Wan, 1985). Substituents on the 9-phenyl ring apparently have a dramatic effect on the lifetimes as the values range from appoximately 28 ns for the *p*-CF_3 substituted cation to subnanosecond values for the *m*- and *p*-OMe substituted cations (Boyd, 1991).

The singlet lifetimes of the xanthyl cation and alkyl substituted xanthyl cations have also been measured. The parent xanthyl cation in acidified solvents has been reported as having a singlet lifetime ranging from 17.5 to 31 ns (Azarani, 1991; Boyd, 1991 and Samanta, 1993) with a fluorescence quantum yield of 0.16 (Samanta, 1993) and 0.12 (Azarani, 1991). The wide variation seen in the lifetimes may also be due to the water present in the solvent medium. Alkyl substitution (Me, *i*-Pr, *c*-Pr) on the 9-position of the xanthyl cation does not cause as dramatic an effect on the lifetime

as seen with the 9-arylxanthyl cations. Lifetimes for the 9-alkylxanthyl cations ranged from only 32.6 to 41 ns (Azarani, 1991 and Boyd, 1991).

Measured fluorescence lifetimes and quantum yields for the thioxanthyl and 9-phenylthioxanthyl cations in acidified solvents differ greatly. A lifetime of 22.8 ns and quantum yield of 0.24 have been reported for the thioxanthyl cation compared to a lifetime of <2 ns and a quantum yield value of 0.025 and 0.031 for the 9-phenyl substituted thioxanthyl cation (Samanta, 1993).

Dibenzosuberenyl cations have characteristic absorption maxima between 370 and 556 nm with a fluorescence emission band between 550 and 580 nm (Azarani, 1991). The same group reports a measured fluorescence lifetime of <1 ns for the phenyl-substituted dibenzosuberenyl cation.

The triplet excited state of 9-arylxanthyl (H, *p*-F, *p*-OMe) and 9-arylthioxanthyl (H, *p*-F) cations have also been characterized (Johnston, 1992 and 1993). Using luminescence and transient absorption techniques, the triplet excited states of these cations were found to have absorption bands in the 300 nm region. At room temperature and in the absence of quenchers, these species are relatively long lived (5-10 μs) in TFE/TFA solution. A weak phosphorescence emission between 600 and 700 nm at 77 K was detected for these cations. Triplet energies were estimated at ~48 kcal/mol for the 9-arylxanthyl cations and at ~41 kcal/mol for the 9-arylthioxanthyl cations based on the onset of phosphorescence.

Singlet excited 9-arylxanthyl cations possess relatively long excited-state

lifetimes making them excellent candidates for the study of bimolecular reactions such as nucleophilic and electron transfer processes. In one particular reactivity study, the 9-phenylxanthyl cation was thermally generated from 9-phenylxanthen-9-ol in trifluoroacetic acid/acetonitrile (Samanta, 1990). The solution was irradiated and the fluorescence of the 9-phenylxanthyl cation was found to decrease in the presence of aromatic donors, such as substituted benzenes and polycyclic aromatic compounds. Bimolecular rate constants for the steady-state fluorescence quenching of the cation were determined using the Stern-Volmer method (Stern, 1919) and ranged from 4.5×10^{9} M^{-1} s^{-1} (benzene) to 2.6×10^{10} M^{-1} s^{-1} (anthracene). An electron-transfer quenching mechanism was proposed based upon transient absorption detection of the 9-phenylxanthyl radical and the radical cation of the aromatic donor. Further evidence in support of the electron-transfer quenching mechanism came from correlation of the quenching rate constants with the oxidation potential of the aromatic donor.

Similarly, the fluorescence from xanthyl, 9-phenylxanthyl and dibenzosuberenyl cations produced in trifluoroacetic acid/trifluoroethanol from their corresponding alcohols was quenched upon the addition of aromatic donors (Azarani, 1991). Singlet excited quenching rate constants were determined by monitoring the fluorescence decay of the cation as a function of the concentration of added aromatic donor (substituted benzenes). Table 1 lists the data obtained for reaction of the singlet excited xanthyl, 9-phenylxanthyl and dibenzosuberenyl cations with a variety of substituted aromatic compounds. Again, a correlation was seen between the observed

TABLE 1

RATE CONSTANTS FOR FLUORESCENCE QUENCHING OF THE XANTHYL I, 9-PHENYLXANTHYL II, AND DIBENZOSUBERENYL III CATIONS WITH AROMATIC DONORS IN TFE.[a]

Quencher	E_{ox}[b] (V)	k_q ($x10^9$ M^{-1} s^{-1})		
		I	II	III
1,2,4,-Trimethoxybenzene	1.12	7.4	-	5.3
Anisole	1.76	7.6	4.9	5.7
Mesitylene	1.80	-	-	4.8
o-Xylene	1.89	-	-	4.6
Toluene	1.98	5.5	-	3.4
Cumene	2.07	5.3	5.2	3.1
Benzyltrimethylsilane	2.09	4.8	4.0	4.3
Benzene	2.30	4.2	0.75	0.010
Chlorobenzene	2.42	4.9	1.3	0.017
Fluorobenzene	-	3.5	0.34	-
Cyanobenzene	-	<0.001	<0.01	-

[a]Source: A. Azarani, A.B. Berinstain, L.J. Johnston and Sophia Kazanis, "Electron Transfer Reactions Between Excited Diarylmethyl and Triarylmethyl Carbocations and Aromatic Donors," J. Photochem. Photobiol. A: Chem. 57 (1991): 182.

[b]In acetonitrile versus saturated calomel electrode (SCE).

rate constant and the oxidation potential of the quencher suggesting an electron-transfer quenching mechanism.

To further investigate the excited-state mechanism, product studies were undertaken. Irradiation of the dibenzosuberenyl cation in the presence of benzyltrimethylsilane produced 5-benzodibenzocycloheptene. This product is proposed to arise from either coupling of the benzyl radical to the dibenzosuberenyl radical or the dibenzosuberenyl cation. With either intermediate, electron transfer is proposed as the initial step of the quenching mechanism.

More recently, Das and co-workers (Samanta, 1993) studied the excited-state reactivity of the 9-phenylxanthyl and 9-phenylthioxanthyl cations in the presence of aromatic donors. These cations were thermally generated from the corresponding alcohols using trifluoroacetic acid or H_2SO_4 in acetonitrile, followed by irradiation. The reactivity of the singlet excited cations with substituted benzenes and polycyclic aromatics was studied using laser flash photolysis. A representative case was reported for the transient absorption changes following laser excitation of the 9-phenylxanthyl cation in the presence of 1-methylnaphthalene. Transient absorption bands corresponding to the 9-phenylxanthyl radical and the 1-methylnaphthalene radical cation were observed.

The magnitude of the steady-state rate constants for quenching of the xanthyl cations by the aromatic donors varied, but were in the diffusion controlled region. The authors also investigated quenching of the singlet excited cations by oxygen. Results

indicate the cations are resistant to quenching by oxygen. An unfavorable charge-transfer interaction and poor capability as an electron-donor were proposed as reasons for the inability of oxygen to quench the singlet cations.

The xanthyl rate constants are generally lower than those for the thioxanthyl carbocations. This is a reflection of the fact that the singlet energy of the thioxanthyl cation is about 5 kcal/mol lower than the xanthyl cation. The rate constants for quenching of the xanthyl cation are 2-3 times larger than for quenching the 9-phenylxanthyl cation. Since the singlet energies (E_s) and reduction potentials ($E_{1/2}^{red}$) for these two cations are nearly equal, the lower rate constants for the 9-phenylxanthyl cation is proposed to be due to steric hindrance of the phenyl ring. Additionally, estimated electron-transfer quantum yields for quenching of the xanthyl and 9-phenylxanthyl singlet cations by biphenyl were 0.01-0.02. This suggests that back electron transfer dominates over the dissociation of the generated radical and radical cation pair.

Another recent study investigated the products formed from reaction of the photoexcited 9-phenylxanthyl cation with aromatic donors (Shukla, 1993). Here, the cation was thermally produced from its alcohol precursor in acidic acetonitrile. Excited-state quenching rate constants were determined using the Stern-Volmer method upon addition of methyl-substituted benzenes. Quenching rate constants were in the range of 5-7.9x10^9 M^{-1} s^{-1}. A solution of the 9-phenylxanthyl cation was irradiated in the presence of 1,3-dimethoxybenzene and photoproducts isolated. The

identification of the radical derived photoproduct, bis(9-phenylxanthen-9-yl) peroxide, provided further evidence for an electron-transfer mechanism.

The triplet state of some 9-arylxanthyl cations were similarly found to undergo electron-transfer reactions with aromatic donors (Johnston, 1992 and Johnston, 1993). The 9-phenylxanthyl, 9-(4-fluorophenyl)xanthyl and 9-phenylthioxanthyl cations were thermally generated in trifluoroacetic acid/trifluoroethanol solution from their respective alcohol precursors. The triplet excited state of these cations were directly observed using transient absorption techniques. The triplet cations were found to undergo efficient electron-transfer reactions in the presence of substituted benzenes, naphthalenes and the precursor alcohols. For example, addition of biphenyl resulted in quenching of the 9-phenylxanthyl triplet cation. The 9-phenylxanthyl radical and the biphenyl radical cation were detected via transient techniques. The quenching rate constants measured in TFE ranged from lower than 10^7 M^{-1} s^{-1} to nearly the diffusion controlled limit. The triplet cations are proposed to be poorer oxidizing agents than the singlet excited state of the same cations due to the lower excitation energy of the triplet cations (Azarani, 1991).

Measured electron-transfer yields for quenching of the triplet 9-phenylxanthyl cation by biphenyl was 0.04, based on biphenyl radical cation formation. Triplet cations are proposed to be potentially useful as sensitizers since they give substantially higher yields of cage escape from the initial pair than the corresponding singlet compounds.

The reactivity of singlet 9-arylxanthyl cations with species other than aromatic donors has also been studied. Minto and Das (Minto, 1989) used a two-laser flash photolysis technique to generate the 9-phenylxanthyl cation from 9-phenylxanthen-9-ol in acetonitrile. This photolytic technique also resulted in the generation of the 9-phenylxanthyl radical. Fluorescence from the 9-phenylxanthyl cation was quenched by water, alkyl alcohols and amines. The Stern-Volmer method was used to determine the excited-state quenching rate constants which ranged from $3.3x10^7$ M^{-1} s^{-1} for quenching of the cation by water to $3.0x10^{10}$ M^{-1} s^{-1} for quenching by triethylamine. Rate constants for quenching of the singlet 9-phenylxanthyl cation by H_2O and amines were several orders of magnitude larger than those measured for the corresponding ground-state reaction (McClelland, 1989). It was suggested that the increased reactivity of the singlet excited cation was due to the increased exothermicity by an amount equal to the singlet energy (~60 kcal/mol). The observed relative order for the quenching of the excited-state cation by water and the alcohols was *i*-PrOH>MeOH>*t*-BuOH>H_2O. This does not follow the steric order of the quenchers. The excited-state quenching of the 9-phenylxanthyl cation by these species was proposed to proceed via nucleophilic attack, with the observed alcohol quenching order rationalized by the steric effect of increasing methyl substitution counter balancing the increase in lone pair availability of the nucleophile. This study also reports that the fluorescence of the 9-phenylxanthyl cation decreased in the presence of tetrahydrofuran. An excited-state rate constant of $6.2x10^8$ M^{-1} s^{-1} was determined

using time-resolved measurements.

The water quenching behavior of singlet excited xanthyl cations in aqueous sulfuric acid solution was also studied (Boyd, 1991). 9-Alkyl (H, Me, *i*-Pr) and 9-aryl (H, *p*-CF_3, *p*-Me, *m*-Me, *p*-OMe, *m*-OMe) substituted xanthyl cations were generated in the ground state by reaction of the corresponding alcohols with aqueous sulfuric acid. The ground state cations were then irradiated, and the fluorescence intensity and measured fluorescence lifetimes of the cations were found to increase as the percent acid increased. This was found not to be due to the formation of additional cation, as absorption spectra showed the alcohol to be completely ionized. Rather it was proposed that the cations were quenched by the water available in the aqueous acid solution. Excited-state quenching rate constants were determined by the Stern-Volmer method. For the 9-alkyl substituted xanthyl cations, k_q values were in the range of 2-9x10^6 M^{-1} s^{-1}, depending on the size of the alkyl group. With the small variance in the rate constants measured for the 9-alkyl substituted cations, a steric effect rather than an electronic effect was proposed to be the controlling factor.

The rate constants determined for water quenching of the singlet excited 9-arylxanthyl cations varied over a much larger range. Rate constants varied from 10^6 to 10^9 M^{-1} s^{-1}, a three order of magnitude difference. Also, the rate constant for quenching of the 9-phenylxanthyl cation by water is higher than the rate constant associated with the xanthyl cation. This result is opposite that seen for quenching of these same cations by aromatic donors (Samanta, 1993). The result suggests a special

electronic effect operating for quenching of the 9-arylxanthyl cations by water. Additionally, the excited-state rate constants were found to increase as the electron donating ability of the substituent increased.

An excited-state Hammett plot was constructed using the $\sigma^{h\nu}$ substituent parameter scale (McEwen, 1991). The $\sigma^{h\nu}$ scale is appropriate for 9-arylxanthyl cation reactivity since it is based on formation of structurally similar benzyl cations in photoprotonation reactions of ring-substituted styrenes and phenylacetylenes. Plots of the relative rate constants versus either the σ or σ^+ substituent parameters (Murov, 1973) gave poor correlation. The poor correlations were primarily due to scatter from the *meta*-substituted cations, whose points fell above the correlation line, indicative of an increased reactivity of these cations. *Meta*-substituents are known to exhibit an enhanced conjugative effect in the excited-state compared to the corresponding ground-state compounds (Zimmerman and Somasekhara, 1963; Zimmerman and Sandel, 1963 and Havinga, 1956).

Plots of $\log[k_q(X)/k_q(H)]$ versus $\sigma^{h\nu}$ gave a negative ρ value, again indicating that electron-donating substituents increase the rate of reaction. This negative ρ value is opposite in sign to that observed for reaction of ground-state 9-arylxanthyl cations with water (McClelland, 1989). In the ground-state study, the cations were photolytically produced from their corresponding alcohols. The rate constants for the reaction of the cations with water decreased as the electron-donating ability of the substituent increased. A Hammett plot was constructed using the σ substituent scale,

resulting in a ρ value of +0.5. This result is consistent with ground-state theory where carbocation molecules are stabilized through inductive effects by electron donating substituents, making them less reactive toward species such as nucleophiles. This stabilization of the cations by electron donating substituents is presumably somewhat attenuated due to twisting of the 9-aryl group away from planarity with the xanthyl backbone.

The results obtained by Boyd and co-workers can not be explained by invoking conventional ground-state theory (Boyd, 1991). Huckel MO calculations provided a possible explanation for the observed substituent dependence. The calculations showed that the size of the lobe and MO coefficient increased as the substituents became more strongly electron donating. The larger k_q values can then be explained by invoking frontier orbital theory (Fleming, 1976), as the larger lobe would provide better overlap with the incoming nucleophile lone pair.

In order to further investigate the photophysics and photochemistry of excited state cations an alternate method for generating excited-state cations is necessary. In the previous studies where the cations were generated in aqueous sulfuric acid solution, the choice of quencher was limited to water. Furthermore, photoproducts from the reaction of the cation could not be isolated. The alternative two-laser flash photolysis method employed by Das successfully generated the 9-phenylxanthyl cation in acetonitrile from its alcohol precursor (Minto, 1989). Unfortunately, cation formation was accompanied by the generation of the 9-phenylxanthyl radical. Xanthyl

cations have also been generated in Nafion matrices (Minto, 1989) and on silica gel surfaces (Berger, 1990), however for these studies we are interested in solution-phase generation of the cations.

The goal of this research is to explore all aspects of carbocation photochemistry, and in particular, understand the fundamental chemical principles leading to the unusual excited-state substituent effects. Classical physical organic chemical methodology will be used, focusing on substituent effects on cation reactivity and the idenfication of photoproducts. Comparison of our results on excited-state cations to the ground-state results, will indicate whether different mechanisms are operating in the ground state and excited state.

CHAPTER II

RESULTS

Substrate Synthesis and Characterization

9-Arylxanthen-9-ols **18b-f** and 9-arylthioxanthen-9-ols **19a-e** were synthesized via a Grignard reaction of the appropriate arylmagnesium bromide with xanthone.

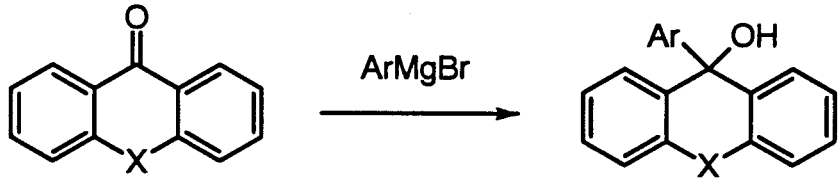

18a-f X = O 19a-e X = S

Aryl Substituent: **a**=H, **b**=*p*-F, **c**=*m*-F, **d**=*p*-CH_3, **e**=*m*-CH_3, **f**=*m*-OCH_3

Reaction of **18a-f** and **19a-e** with fluoroboric acid in propionic anhydride (Dauben, 1960) gave 9-arylxanthylium tetrafluoroborate salts **20a-f** and 9-arylthioxanthylium tetrafluoroborate salts **21a-e** as crystalline solids. The cations were stable indefinitely both in the solid phase and dissolved in dry acetonitrile.

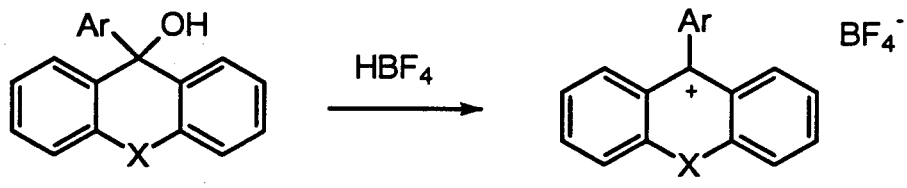

20a-f X = O 21a-e X = S

Aryl substituent: **a**=H, **b**=*p*-F, **c**=*m*-F, **d**=*p*-CH_3, **e**=*m*-CH_3, **f**=*m*-OCH_3

UV/Visible spectra of **20a-f** in acetonitrile were identical to the spectra reported for the same cations generated in acidified organic solvents (Azarani, 1991; Johnston, 1992 and 1993; Minto, 1989; Samanta, 1990 and 1993) or aqueous acidic solutions (Boyd, 1985 and 1991) with absorption maxima at 260, 374 and 450 nm. UV/visible spectra of **21a-e** in acetonitrile exhibit absorption maxima at 246, 280, 386 and 492 nm, identical to the spectra reported for the 9-phenylthioxanthyl cation in acidified organic solvents (Samanta, 1993) and the 9-phenylthioxanthyl and 9-(4-fluoro-phenyl)thioxanthyl cations generated by laser flash photolysis in 1% TFA in TFE (Johnston, 1993). There is no substituent dependence on the position of the absorbance maxima for **20a-f** or **21a-e**.

Excitation of **20a-f** at 374 nm in acetonitrile gave steady-state fluorescence spectra that were identical to the emission spectra previously reported, with a broad band centered at 540 nm (Azarani, 1991; Boyd, 1991; Minto, 1989; Samanta, 1990 and 1993; Wan, 1985). Excitation of **21a-e** at 386 nm in acetonitrile gave steady-state fluorescence spectra that were also identical to emission spectra previously

reported, with a band centered at 580 nm (Johnston, 1992 and 1993). There is no substituent effect observed on the position of the fluorescence maxima for **20a-f** or **21a-e**.

Fluorescence lifetimes, τ_f^o, for **20a-e** and **21a-e** were measured in acetonitrile and are listed in Table 2. The measured lifetimes were obtained from primarily single exponential decays. The lifetime of compound **20f** was below the range of our instrument and was estimated from relative fluorescence quantum yields according to the method previously described for weakly fluorescent compounds (Boyd, 1991).

Substituents apparently have a dramatic effect on the lifetimes of **20a-f** with values ranging from 28 ns for **20a** to a subnanosecond value for **20f**. The lifetime for **20a** is in excellent agreement with a previous measurements of 25 ns for the cation generated in acetonitrile using a double-laser photolysis technique (Minto, 1989) and 28.5 ns for the cation generated in 1:1 TFA-acetonitrile (Samanta, 1993). Lifetimes of **20a, 20b** and **20e** are also in very good agreement with the values obtained for the same cations generated in strongly acidic aqueous media (Boyd, 1991). Lifetime values for **20a** and **20b** agree reasonably well with those measured in trifluoroethanol acidified with trifluoroacetic acid, after making allowance for possible solvent effects (Azarani, 1991).

In contrast to the measured lifetimes for **20a-f**, there is no substituent effect on the lifetimes of **21a-e** with all τ_F^o values about 1 ns. The measured lifetimes were obtained from single exponential decays. The lifetimes for **21a** and **21b** are in excel-

TABLE 2

FLUORESCENCE LIFETIMES, τ_f^o, OF 9-ARYLXANTHYL CATIONS **20a-f** AND 9-ARYLTHIOXANTHYL CATIONS **21a-e**

Compound	9-Aryl Substituent	τ_F^o (ns)
20a	H	27.6
20b	*p*-F	18.8
20c	*m*-F	14.0
20d	*p*-Me	2.1
20e	*m*-Me	2.0
20f	*m*-OMe	0.028
21a	H	1.0
21b	*p*-F	1.0
21c	*m*-F	1.3
21d	*p*-Me	1.0
21e	*m*-Me	1.0

lent agreement with a previous measurement of <2 ns for the cations generated from the corresponding alcohols via laser flash photolysis in 1% TFA in TFE (Johnston, 1993). The lifetime of **21a** is also in excellent agreement with the values of 1.0 ns for the cation generated in acidified acetonitrile (Samanta, 1993) and <1 ns for the cation generated in TFA-TFE solution (Azarani, 1991).

Fluorescence quantum yields relative to quinine sulfate, Φ_F, for **20a-f** and **21a, 21b** and **21d** were measured in acetonitrile and are listed in Table 3. As seen with the fluorescence lifetimes of **20a-f,** there is a significant substituent effect on the fluorescence quantum yields of the xanthyl cations with values ranging from 0.47 for **20a** down to 6.6×10^{-4} for **20f.** The fluorescence quantum yield of 0.47 measured for **20a** is in excellent agreement with values of 0.48 and 0.45 for the same cation generated in TFA-acetonitrile (Samanta, 1990 and 1993) and 0.42 for the cation generated in 8% H_2SO_4 in acetonitrile (Minto, 1989). The value is in good agreement with the fluorescence quantum yield reported by Johnston and co-workers of 0.33 for the cation generated in TFA-TFE (Azarani, 1991). However, the value is somewhat lower than the reported value of 0.80 for the 9-phenylxanthyl cation in 1% TFA in TFE (Johnston,1993). Since the 9-phenylxanthyl cation is quenched by water with a rate constant of 3.3×10^7 M^{-1} s^{-1} (Minto, 1989), the lower quantum yield value may be explained by traces of water in the solvent, although it is remarkable that three separate measurements would give such consistent results. Similarly, the quantum yield for **20b** is lower than the reported value of 0.55 for the 9-(4-fluorophenyl)xanthyl

TABLE 3

FLUORESCENCE QUANTUM YIELDS, Φ_F, OF 9-ARYLXANTHYL CATIONS **20a-f** AND 9-ARYLTHIOXANTHYL CATIONS **21a-e**

Compound	9-Aryl Substituent	Φ_F
20a	H	0.47
20b	*p*-F	0.28
20c	*m*-F	0.18
20d	*p*-Me	0.014
20e	*m*-Me	0.084
20f	*m*-OMe	6.6×10^{-4}
21a	H	0.020
21b	*p*-F	0.018
21d	*p*-Me	0.011

cation in 1% TFA in TFE (Johnston, 1993). Again it is possible that trace amounts of water may be responsible for the lower value reported here.

In contrast to the measured fluorescence quantum yields for **20a-f**, there is little to no substituent effect observed in the measured fluorescence quantum yield for **21a, 21b** and **21d**. A fluorescence quantum yield of 0.020 for **21a** was measured and is in very good agreement with a value of 0.025 measured for the cation generated in TFA-acetonitrile (Samanta, 1993). The quantum yields measured for **21a** and **21b** are in very good agreement with the values of 0.031 and 0.020, respectively, for these cations generated in 1% TFA in TFE (Johnston, 1993).

Total decay rate constants, k_{dt}, were calculated from the measured lifetimes of **20a-f** and **21a-e** and are listed in Table 4. As indicated by the lifetimes, a dramatic substituent effect is observed in the k_{dt} values for the 9-arylxanthyl cations. Total decay rate constants range from 3.6×10^7 s^{-1} for **20a** up to 3.6×10^9 s^{-1} for **20f**. In contrast to the decay rate constants for the xanthyl cations, there is no substituent effect observed on the k_{dt} values for the 9-arylthioxanthyl cations, where all total decay rate constants are about 1×10^9 s^{-1}.

Fluorescence rate constants, k_f, and non-radiative rate constants, k_{nr}, were calculated from the fluorescence quantum yields and lifetimes for **20a-f** and **21a, 19b** and **21d** and are listed in Table 4. The k_f values of 1.7×10^7 s^{-1} for **20a** and 2.0×10^7 s^{-1} for **21a** are in excellent agreement with the k_f values of 1.7×10^7 s^{-1} and 2.5×10^7 s^{-1}, respectively, determined by Das from fluorescence quantum yield and lifetime measurements

TABLE 4

PHOTOPHYSICAL DATA FOR 9-ARYLXANTHYL CATIONS **20a-f** AND 9-ARYLTHIOXANTHYL CATIONS **21a-e**

Compound	k_{dt} (s^{-1})	k_f (s^{-1})	k_{nr} (s^{-1})
20a	3.6×10^{7}	1.7×10^{7}	1.9×10^{7}
20b	5.3×10^{7}	1.5×10^{7}	3.8×10^{7}
20c	7.1×10^{7}	1.3×10^{7}	5.8×10^{7}
20d	4.8×10^{8}	6.6×10^{6}	4.6×10^{8}
20e	5.0×10^{8}	4.2×10^{7}	4.6×10^{8}
20f	3.6×10^{9}	2.4×10^{7}	3.6×10^{9}
21a	1.0×10^{9}	2.0×10^{7}	9.8×10^{9}
21b	1.0×10^{9}	1.8×10^{7}	9.8×10^{9}
21c	7.8×10^{8}		
21d	1.0×10^{9}	1.1×10^{7}	9.9×10^{9}
21e	1.0×10^{9}		

(Samanta, 1993). Das also used the Strickler-Berg formula (Strickler, 1962) to calculate k_f values of $2.5x10^7$ s^{-1} for the 9-phenylxanthyl cation and $2.4x10^7$ s^{-1} for the 9-phenylthioxanthyl cation which are also in very good agreement with our fluorescence rate constants.

The fluorescence rate constants show a modest substituent effect in both the xanthyl and thioxanthyl series, ranging from a low value of $6.6x10^6$ s^{-1} for **20d** to a high value of $4.2x10^7$ s^{-1} for **20e**, and ranging from a low of $1.1x10^7$ s^{-1} for **21a** to a high of $2.0x10^7$ s^{-1} for **21d**. A significant substituent effect is observed on the non-radiative decay rate constants for the 9-arylxanthyl cations, ranging from $1.9x10^7$ for **20a** to $3.6x10^9$ s^{-1} for **20f**. As observed in the k_{dt} values, the larger values for k_{nr} are associated with the xanthyl cations substituted with the more strongly electron donating substituents. In contrast to the xanthyl cations, no substituent effect is observed for k_{nr} with the thioxanthyl cations, where k_{nr} values vary slightly from $9.8x10^8$ s^{-1} for **21a** and **21b** to $9.9x10^8$ s^{-1} for **21d**.

Measurement of Quenching Rate Constants

The fluorescence of **20a-f** in acetonitrile was quenched by the addition of water, alcohols (MeOH, *i*-PrOH, *t*-BuOH) and ethers (Et_2O, *i*-Pr_2O, *t*-BuOMe, *t*-BuOEt, THF). Relative fluorescence quantum yields (Φ_f^o/Φ_f) were measured for all cations and plotted versus the quencher concentration. Excellent linear plots ($r>0.98$) were obtained in each case. Stern-Volmer analysis gave excited state bimolecular rate

constants, k_q, for the reaction of the singlet excited cations with the quenchers. Representative Stern-Volmer plots for each quencher (H_2O, three alcohols and five ethers) are illustrated in Figures 1-9. The rate constants for quenching of singlet excited **20a-f** by H_2O, MeOH, *i*-PrOH and *t*-BuOH are listed in Table 5. Excited-state rate constants for quenching of **20a-f** by Et_2O, *i*-Pr_2O, *t*-BuOMe, *t*-BuOEt and THF are listed in Table 6. For each quencher, the excited-state rate constants show a substantial substituent dependence, with the larger k_q values associated with the electron-donating substituents.

For quenching of singlet excited **20a-f** by water and alcohols, the rate constants vary from about 10^6-10^7 M^{-1} s^{-1} for **20b** up to the diffusion-controlled limit for **20f.** Each substituent exhibits a much smaller k_q range along the quencher series. Using **20a** as an example, k_q values range from 2.02×10^7 M^{-1} s^{-1} for quenching by H_2O, to 8.94×10^7 M^{-1} s^{-1} for quenching by *i*-PrOH. The rate constants vary on average by a factor of 4-6, and for **20b**, by a factor of 9.

The excited-state rate constant of 2.02×10^7 M^{-1} s^{-1} for quenching of **20a** by water, is in very good agreement with a rate constant of 1.5×10^7 M^{-1} s^{-1} obtained by steady-state measurement for the 9-phenylxanthyl cation generated in strongly acidic aqueous solution (Boyd, 1991) and with the value of 1.6×10^7 M^{-1} s^{-1} obtained by time-resolved measurement of the fluorescence decay for the cation generated in acidic acetonitrile (Minto, 1989). The slightly lower values obtained in acidic media can be attributed to a lowering of the water activity. A rate constant of 3.3×10^7 M^{-1} s^{-1} was

Figure 1

Stern-Volmer plot of the relative fluorescence quantum yield, Φ_f°/Φ_f, versus H_2O concentration for quenching of 9-phenylxanthylium tetrafluoroborate **20a**.

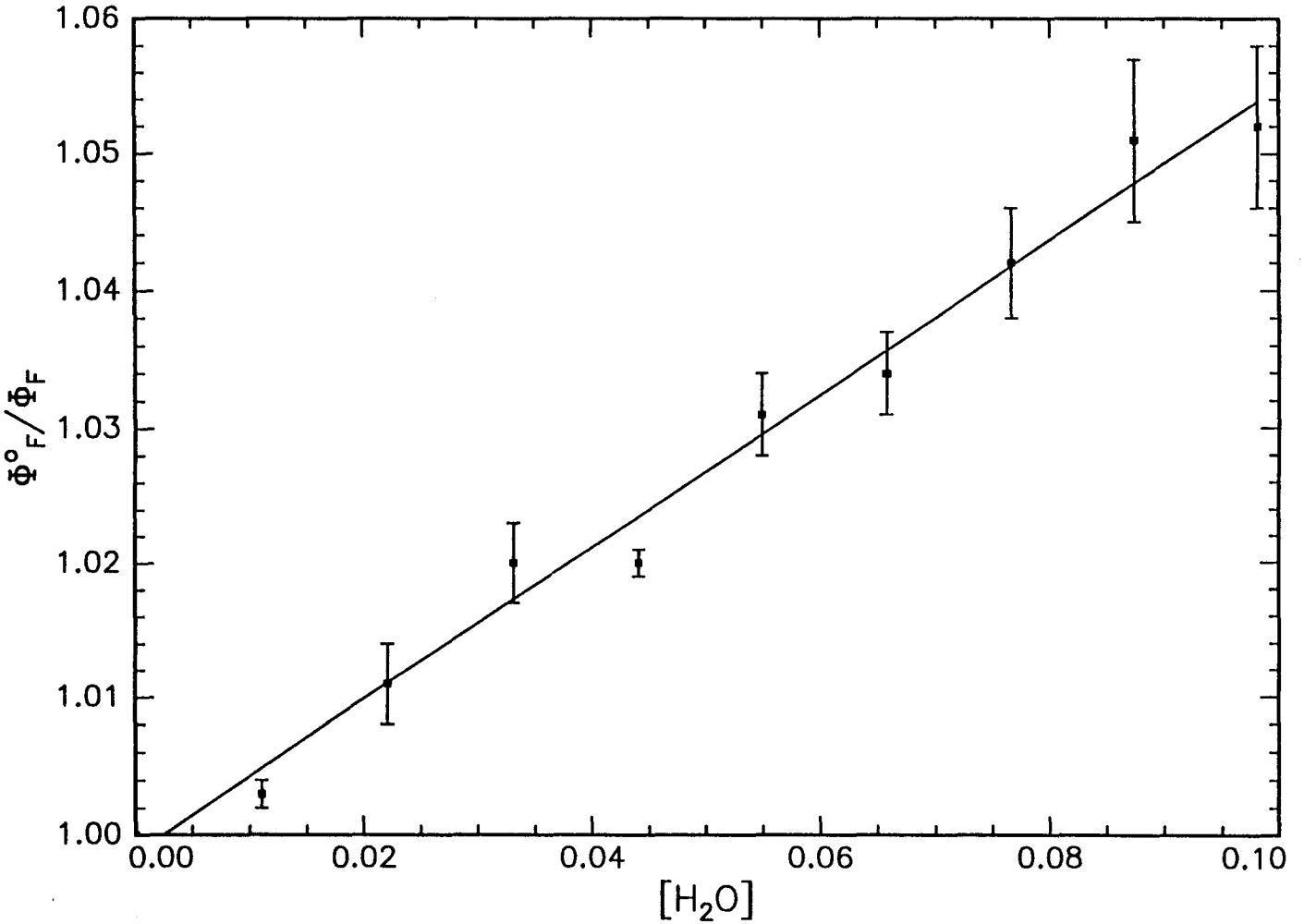
1.06
1.05
1.04
1.03
1.02
1.01
1.00
Φ^o_F/Φ_F
0.00
0.02
0.04
0.06
0.08
0.10
$[H_2O]$

Figure 2

Stern-Volmer plot of the relative fluorescence quantum yield, Φ_f^o/Φ_f, versus MeOH concentration for quenching of 9-(4-fluorophenyl)xanthylium tetrafluoroborate **20b**.

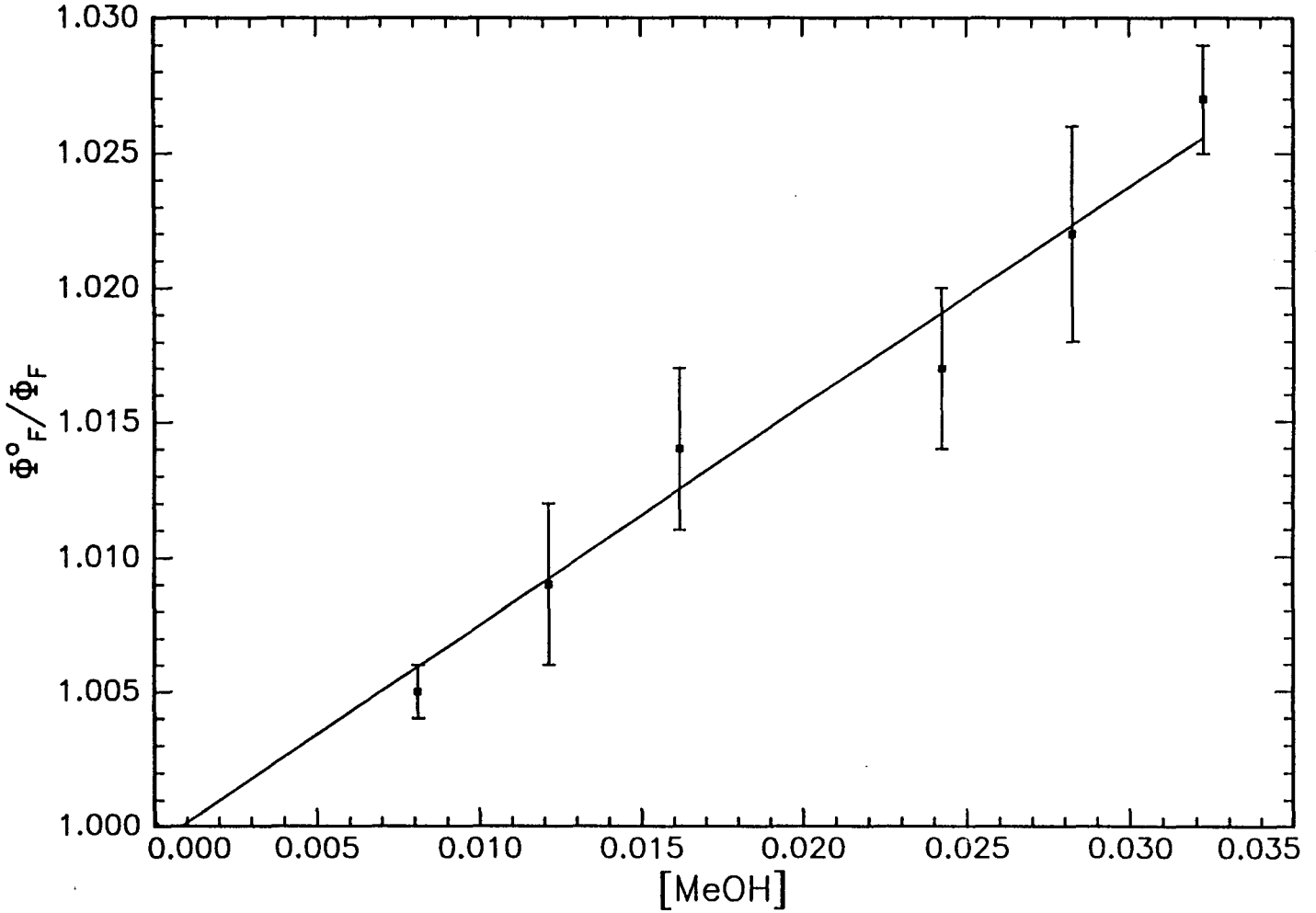
1.030
1.025
1.020
1.015
1.010
1.005
1.000
Φ°_F/Φ_F
0.000
0.005
0.010
0.015
0.020
0.025
0.030
0.035
[MeOH]

Figure 3

Stern-Volmer plot of the relative fluorescence quantum yield, Φ_f^o/Φ_f, versus *i*-PrOH concentration for quenching of 9-(3-methylphenyl)xanthylium tetrafluoroborate **20e**.

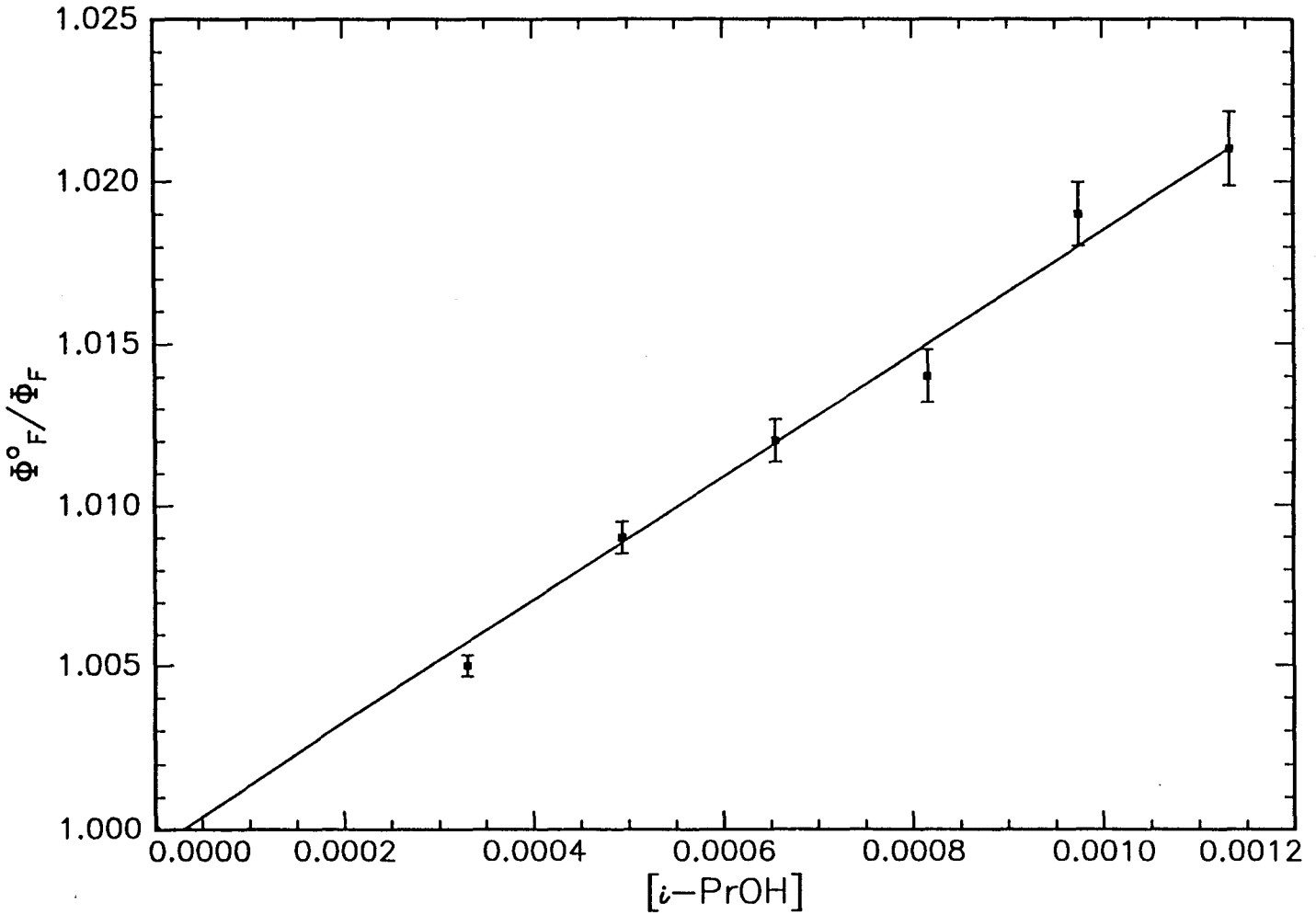
1.025
1.020
1.015
1.010
1.005
1.000
Φ°_F/Φ_F
0.0000
0.0002
0.0004
0.0006
0.0008
0.0010
0.0012
[i–PrOH]

Figure 4

Stern-Volmer plot of the relative fluorescence quantum yield, Φ_f^o/Φ_f, versus *t*-BuOH concentration for quenching of 9-(4-methylphenyl)xanthylium tetrafluoroborate **20d**.

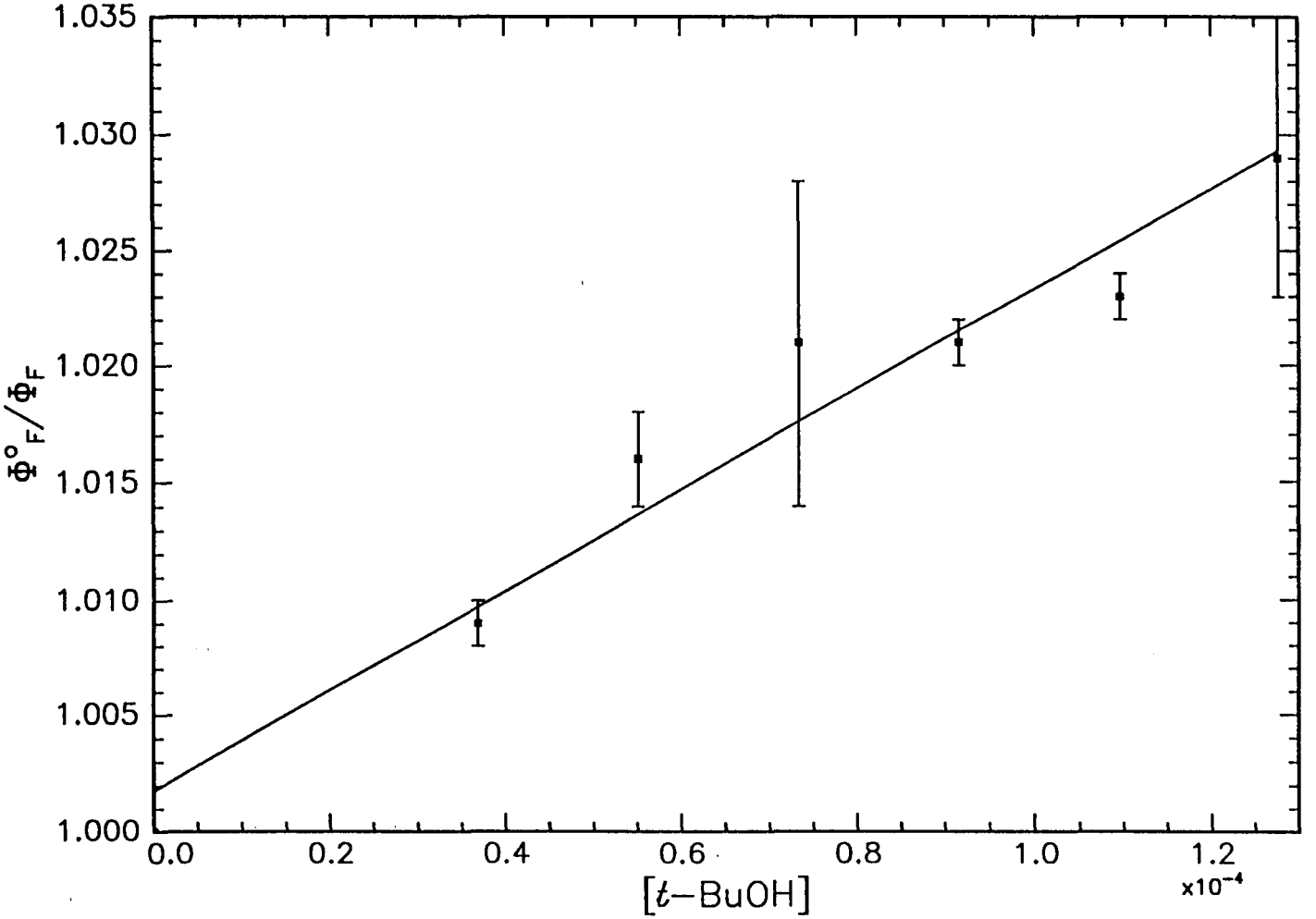
1.035
1.030
1.025
1.020
1.015
1.010
1.005
1.000
Φ°_F/Φ_F
0.0
0.2
0.4
0.6
0.8
1.0
1.2
x10^{-4}
[t–BuOH]

Figure 5

Stern-Volmer plot of the relative fluorescence quantum yield, Φ_f^o/Φ_f, versus *i*-Pr_2O concentration for quenching of 9-(3-fluorophenyl)xanthylium tetrafluoroborate **20c**.

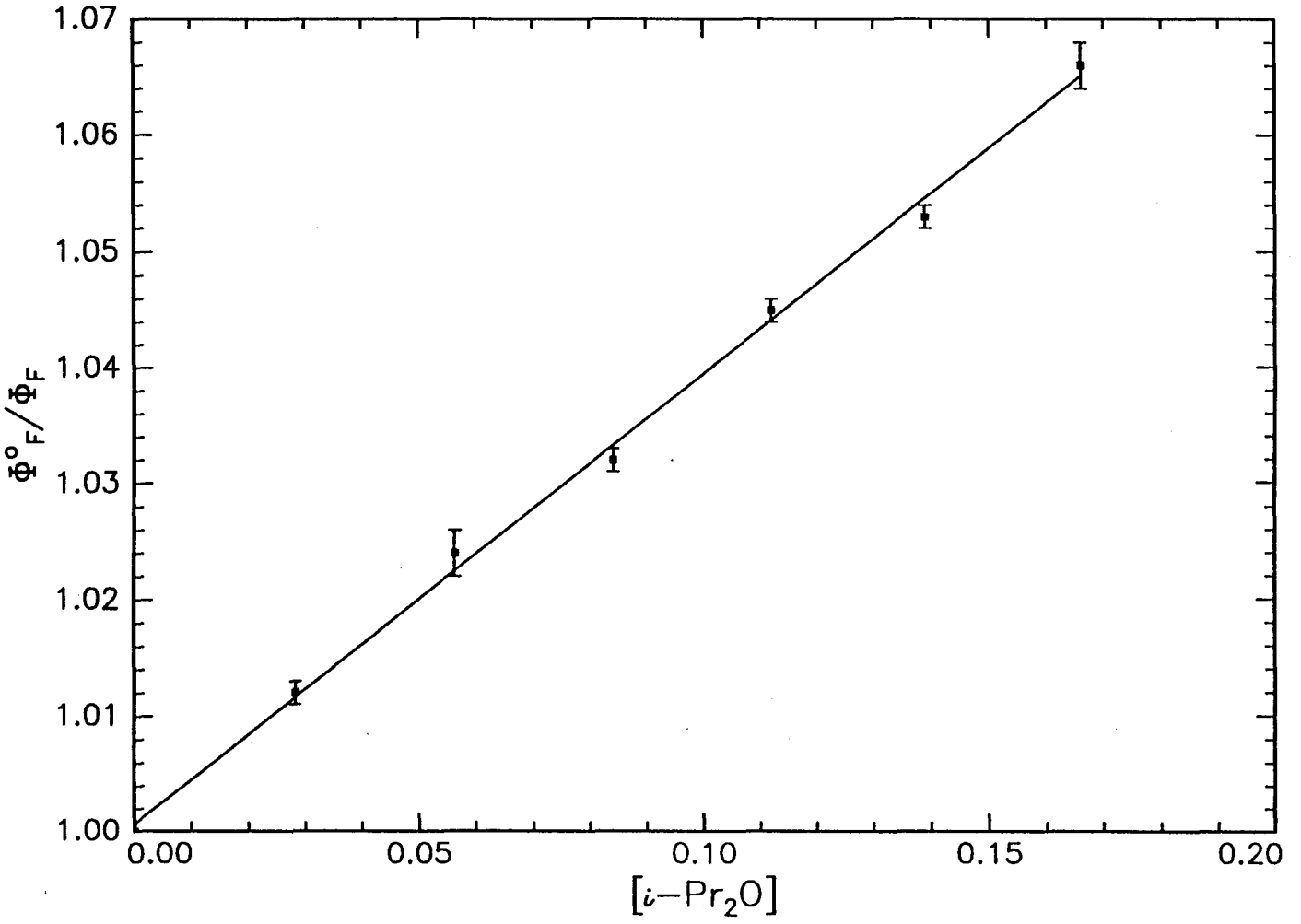
1.07
1.06
1.05
1.04
1.03
1.02
1.01
1.00
Φ°_F/Φ_F
0.00
0.05
0.10
0.15
0.20
[i–Pr_2O]

Figure 6

Stern-Volmer plot of the relative fluorescence quantum yield, Φ_f^o/Φ_f, versus Et_2O concentration for quenching of 9-(4-fluorophenyl)xanthylium tetrafluoroborate **20b.**

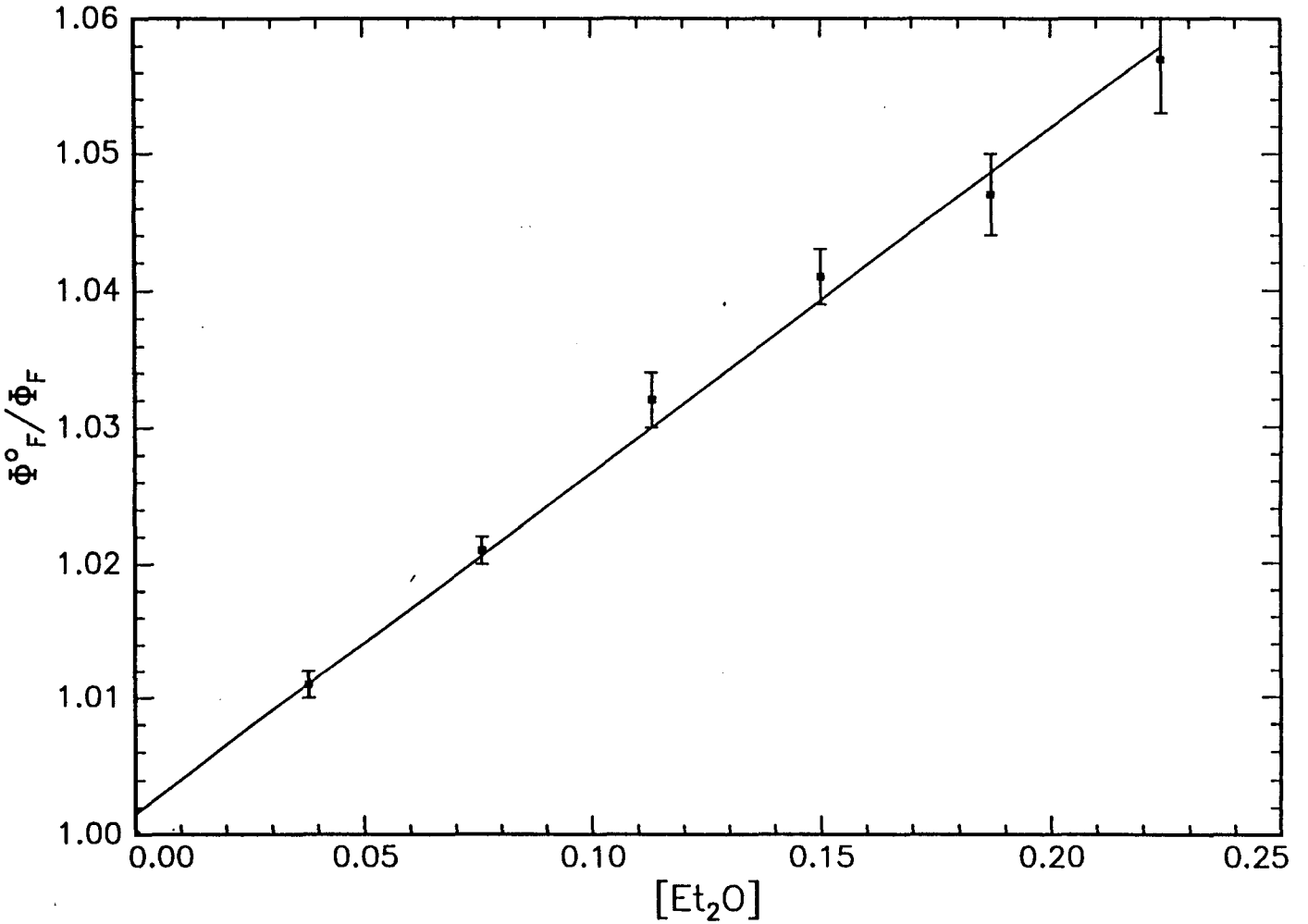
1.06
1.05
1.04
1.03
1.02
1.01
1.00
Φ°_F/Φ_F
0.00
0.05
0.10
0.15
0.20
0.25
$[Et_2O]$

Figure 7

Stern-Volmer plot of the relative fluorescence quantum yield, Φ_f^o/Φ_f, versus *t*-BuOMe concentration for quenching of 9-phenylxanthylium tetrafluoroborate **20a**.

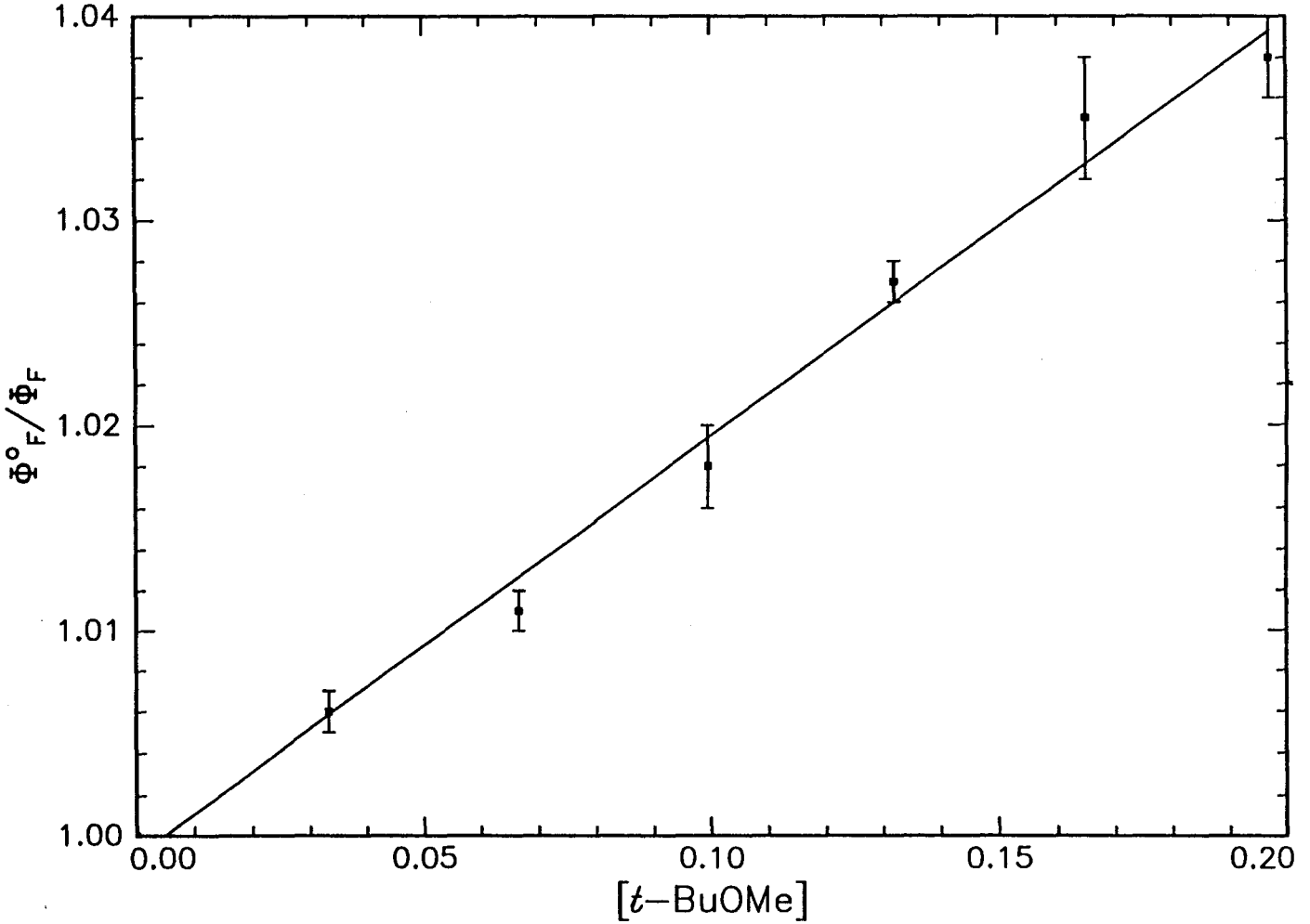
1.04
1.03
1.02
1.01
1.00
Φ°_F/Φ_F
0.00
0.05
0.10
0.15
0.20
[t–BuOMe]

Figure 8

Stern-Volmer plot of the relative fluorescence quantum yield, Φ_f^o/Φ_f, versus *t*-BuOEt concentration for quenching of 9-(3-methoxyphenyl)xanthylium tetrafluoroborate **20f**.

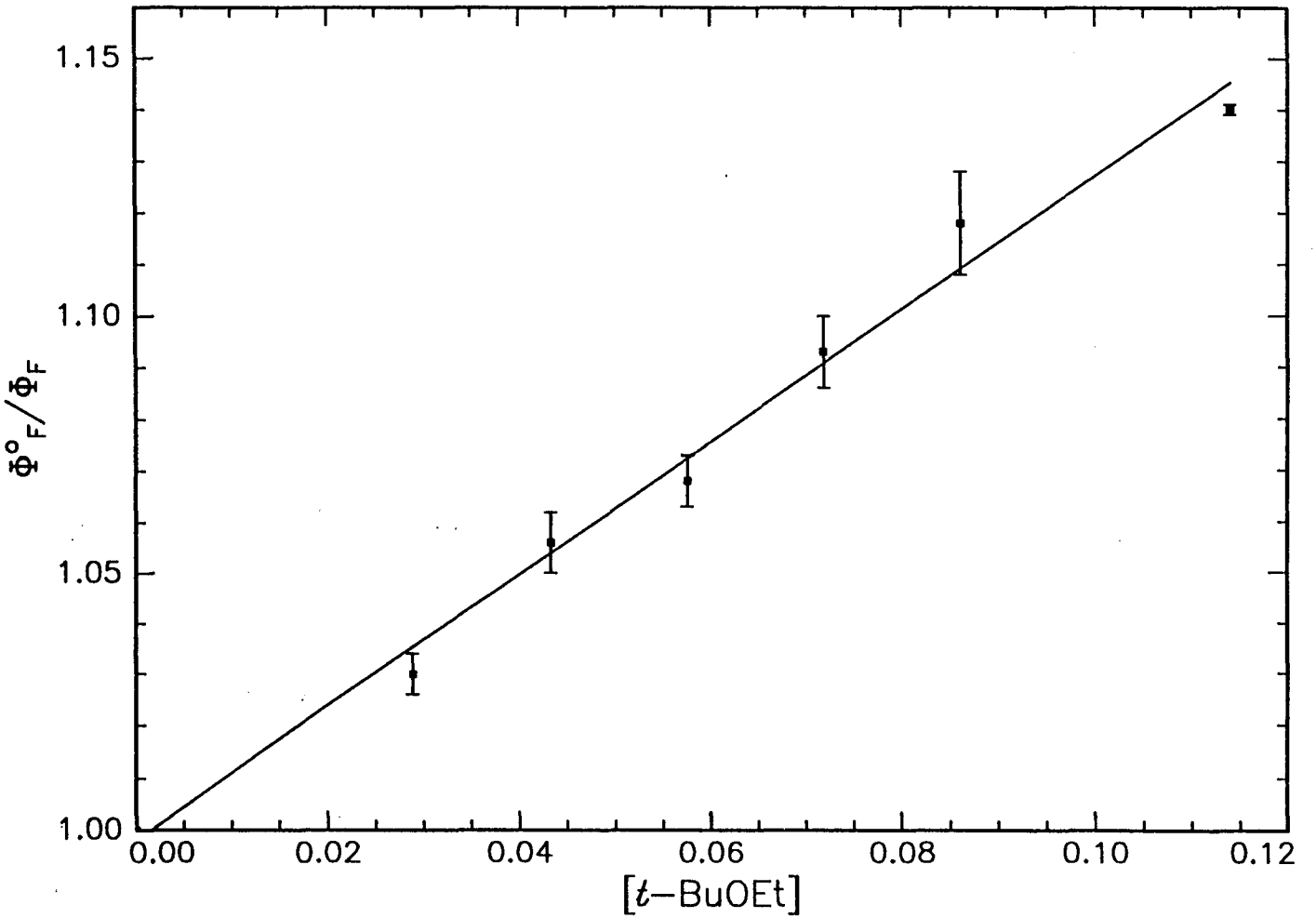
1.15
1.10
1.05
1.00
Φ°_F/Φ_F
0.00
0.02
0.04
0.06
0.08
0.10
0.12
[t–BuOEt]

Figure 9

Stern-Volmer plot of the relative fluorescence quantum yield, Φ_f°/Φ_f, versus THF concentration for quenching of 9-(3-methylphenyl)xanthylium tetrafluoroborate **20e**.

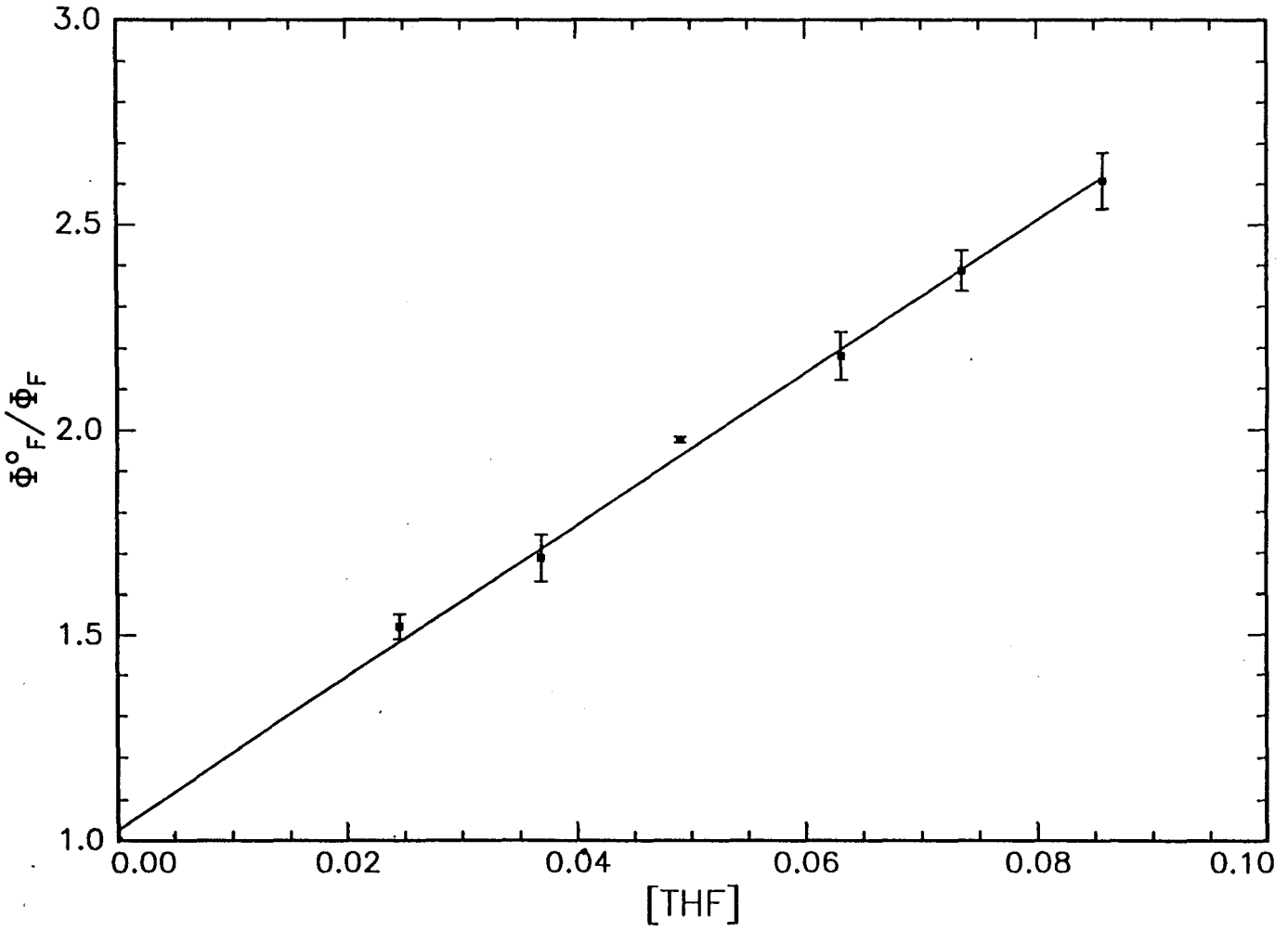
3.0
2.5
2.0
1.5
1.0
Φ°_F/Φ_F
0.00
0.02
0.04
0.06
0.08
0.10
[THF]

TABLE 5

EXCITED-STATE RATE CONSTANTS ($M^{-1}s^{-1}$)[a] FOR QUENCHING OF **20a-f**

BY WATER AND ALCOHOLS

	Quencher			
Substituent	**H_2O**	**MeOH**	***i*-PrOH**	***t*-BuOH**
H	$(2.02\pm0.02)\times10^{7}$	$(4.56\pm0.52)\times10^{7}$	$(8.94\pm0.23)\times10^{7}$	$(3.33\pm0.54)\times10^{7}$
***m*-F**	$(1.20\pm0.01)\times10^{8}$	$(8.10\pm0.02)\times10^{7}$	$(1.05\pm0.05)\times10^{8}$	$(2.34\pm0.03)\times10^{7}$
***p*-F**	$(8.88\pm0.11)\times10^{6}$	$(4.11\pm0.27)\times10^{7}$	$(8.05\pm0.69)\times10^{7}$	$(1.80\pm0.02)\times10^{7}$
***m*-CH_3**	$(2.16\pm0.30)\times10^{9}$	$(8.03\pm0.25)\times10^{9}$	$(1.02\pm0.02)\times10^{10}$	$(3.36\pm0.14)\times10^{9}$
***p*-CH_3**	$(6.23\pm0.66)\times10^{8}$	$(2.06\pm0.26)\times10^{9}$	$(3.28\pm0.38)\times10^{9}$	$(1.02\pm0.16)\times10^{9}$
***m*-OCH_3**	$(1.76\pm0.34)\times10^{10}$	$(4.97\pm0.02)\times10^{10}$	$(6.14\pm0.30)\times10^{10}$	$(3.12\pm0.27)\times10^{10}$

[a]Errors quoted are the standard deviations obtained from repeated measurements.

TABLE 6

EXCITED-STATE RATE CONSTANTS ($M^{-1}s^{-1}$)[a] FOR QUENCHING OF **20a-f**

BY ETHERS

	Quencher				
Substituent	*i*-Pr$_2$O	Et$_2$O	*t*-BuOMe	*t*-BuOEt	THF
H	$(2.28\pm0.02)\times10^{7}$	$(2.35\pm0.09)\times10^{7}$	$(6.94\pm0.46)\times10^{6}$	$(5.71\pm0.09)\times10^{7}$	$(4.86\pm0.01)\times10^{8}$
***p*-F**	$(1.91\pm0.14)\times10^{7}$	$(1.34\pm0.01)\times10^{7}$	$(4.90\pm0.52)\times10^{6}$	$(5.17\pm0.07)\times10^{7}$	$(5.02\pm0.04)\times10^{8}$
***m*-F**	$(2.80\pm0.04)\times10^{7}$	$(2.24\pm0.03)\times10^{7}$	$(6.22\pm0.06)\times10^{6}$	$(6.72\pm0.42)\times10^{7}$	$(7.60\pm0.10)\times10^{8}$
***p*-Me**	$(1.70\pm0.01)\times10^{8}$	$(1.88\pm0.12)\times10^{8}$	$(7.42\pm0.76)\times10^{7}$	$(7.76\pm0.52)\times10^{8}$	$(2.28\pm0.14)\times10^{9}$
***m*-Me**	$(4.40\pm0.06)\times10^{8}$	$(3.77\pm0.22)\times10^{8}$	$(2.01\pm0.09)\times10^{8}$	$(1.22\pm0.04)\times10^{9}$	$(8.88\pm0.42)\times10^{8}$
***m*-OMe**	$(2.11\pm0.22)\times10^{10}$	$(1.88\pm0.06)\times10^{10}$	$(5.86\pm0.28)\times10^{9}$	$(4.59\pm0.02)\times10^{10}$	

[a]Errors quoted are the standard deviations obtained from repeated measurements.

obtained using time-resolved measurements for the 9-phenylxanthyl cation generated in acetonitrile by a two-laser flash photolysis technique (Minto, 1989). The slightly higher value obtained using laser flash photolysis agrees with an earlier suggestion that ion-paired photoexcited cations are less susceptible to quenching (Minto, 1989).

For quenching of the singlet excited **20a-f** by the acyclic ethers (Et_2O, *i*-Pr_2O, *t*-BuOMe and *t*-BuOEt), the k_q values range from 10^6 to 10^{10} M^{-1} s^{-1} and are similar in magnitude to the rate constants determined for quenching of **20a-f** by H_2O and alcohols. Excited-state rate constants for quenching of **20a-e** by THF range from $4.9x10^8$ M^{-1} s^{-1} for **20a** to $8.9x10^9$ M^{-1} s^{-1} for **20e**.

The rate constant of $4.86x10^8$ M^{-1} s^{-1} for quenching of singlet excited **20a** by THF is in very good agreement with the value of $6.2x10^8$ M^{-1} s^{-1} determined by Das using time-resolved measurements for the 9-phenylxanthyl cation generated via a two-laser flash photolysis technique (Minto, 1989). As with quenching of the 9-phenylxanthyl cation by water using this photolysis technique, the slightly higher value obtained suggests that ion-paired photoexcited cations are less susceptible to quenching (Minto, 1989).

The excited-state quenching of **21a-e** by H_2O and MeOH in acetonitrile was also investigated. The excited-state quenching of two 9-arylthioxanthyl cations **21a** and **21d** by the alcohol series (MeOH, *i*-PrOH, *t*-BuOH) was also studied. Relative fluorescence quantum yields (Φ_f^o/Φ_f) were measured for **21a-e** and plotted versus the quencher concentration. Excellent linear plots ($r>0.98$) were obtained in each case.

Stern-Volmer analysis gave excited state bimolecular rate constants, k_q, for the reaction of the singlet excited 9-arylthioxanthyl cations with the quenchers. A representative Stern-Volmer plot for quenching of the *p*-F cation by MeOH is illustrated in Figure 10. The quenching rate constants are listed in Table 7 for quenching of singlet excited 9-arylthioxanthyl cations **21a-e** by water and alcohols.

In contrast to the substituent effect observed in the k_q values for quenching of the 9-arylxanthyl cations, there is no substituent dependence observed in the rate constants for quenching of **21a-e** by water and methanol. The k_q values for quenching of singlet excited **21a-e** by H_2O vary only over a small range, with a low k_q value of 3.9×10^8 M^{-1} s^{-1} (**21a**) to an upper k_q value of 6.9×10^8 M^{-1} s^{-1} (**21d**). Additionally, a small k_q range is observed for quenching of **21a-e** by MeOH where k_q values vary from 1.6×10^9 M^{-1} s^{-1} for **21d** to 5.4×10^9 M^{-1} s^{-1} for **21b**.

For quenching of singlet excited **21a** and **21d** by water and alcohols, the rate constants vary from about 10^8-10^9 M^{-1} s^{-1}. The unsubstituted cation **21a** and the *p*-Me compound **21d** exhibit a very small k_q range along the quencher series. For **21a**, k_q values range from 3.92×10^8 M^{-1} s^{-1} for quenching by H_2O up to 1.39×10^9 M^{-1} s^{-1} for quenching by *i*-PrOH, differing by a factor of only 1.2. For **21d**, k_q values range from 6.92×10^8 M^{-1} s^{-1} for quenching by H_2O up to 4.80×10^9 M^{-1} s^{-1} for quenching by *i*-PrOH, a factor of only 0.7.

Figure 10

Stern-Volmer plot of the relative fluorescence quantum yield, Φ_f^o/Φ_f, versus MeOH concentration for quenching of 9-(4-fluorophenyl)thioxanthylium tetrafluoroborate **21b.**

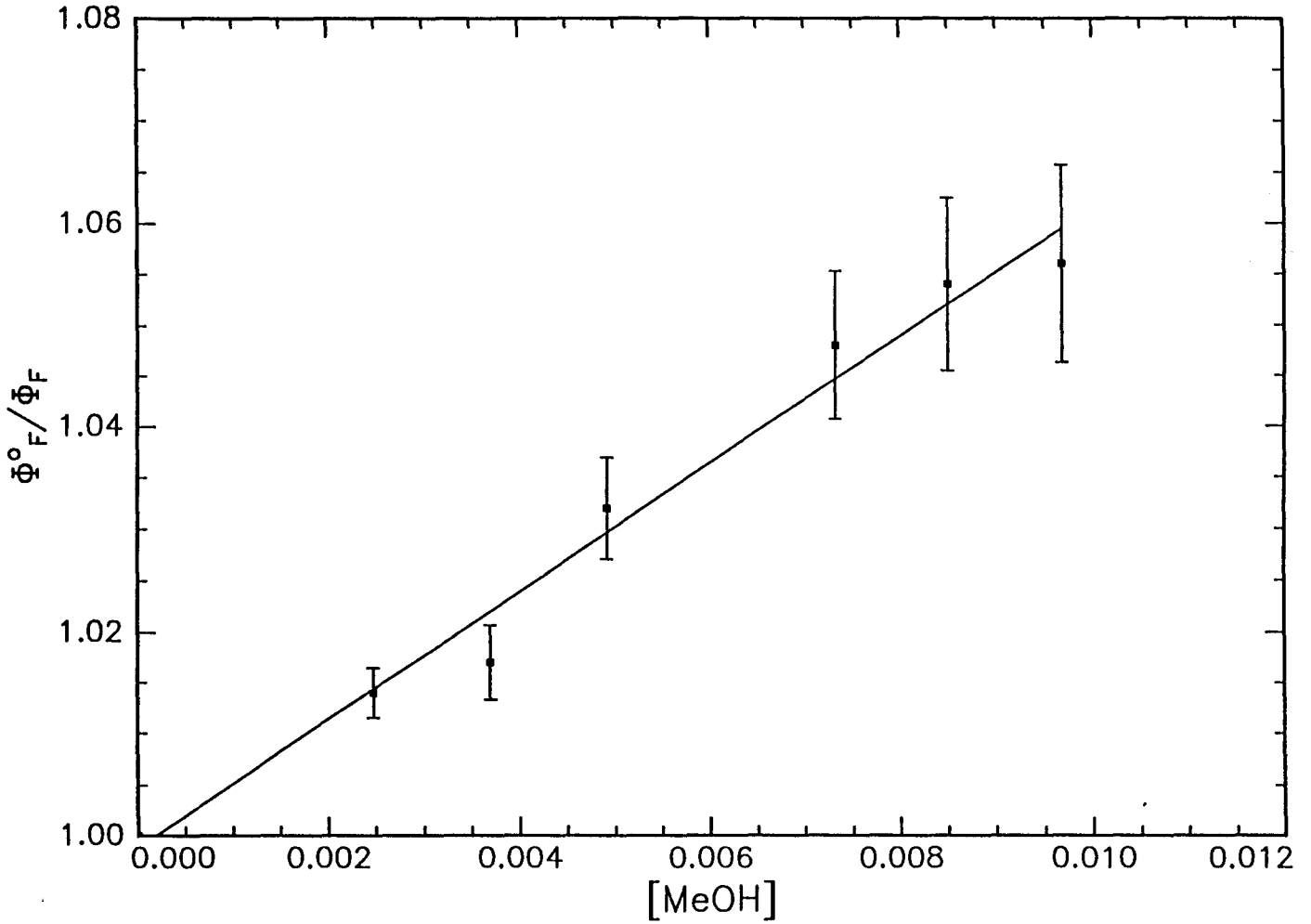
1.08
1.06
1.04
1.02
1.00
Φ°_F/Φ_F
0.000
0.002
0.004
0.006
0.008
0.010
0.012
[MeOH]

TABLE 7

EXCITED-STATE RATE CONSTANTS (M^{-1} s^{-1})[a] FOR QUENCHING OF **21a-e**

BY WATER AND ALCOHOLS

	Quencher			
Substituent	**H_2O**	**MeOH**	***i*-PrOH**	***t*-BuOH**
H	$(3.92\pm0.16)\times10^8$	$(4.12\pm0.29)\times10^9$	$(4.74\pm0.16)\times10^9$	$(1.42\pm0.04)\times10^9$
***p*-F**	$(6.70\pm0.68)\times10^8$	$(5.39\pm0.87)\times10^9$		
***m*-F**	$(4.58\pm0.44)\times10^8$	$(3.54\pm0.14)\times10^9$		
***p*-Me**	$(6.92\pm0.31)\times10^8$	$(1.65\pm0.04)\times10^9$	$(4.80\pm0.29)\times10^9$	$(1.20\pm0.02)\times10^9$
***m*-Me**	$(4.36\pm0.20)\times10^8$	$(2.26\pm0.36)\times10^9$		

[a]Errors quoted are the standard deviations obtained from repeated measurements.

Photoproduct Studies

Photoproducts from the reaction of the 9-arylxanthyl cations with H_2O or alcohols could not be isolated due to the competing thermal reaction at the high concentration of reactants necessary for preparative photolysis. Instead, a solution of **20a** (0.001 M) in acetonitrile was irradiated in the presence of *i*-Pr_2O (1 M). Unique photoproducts **22** and **24-27** have been identified by HPLC and are shown in Scheme 4. Independent synthesis and characterization of 9-hydroperoxy-9-phenylxanthene **22** and 9-phenylxanthene **24** confirmed the structures of isolated compounds **22** and **24**. Spectral analysis comfirmed the structures of xanthone **26** and *o*-hydroxybenzophenone **27** by comparison to authentic samples. A precipitate **23** formed upon irradiation and was identified as bis(9-phenylxanthen-9-yl) peroxide **22** by melting point comparison to an authentic sample.

Scheme 4

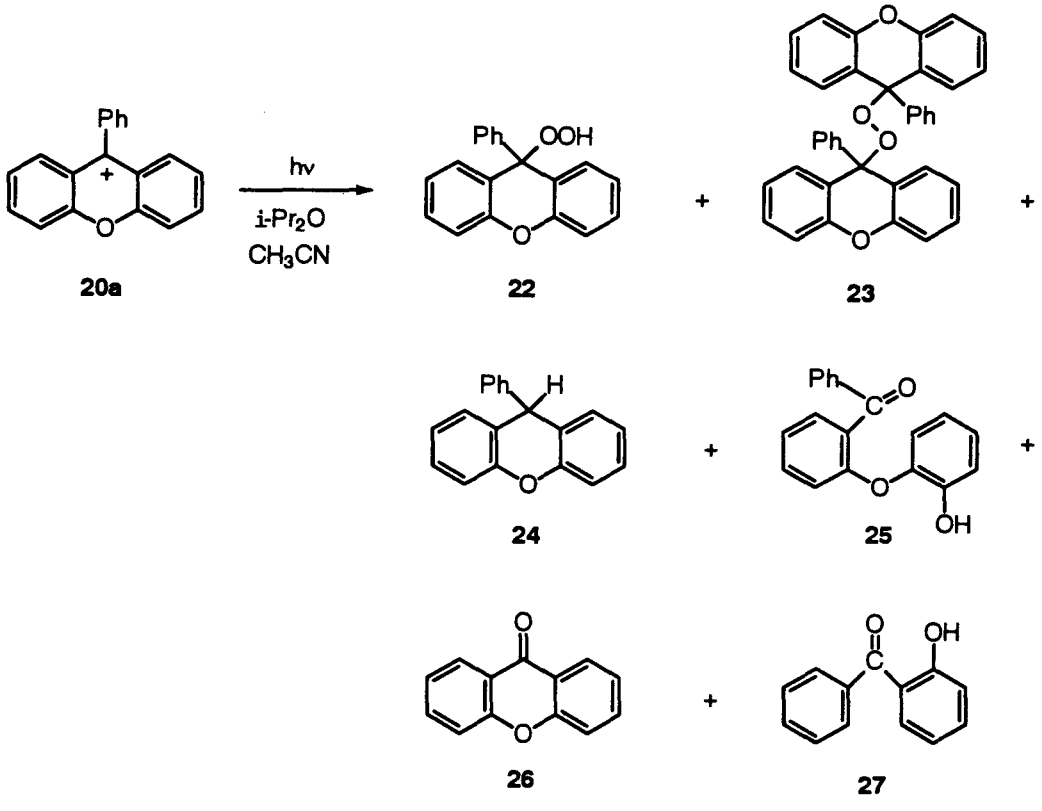

The major photoproduct **25** was isolated and characterized via spectral analysis. An independent synthesis and characterization of 2-(*o*-hydroxyphenoxy)benzophenone confirmed the structure of photoproduct **25**. Irradiation of **20a** in the absence of ether shows no reaction.

Percent conversion of **20a** over the irradiation time (40 minutes) was also monitored by HPLC. The relative amounts of photoproducts **22** and **24-27** resulting from the irradiation of oxygen saturated or argon purged solutions of **20a** were identical. Time profiles for the formation of photoproducts **22** and **24-27** are shown in Figure 11. The amount of unreacted cation **20a** was represented by the amount of

Figure 11

Plot of the percent composition of photoproducts **22** and **24-27** versus time for the irradiation of **20a** in acetonitrile in the presence of *i*-Pr_2O: ● = **20a**; ★ = **25**; ▲ = **26**; ■ = **27**; ☆ = **24**; ○ = **22**.

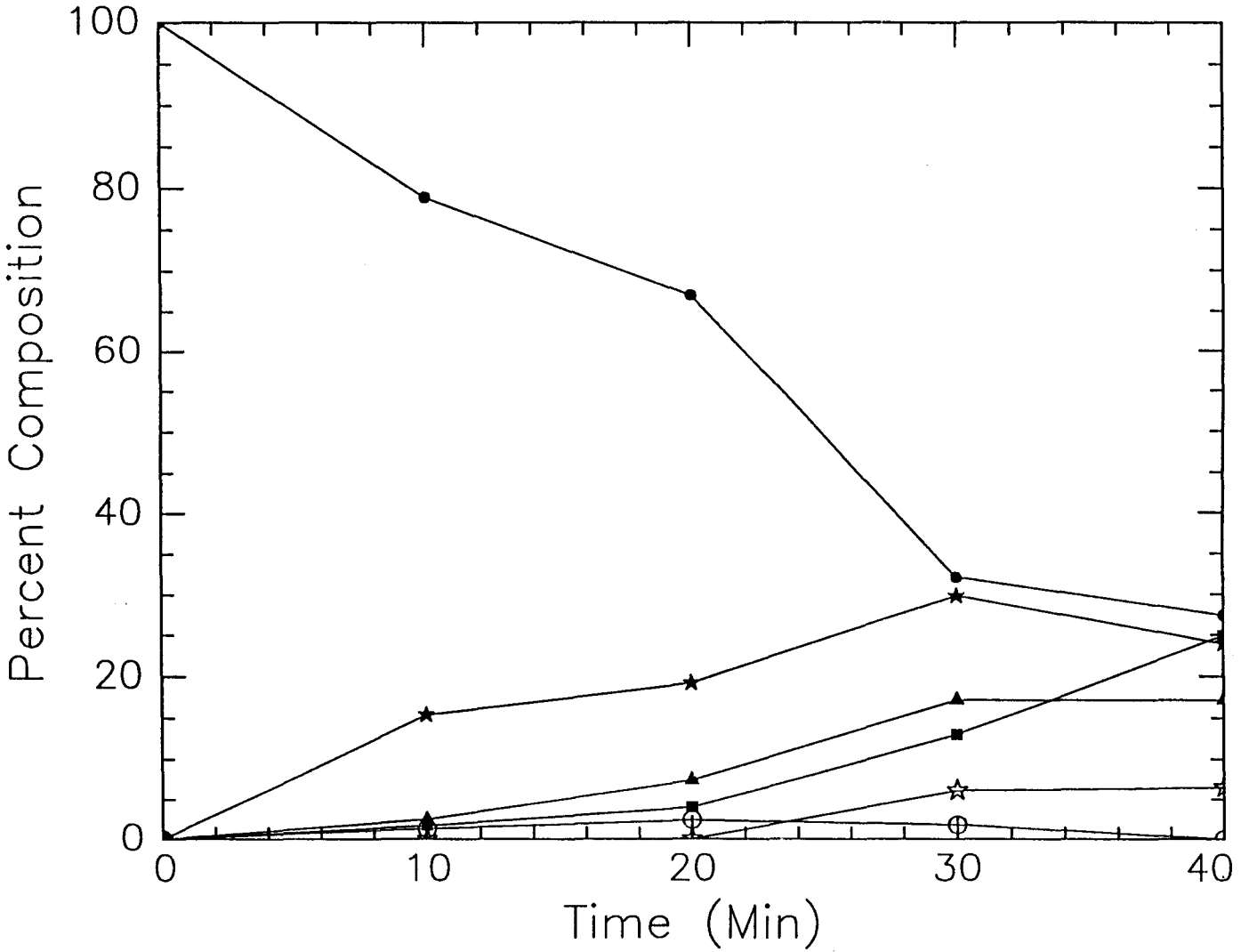
100
80
60
40
20
0
Percent Composition
0
10
20
30
40
Time (Min)

9-methoxy-9-phenyl xanthene **28** present after quenching each photolysis solution with methanol.

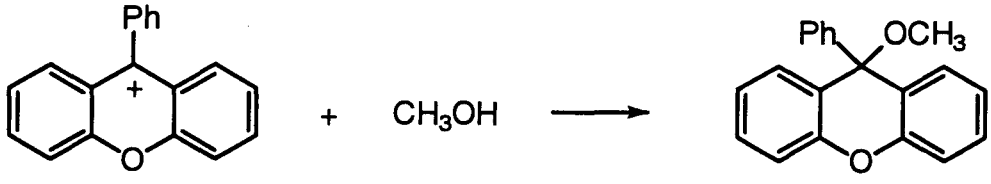

20a **28**

Compounds **22-25** and **27** were not produced in a "dark" reaction under the same conditions with only trace amounts of xanthone **26** produced. Irradiation of 9-phenylxanthen-9-ol **18a**, xanthone **26** and 9-phenylxanthene **24** in acetonitrile in the presence or absence of ether showed no reaction. Irradiation of 9-hydroperoxide-9-phenylxanthene **22** in the presence or absence of ether showed no reaction. Irradiation of 9-hydroperoxide-9-phenylxanthene **22** in the presence of ether and a trace of acid resulted in formation of **25-27**.

CHAPTER III

DISCUSSION

Substituent Effects on Quenching Rate Constants

Singlet excited 9-arylxanthyl cations **20a-f** are quenched by H_2O, acohols and ethers with excited-state bimolecular rate constants ranging from 10^7-10^{10} M^{-1} s^{-1}. A substantial substituent dependence is observed in the k_q values, with the larger rate constants associated with the electron-donating substituted cations. This substituent dependence can be further examined by construction of Hammett plots. Correlation was first attempted with plots of $\log[k_q(X)/k_q(H)]$ versus the σ and σ^+ substituent parameters (Murov, 1973), with very poor results for each of the quenchers. The poor correlation was largely due to scatter of the *meta*-substituted cations, whose points fell above the correlation line, indicating an enhanced reactivity of these cations. This behavior by excited-state *meta*-substituted compounds was first reported by Havinga (1956) and later by Zimmerman (1963), where substituents in the *meta* position exhibit greater conjugative effects than those in the *para* position. Further support for the *meta* effect is also obtained through comparison of the k_q values in Tables 5 and 6 obtained for the same substituent in the *meta* or *para* position. For both the fluoro and methyl substituted cations, the larger k_q value is associated with the *meta*

substituted cations, **20c** and **20e**, compared to the *para* substituted cations, **20b** and **20d**.

Excellent correlation was obtained with a plot of $\log[k_q(X)/k_q(H)]$ versus $\sigma^{h\nu}$, an excited-state substituent parameter (McEwen, 1991). This scale is appropriate for singlet excited xanthyl cations since it is based on the photoprotonation reaction of ring-substituted styrenes and phenylacetylenes to give the structurally similar benzyl cation. A plot of $\log[k_q(X)/k_q(H)]$ versus $\sigma^{h\nu}$ for H_2O quenching gave a ρ value of -2.07 and excellent correlation with a correlation coefficient of 0.98. Figure 12 illustrates the Hammett plot obtained for quenching of singlet excited cations **20a-f** by water. This ρ value is in very good agreement with a ρ value of -1.45 determined for H_2O quenching of the excited state 9-arylxanthyl cations in strongly acidic aqueous media (Boyd, 1991).

Plots of $\log[k_q(X)/k_q(H)]$ versus $\sigma^{h\nu}$ for quenching by MeOH, *i*-PrOH and *t*-BuOH also gave excellent correlation ($r>0.98$), with the exception of the point corresponding to **20c**, the *m*-F substituted cation. This point fell below the correlation line, with the extent of deviation from the line increasing with increasing steric bulk of the alkyl portion of the alcohol. That is, the *m*-F point is only slightly below the line for MeOH quenching, somewhat further from the line for *i*-PrOH quenching and furthest from the correlation line for *t*-BuOH quenching. Figures 13-15 illustrate the excited state Hammett plots obtained for quenching of **20a-f** by the alcohols.

Plots of $\log[k_q(X)/k_q(H)]$ versus $\sigma^{h\nu}$ for quenching by Et_2O, *i*-Pr_2O, *t*-BuOMe,

Figure 12

Plot of the $\log[k_q(X)/k_q(H)]$ versus σ^{hv} for quenching of **20a-f** by H_2O.

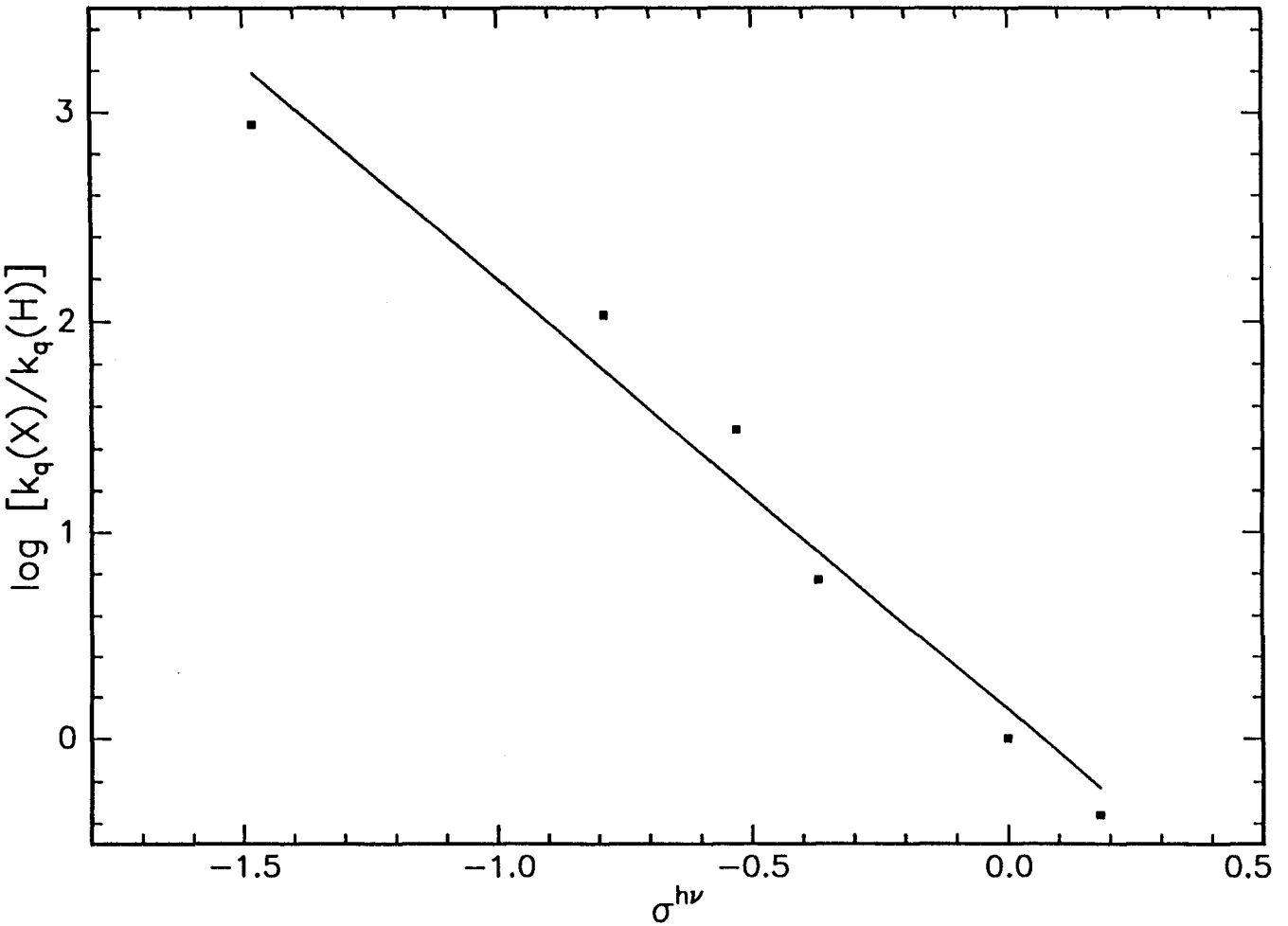
log [$k_b(X)/k_b(H)$]
3
2
1
0
−1.5
−1.0
−0.5
0.0
0.5
$\sigma^{h\nu}$

Figure 13

Plot of the $\log[k_q(X)/k_q(H)]$ versus $\sigma^{h\nu}$ for quenching of **20a-f** by MeOH.

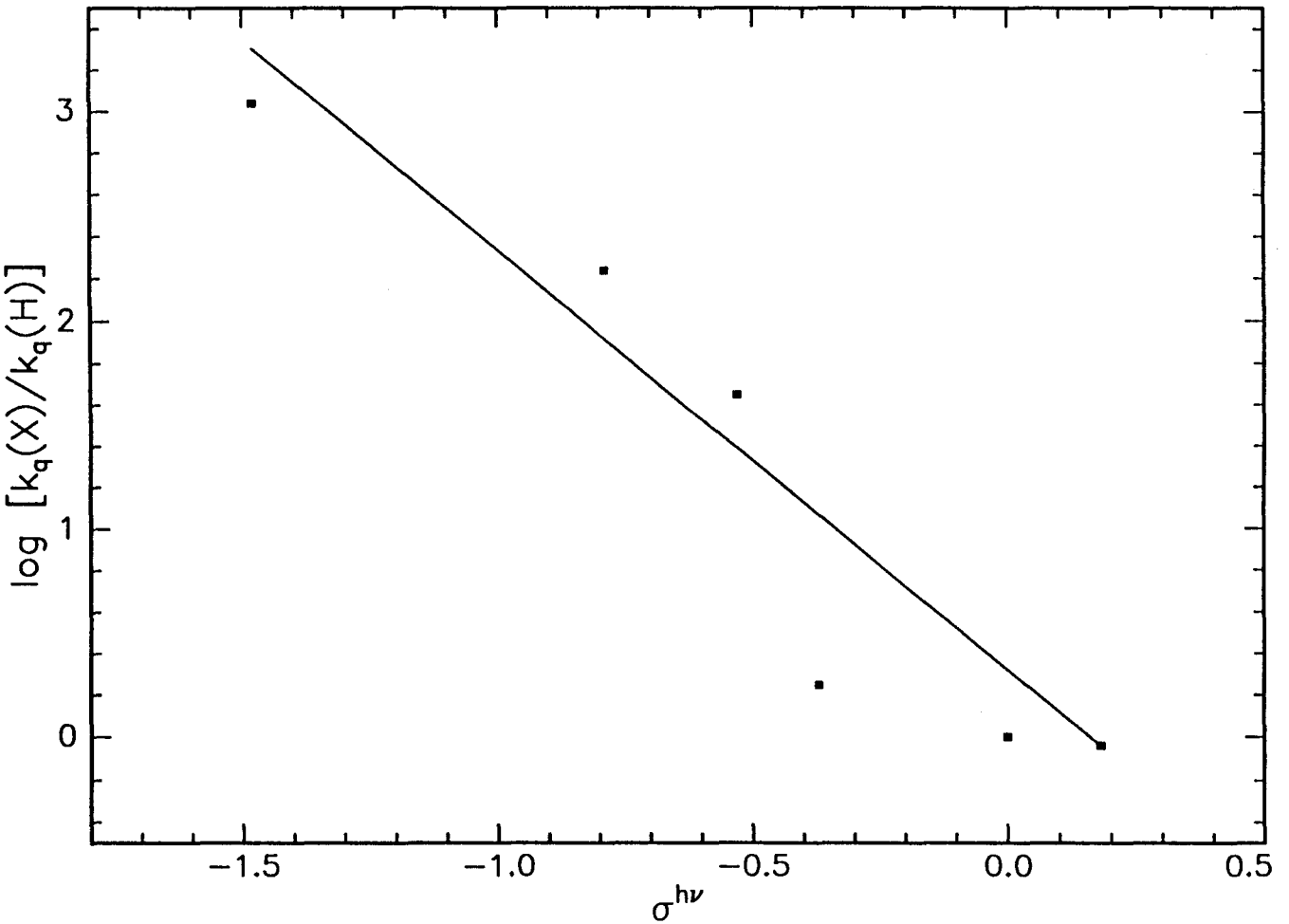
log [$k_q(X)/k_q(H)$]
3
2
1
0
−1.5
−1.0
−0.5
0.0
0.5
$\sigma^{h\nu}$

Figure 14

Plot of the $\log[k_q(X)/k_q(H)]$ versus σ^{hv} for quenching of **20a-f** by *i*-PrOH.

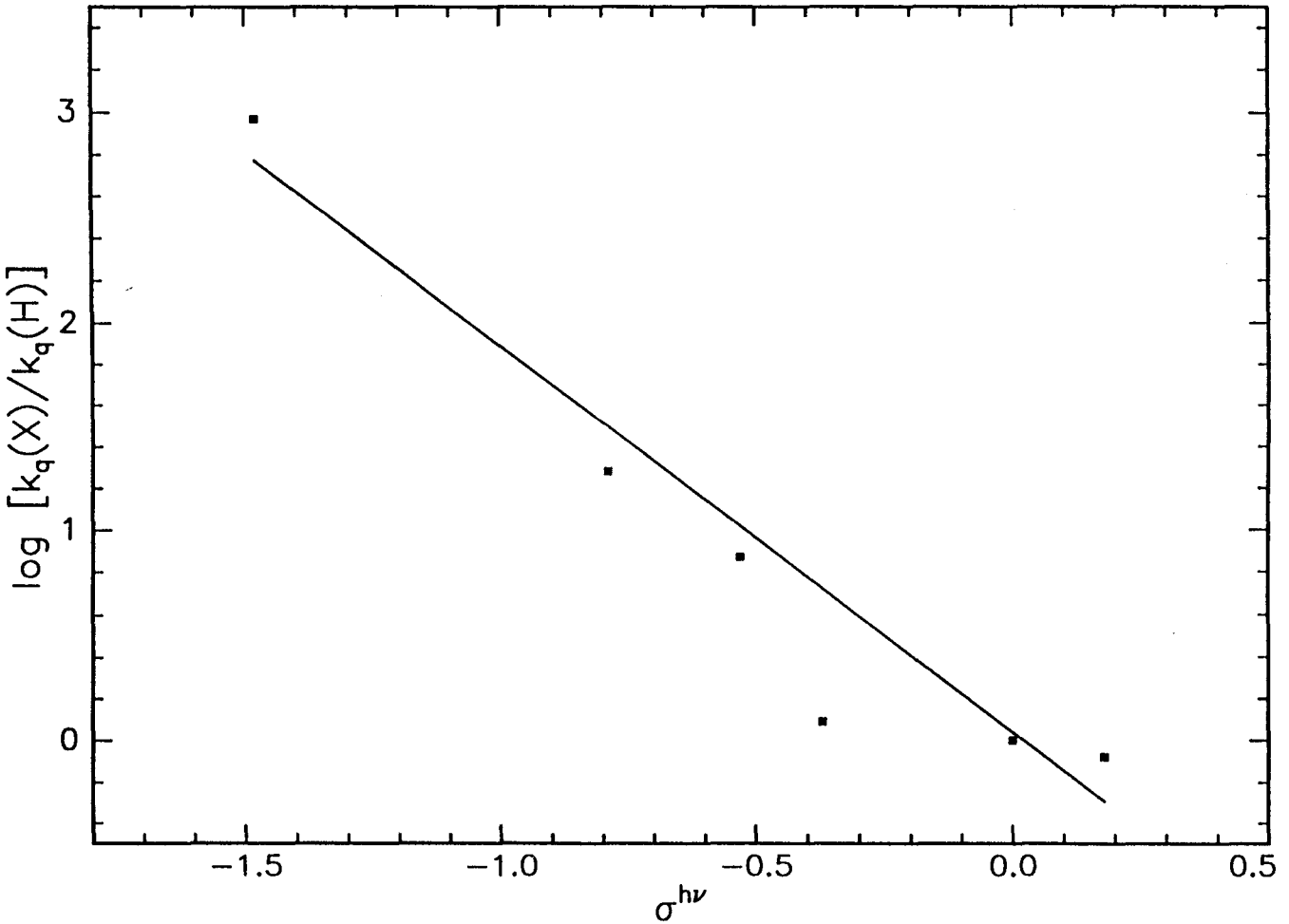
log [$k_q(X)/k_q(H)$]
3
2
1
0
−1.5
−1.0
−0.5
0.0
0.5
$\sigma^{h\nu}$

Figure 15

Plot of the $\log[k_q(X)/k_q(H)]$ versus σ^{hv} for quenching of **20a-f** by *t*-BuOH.

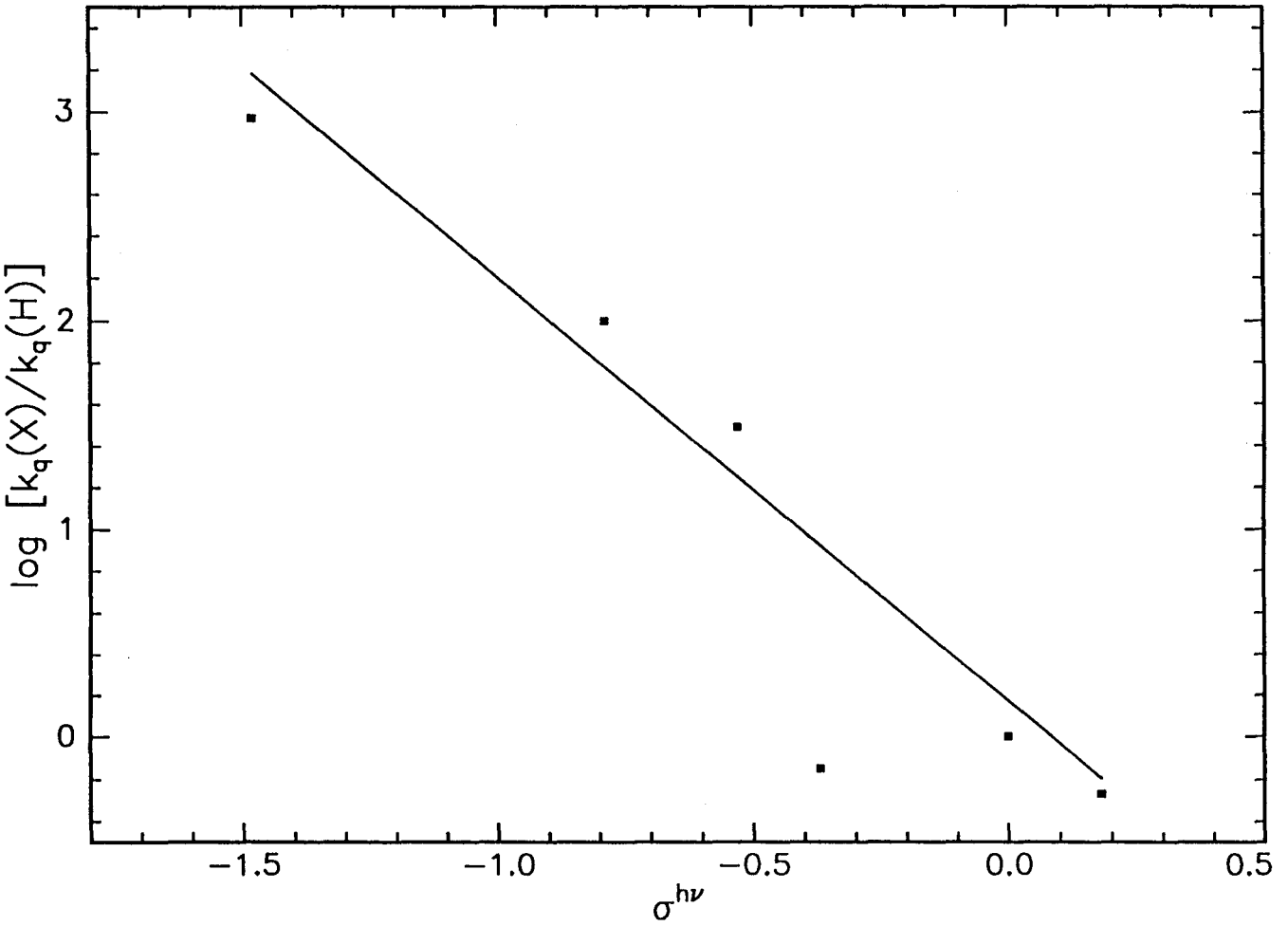
3
2
1
0
log [$k_q(X)/k_q(H)$]
−1.5
−1.0
−0.5
0.0
0.5
$\sigma^{h\nu}$

t-BuOEt and THF also gave excellent correlation (r>0.98), again with the exception of the point corresponding to the *m*-F substituted cation. In contrast to the increasing deviation of the point from the line with increasing steric bulk of the alcohol, the *m*-F point shows approximately the same deviation from the line for each of the ether quenchers. Figures 16-19 illustrate the excited-state Hammett plots obtained for quenching of **20a-f** by Et_2O, *i*-Pr_2O, *t*-BuOMe and *t*-BuOEt. Figure 20 illustrates the excited-state Hammett plot obtained for quenching of **20a-e** by THF.

Values of ρ were calculated from the excited-state Hammett plots for quenching of **20a-f** by the three alcohols and are listed in Table 8 for water and the alcohols and in Table 9 for the ethers. These calculations of ρ exclude the points corresponding to the *m*-F substituted cation. It is worth noting however, that the calculated ρ values were not greatly different if the *m*-F data were included or excluded. For each of the alcohol and ether quenchers a negative ρ value was obtained, showing that the substituent dependence observed for quenching of the singlet excited 9-arylxanthyl cations is not unique for quenching by water. Hammett plots for nucleophilic reactions of ground state 9-arylxanthyl cations with water and anionic species gave weakly positive ρ values (ρ=0.4-1.1) in every case (McClelland, 1989). The ground-state substituent effect can be rationalized by weak electronic stabilization of the positively charged species by electron-donating substituents, with the effect somewhat attenuated due to the twisting of the 9-aryl ring out of planarity of the xanthyl backbone.

Figure 16

Plot of the $\log[k_q(X)/k_q(H)]$ versus σ^{hv} for quenching of **20a-f** by Et_2O.

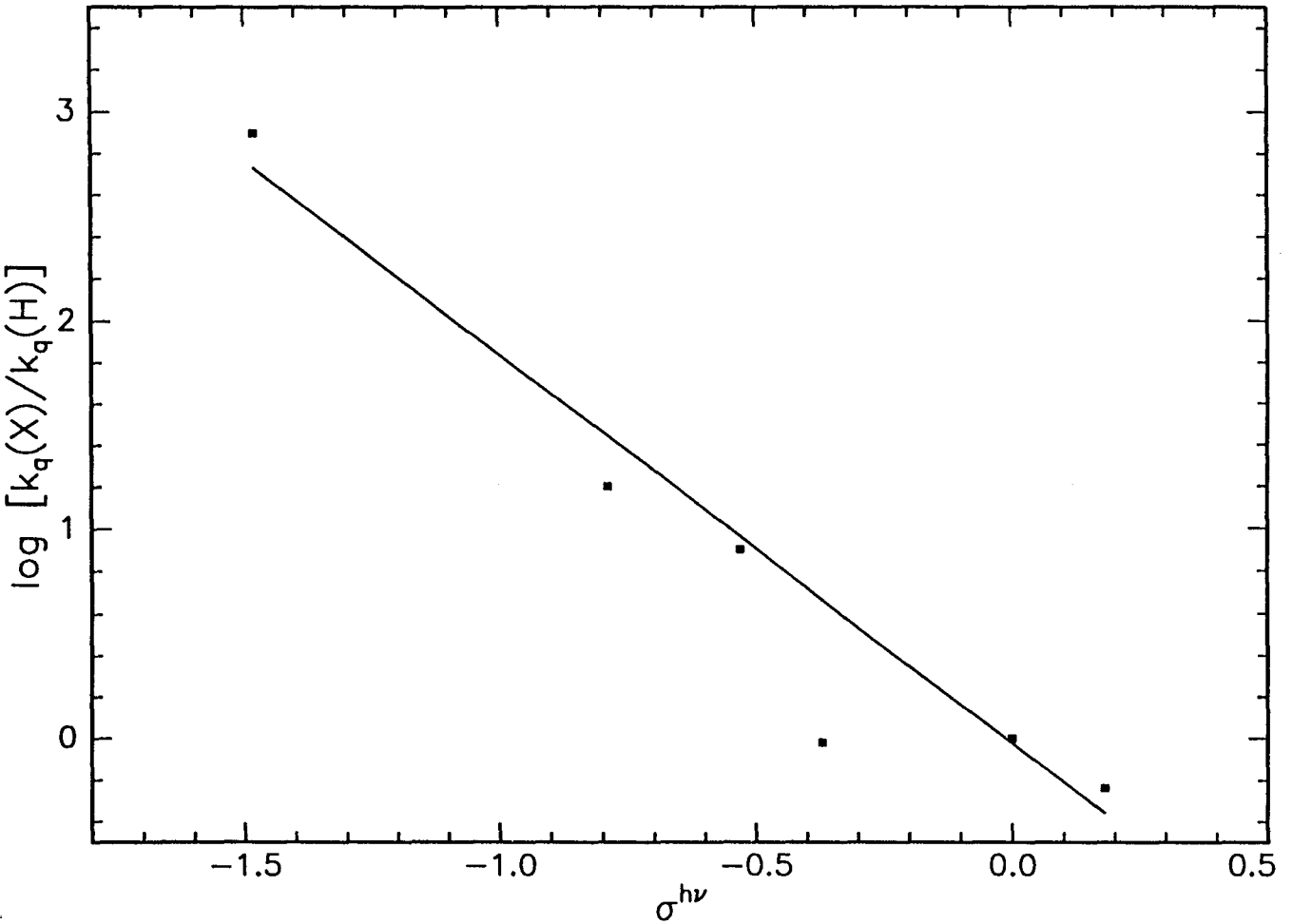
log [$k_q(X)/k_q(H)$]
3
2
1
0
−1.5
−1.0
−0.5
0.0
0.5
$\sigma^{h\nu}$

Figure 17

Plot of the $\log[k_q(X)/k_q(H)]$ versus σ^{hv} for quenching of **20a-f** by *i*-Pr_2O.

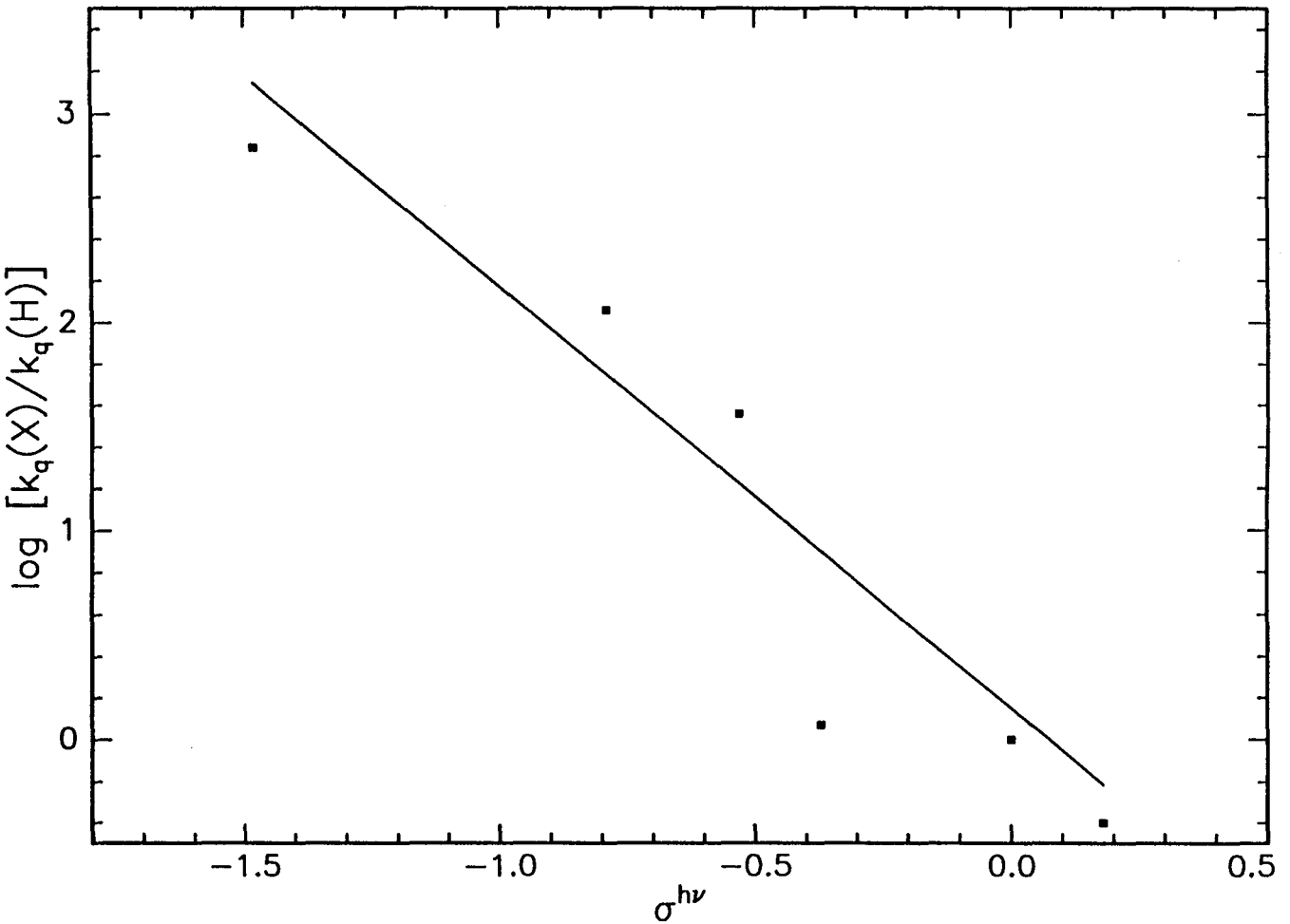
log [$k_q(X)/k_q(H)$]
3
2
1
0
−1.5
−1.0
−0.5
0.0
0.5
$\sigma^{h\nu}$

Figure 18

Plot of the $\log[k_q(X)/k_q(H)]$ versus σ^{hv} for quenching of **20a-f** by *t*-BuOMe.

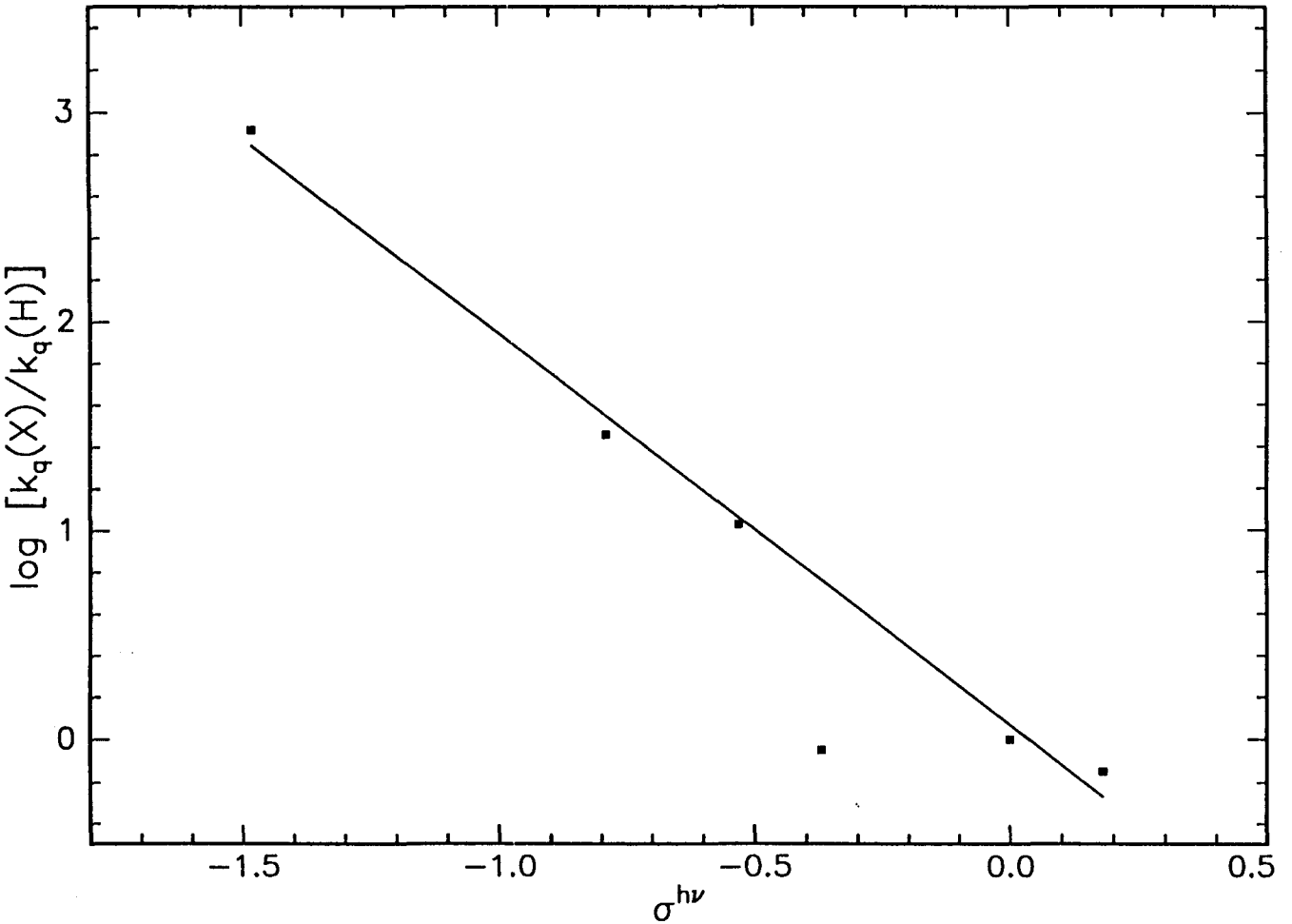
3
2
1
0
log [$k_q(X)/k_q(H)$]
−1.5
−1.0
−0.5
0.0
0.5
$\sigma^{h\nu}$

Figure 19

Plot of the $\log[k_q(X)/k_q(H)]$ versus σ^{hv} for quenching of **20a-f** by *t*-BuOEt.

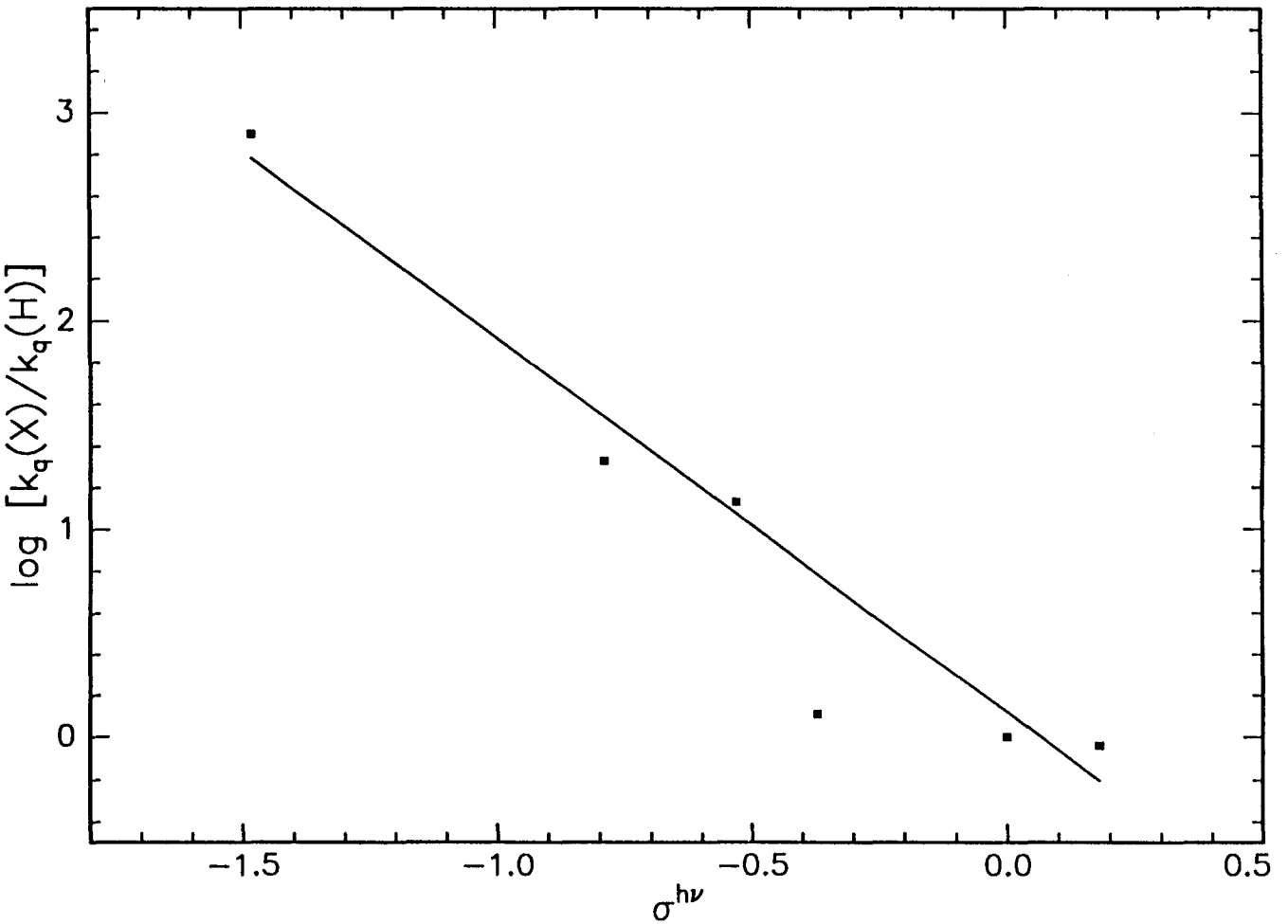
log [$k_q(X)/k_q(H)$]
3
2
1
0
−1.5
−1.0
−0.5
0.0
0.5
$\sigma^{h\nu}$

Figure 20

Plot of the $\log[k_q(X)/k_q(H)]$ versus σ^{hv} for quenching of **20a-f** by THF.

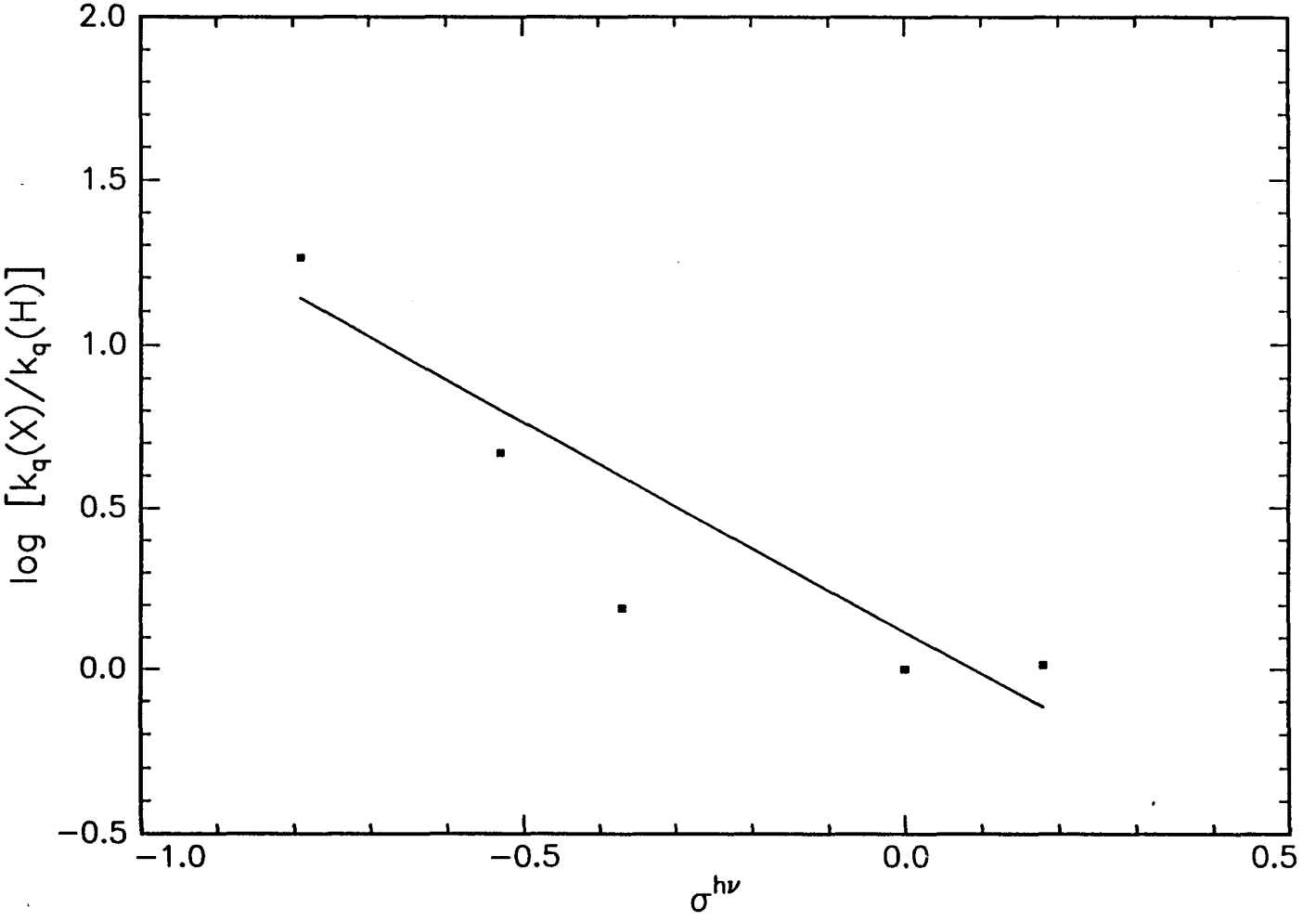
2.0
1.5
1.0
0.5
0.0
−0.5
log [$k_q(X)/k_q(H)$]
−1.0
−0.5
0.0
0.5
$\sigma^{h\nu}$

TABLE 8

CORRELATION OF $\log[k_q(X)/k_q(H)]$ VERSUS σ^{hv}

FOR QUENCHING OF **20a-f**

	quencher			
	H_2O	MeOH[a]	*i*-PrOH[a]	*t*-BuOH[a]
slope (ρ)	-2.07	-2.02	-1.88	-2.03
r[b]	0.98	0.98	0.98	0.99
intercept[c]	0.11	0.32	0.30	0.17
σ_y[d]	0.14	0.20	0.19	0.15
σ_{slope}[e]	0.19	0.26	0.24	0.19

[a]The data corresponding to **20c** were omitted from the linear regression analysis (see Discussion for details).

[b]Correlation coefficient.

[c]Intercept obtained from linear regression.

[d]Standard deviation on $\log[k_q(X)/k_q(H)]$ axis.

[e]Standard deviation in the slope.

TABLE 9

CORRELATION OF $\log[k_q(X)/k_q(H)]$ VERSUS σ^{hv}

FOR QUENCHING OF **20a-f**

	quencher				
	i-Pr_2O[a]	Et_2O[a]	*t*-BuOMe[a]	*t*-BuOEt[a]	THF[a]
slope (ρ)	-1.84	-1.86	-1.87	-1.80	-1.30
r[b]	0.99	0.99	0.99	0.99	0.97
intercept[c]	-0.04	-0.23	0.07	0.12	0.12
σ_y[d]	0.14	0.11	0.06	0.11	0.11
σ_{slope}[e]	0.17	0.14	0.08	0.14	0.23

[a]The data corresponding to **20c** were omitted from the linear regression analysis (see Discussion for details).

[b]Correlation coefficient.

[c]Intercept obtained from linear regression.

[d]Standard deviation on $\log[k_q(X)/k_q(H)]$ axis.

[e]Standard deviation in the slope.

In contrast to the large substituent effect observed in the excited-state quenching rate constants for the 9-arylxanthyl cations **20a-f**, there is apparently no substituent effect observed for quenching of the 9-arylthioxanthyl cations **21a-e**. Plots of $\log[k_q(X)/k_q(H)]$ versus σ^{hv} for H_2O and MeOH were constructed and are shown in Figures 21 and 22.

Values of ρ were calculated from the excited-state Hammett plots for quenching of **21a-e** by H_2O and MeOH and are 0.04 and 0.45, respectively. A ρ value of 0.04 clearly indicates no substitutent effect for quenching of the thioxanthyl cations. Although the ρ value determined for quenching by MeOH is slightly positive, a correlation line with zero slope can visually be drawn on the MeOH Hammett plot in Figure 22.

Relative Quenching Order

The relative order for quenching of **20a-b** and **20d-f** by water and the alcohols is *i*-PrOH>MeOH>*t*-BuOH>H_2O although the effect is modest, with the k_q values varying by a factor of 4-6 and in one case (**20b**) by a factor of 9. This order was previously observed for quenching of the 9-phenylxanthyl cation generated in acetonitrile by two-laser flash photolysis, with the observed alcohol quenching order rationalized by the steric effect of increasing methyl substitution counter balancing the increase in lone pair availability of the nucleophile (Minto, 1989). The *m*-F substituted cation **20c** exhibits a quenching order different than the other cations:

Figure 21

Plot of the $\log[k_q(X)/k_q(H)]$ versus σ^{hv} for quenching of **21a-e** by H_2O.

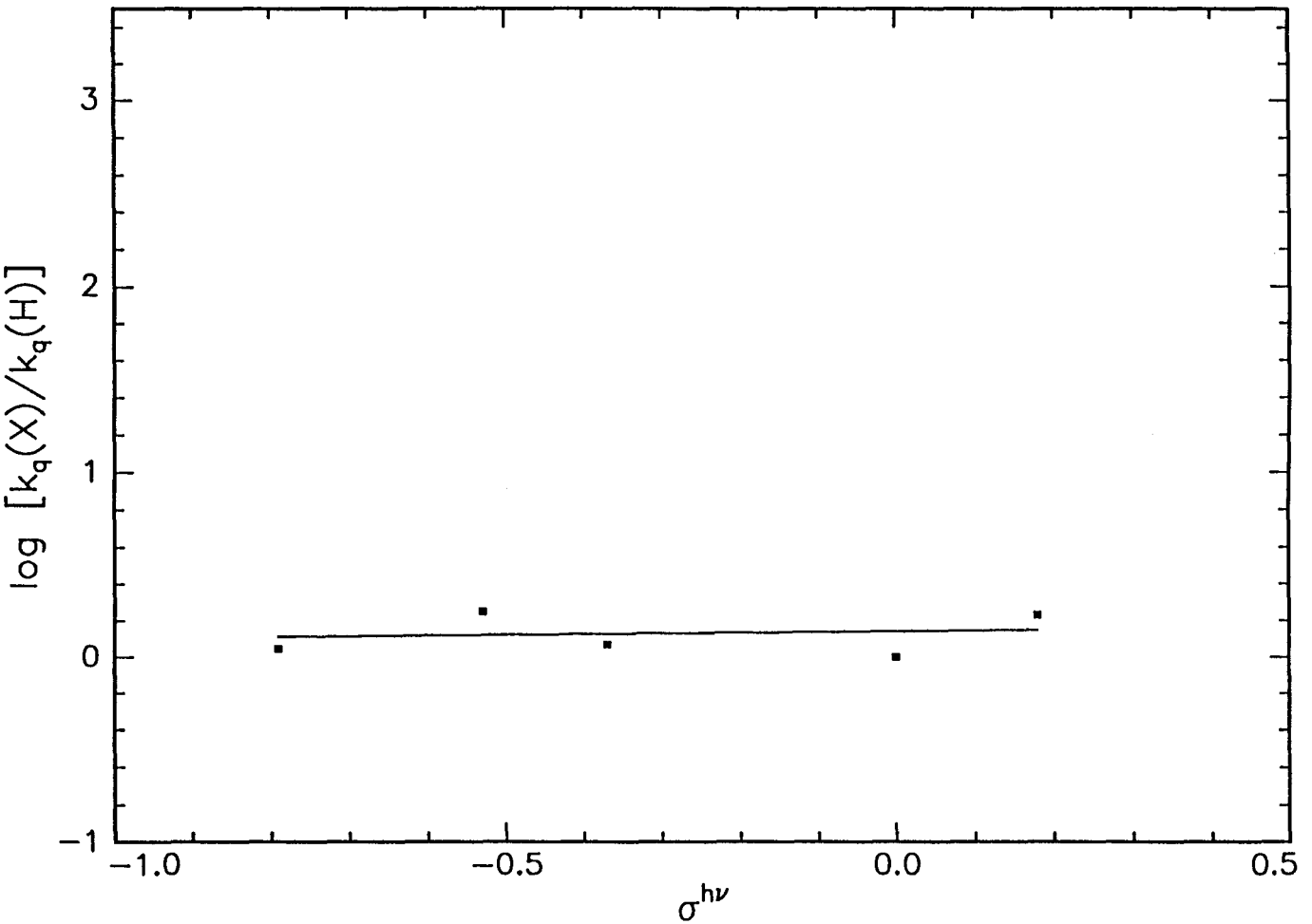
3
2
1
0
−1
log [$k_q(X)/k_q(H)$]
−1.0
−0.5
0.0
0.5
$\sigma^{h\nu}$

Figure 22

Plot of the $\log[k_q(X)/k_q(H)]$ versus σ^{hv} for quenching of **21a-e** by MeOH.

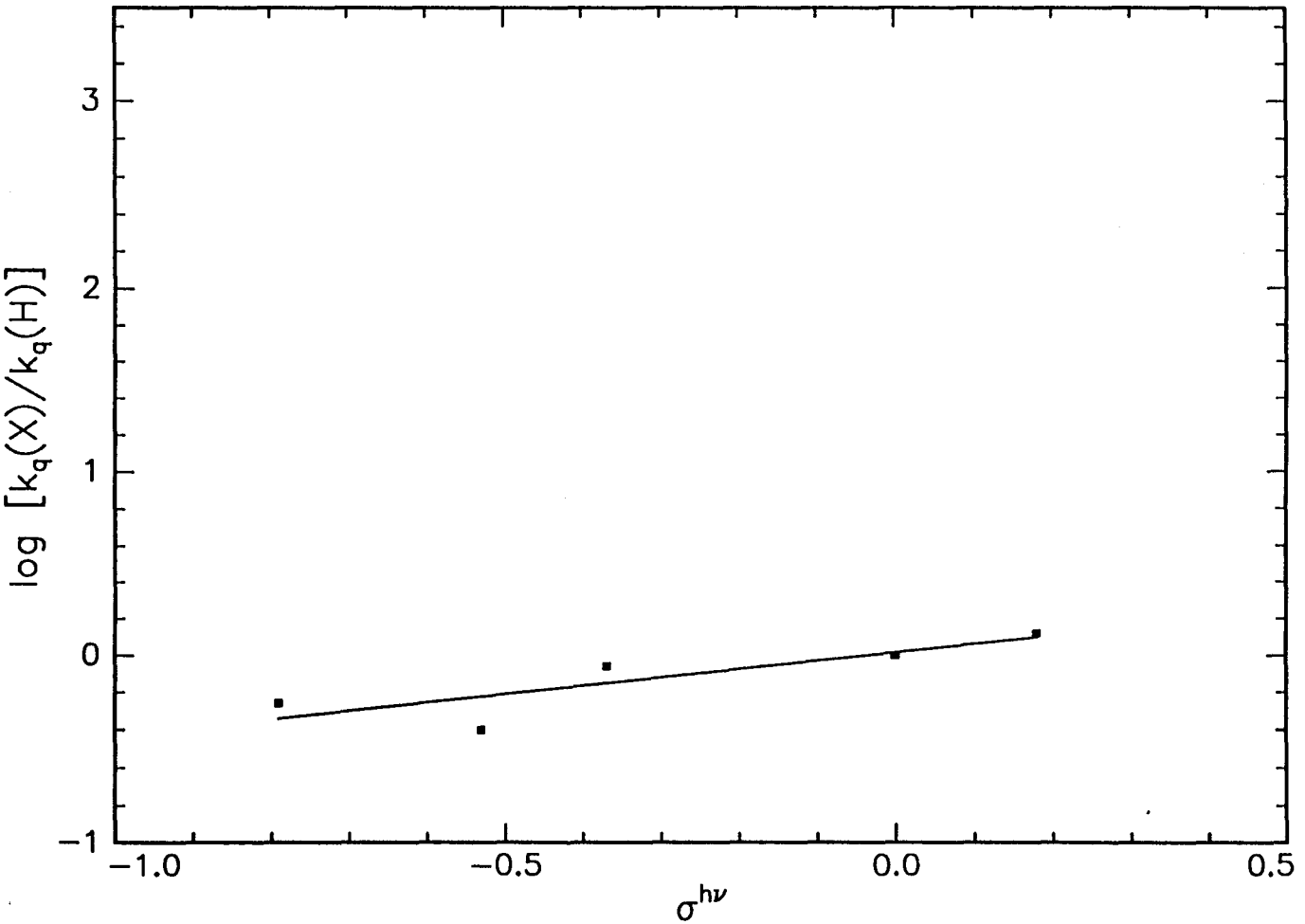
log [$k_q(X)/k_q(H)$]
3
2
1
0
−1
−1.0
−0.5
0.0
0.5
$\sigma^{h\nu}$

H_2O>*i*-PrOH>MeOH>*t*-BuOH. The different behavior of the *m*-F substituted cation **20c** was also observed in the alcohol-quenching Hammett plots, where the *m*-F points fell below the correlation line, indicating a decreased reactivity with alcohols in comparison to the other substituted cations. A steric effect is suggested since the decrease in the reactivity of **20c** (relative to the other substituted cations) correlates with an increase in the steric bulk of the alcohol. However, it seems unlikely that this behavior of **20c** is due to a steric effect of the substituent. A fluoro substituent would not exhibit a greater steric influence compared to either a methyl or methoxy substituent in the *meta* position. Furthermore, any excited-state electronic effects associated with the *m*-F substituent should already be accounted for by use of the σ^{hv} substituent parameter scale.

The relative order for quenching of **20a-f** by the ethers is THF>*t*-BuOEt>Et_2O~*i*-Pr_2O>*t*-BuOMe. For each substituent, the variation in the quenching rate constants is small, with the k_q values varying by a factor of 6 for **20e** up to 11 for **20c**. The rate constants do not appear to depend solely on steric factors, as the rate constants for quenching of **20a-f** by *t*-BuOEt are larger than for quenching by Et_2O.

The relative order for quenching of **21a** and **21d** by water and the alcohols is *i*-PrOH>MeOH>*t*-BuOH>H_2O. This is the same relative quenching order observed for quenching of the 9-arylxanthyl cations **20a-f** by water and the alcohols.

Quenching Mechanism

Quenching of the singlet excited 9-arylxanthyl cations by water and alcohols was previously suggested to occur via a nucleophilic mechanism (Boyd, 1991 and Minto, 1989). The substituent effects for quenching of these cations by H_2O and alcohols in the excited state are opposite that seen in the ground state reactivities. In order to examine the possibility of a nucleophilic mechanism, it would be advantageous to analyze the water and alcohol reactivity data using one of the nucleophilicity parameters (Ritchie, 1975 and 1978). The N^+ scale would be particularly appropriate since it is based on the reactivity of structurally similar triarylmethyl cations (Ritchie, 1975). Unfortunately, N^+ values are not available for these four quenchers in acetonitrile.

Instead we compared the excited-state relative quenching order to the quenching order observed for the reaction of ground-state cations with nucleophiles. Rate constants have been measured for reaction of vinyl (Kobayashi, 1983 and 1987), diarylmethyl (Bartl, 1991) and cyclopropyl radical (Dinnocenzo, 1990) cations with H_2O and alcohols in acetonitrile. Although these cations are less stable than the 9-arylxanthyl cations, their bimolecular rate constants with these nucleophiles are of a similar magnitude ($\sim 10^7$ M^{-1} s^{-1}). The observed trend followed the order MeOH>EtOH>*i*-PrOH>H_2O>*t*-BuOH for quenching of these ground-state cations. Additionally, rate constants have been measured for reaction of 9-carbomethoxyfluoren-9-yl and diphenylmethyl cations with H_2O and alcohols in

acetonitrile (Johnston, 1993). The quenching order observed for these ground-state cations was MeOH>EtOH>*i*-PrOH>H_2O (quenching by *t*-BuOH was not studied). The ground-state reactivities of these cations in acetonitrile also show an insensitivity to the nucleophile, exhibiting similar small differences in rate constants. The observed trend in the alcohol reactivity order is completely dependent on the steric size of alkyl group. In contrast to the relative quenching order of these ground-state cations, the excited-state quenching order does not depend solely on steric considerations of the alcohols, since the k_q values for quenching by *i*-PrOH is larger than the k_q values for quenching by MeOH for **20a-f**.

Both the quenching reactivity order and substituent effects in the excited state reaction differ compared to the ground-state cation-nucleophile reactions. We considered the possibility of a different mechanism operating in the excited-state, namely electron transfer. The Rehm-Weller equation (Rehm, 1969 and 1970) can be used to determine the free energy change for electron transfer to the singlet excited cations.

$$\Delta G_{ET} = E^{ox}_{1/2} - E^{red}_{1/2} - E_S$$

$E^{ox}_{1/2}$ is the oxidation potential of the electron donor (water, alcohol or ether), $E^{red}_{1/2}$ is the reduction potential of the electron acceptor (9-arylxanthyl cations) and E_S is the excited singlet energy of the cations. For any particular quencher, $E^{ox}_{1/2}$ will remain constant for all 9-arylxanthyl cations. E_S is ~60 kcal/mol for each 9-arylxanthyl cation, based on the wavelength for onset of fluorescence (Johnston, 1992 and 1993).

$E_{1/2}^{red}$ must then account for the reactivity difference of the cations should an electron transfer process be operating. In qualitative terms, the ease of reduction of the cations should parallel an increase in the quenching rate constants.

The reduction potentials for the 9-arylxanthyl cations **20a, 20b, 20d** and **20f** have been reported and are listed in Table 10 (Arnett, 1993 and Flowers II, 1994). These $E_{1/2}^{red}$ values were measured in sulfolane against a ferrocene/ferrocenium couple. Although the electrochemical measurements were performed in a solvent system different from the acetonitrile used for measurements of the k_q values, the reduction potentials will nevertheless indicate the substituent effect for the 9-arylxanthyl cations. The $E_{1/2}^{red}$ values (Table 10) and k_q values (Table 5 for H_2O and alcohols and Table 6 for ethers) for quenching of **20a-f** by H_2O, alcohols and ethers demonstrate that the trend for ease of reduction *decreases* with a concomitant *increase* in the magnitude of the quenching rate constants. This trend is *opposite* to that predicted should an electron transfer mechanism be operating in the quenching of the singlet excited 9-arylxanthyl cations **20a-f** by water, alcohols or ethers.

Photoproduct Studies

Photoproducts from the reaction of the 9-arylxanthyl cations with water or alcohols could not be isolated due to the competing thermal reaction at the high concentration of reactants necessary for preparative photolysis. Instead, preparative

TABLE 10

REDUCTION POTENTIALS FOR 9-ARYLXANTHYL CATIONS

Compound	$E^{red}_{1/2}(V)^a$
20a	-0.356[b]
20b	-0.323[b]
20d	-0.363[b]
20f	-0.387[c]

[a]In sulfolane versus a ferrocene/ferrocenium couple.

[b]Source: E.M. Arnett, R.A. Flowers II, A.E. Meekhof and L. Miller, "Energetics of Formation for Conjugate Xanthyl Carbenium Ions, Carbanions, and Radicals by Hydride, Proton, and Electron Transfer in Solution and Their Reactions To Give Symmetrical Bixanthyls," J. Am. Chem. Soc. 115 (1993): 12603.

[c]Source: R.A. Flowers, private communication.

photolyses were conducted for the reaction of **20a** with *i*-Pr_2O. Unique photoproducts **22-25** and **27** were produced upon irradiation of **20a** in acetonitrile in the presence of *i*-Pr_2O that were not formed in a "dark" reaction under the same reaction conditions. The photoproducts are shown in Scheme 4 (Results chapter). Photoproduct **26** was also produced upon irradiation, in addition to trace amounts in the corresponding "dark" reaction. Irradiation of 9-phenylxanthen-9-ol and xanthone in the absence and presence of *i*-Pr_2O was also investigated as a possible source of the photoproducts (see Experimental chapter). Both the alcohol and xanthone were unreactive.

The percent conversion of **20a** over time was monitored by HPLC (see Figure 11, Results chapter) and indicates that 2-(*o*-hydroxyphenoxy)benzophenone **25** is the major photoproduct and **22, 24** and **26** are produced in minor amounts. Bis(9-phenylxanthen-9-yl) peroxide **23** was not included in this time-conversion study due to its insolubility in the acetonitrile solvent. *o*-Hydroxybenzophenone **27** is a secondary photoproduct generated upon the irradiation of 2-(*o*-hydroxyphenoxy)-benzophenone **25**.

There is literature precedence to account for two of our observed photoproducts. It has been established that the ground-state hydroperoxide **22** can rapidly rearrange in the presence of acid to form 2-(*o*-hydroxyphenoxy)benzophenone **25** or xanthone **26** and phenol (Koorts, 1987). Phenol could not be detected using our experimental procedure. This mechanism is proposed to proceed by protonation of the hydroperoxide terminal oxygen, followed by rearrangement, and is shown in Scheme

5. Irradiation of 9-hydroperoxy-9-phenylxanthene **22** in acetonitrile in the presence of acid (see Experimental chapter) produced 2-(*o*-hydroxyphenoxy)benzophenone **25**, xanthone **26** and *o*-hydroxybenzophenone **27**. Compounds **25-27** were also generated in the corresponding thermal reaction, but in lesser amounts. Thus, this rearrangement is suggested to be photocatalyzed.

Scheme 5

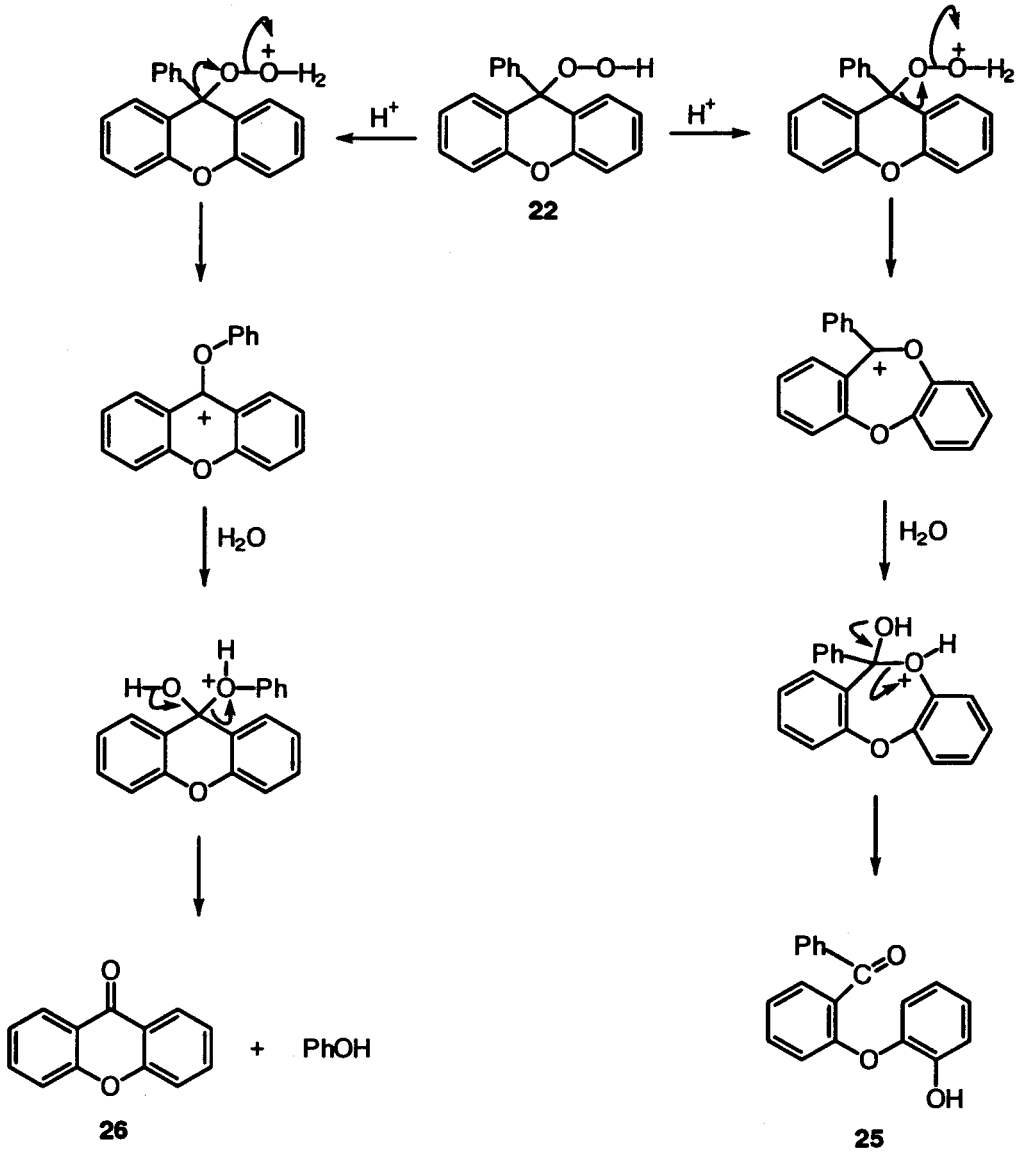

Photoproducts **22-27** suggest the intermediacy of the 9-phenylxanthyl radical. However, an electron-transfer mechanism to form the 9-phenylxanthyl radical was ruled out based on the reduction potentials of the 9-arylxanthyl cations and quenching rate constants. Instead, we propose that the excited-state mechanism proceeds via

nucleophilic attack of the ether on **20a** to form the intermediate oxonium ion **29**. Homolytic cleavage of the bond between the C(9) and oxygen generates the resonance-stabilized 9-phenylxanthyl radical **30** and the corresponding ether radical cation **31** shown in Scheme 6.

Scheme 6

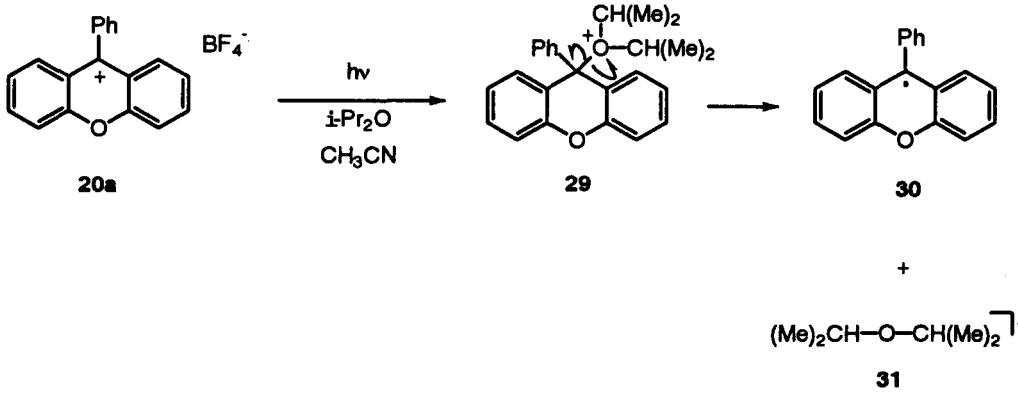

With the formation of the 9-phenylxanthyl radical **30**, the remaining photoproducts can be accounted for, with a mechanism shown in Scheme 7. The 9-phenylxanthyl radical **30** can partition between being trapped by O_2 to produce the 9-phenylxanthene-9-peroxyl radical **32** followed by hydrogen atom abstraction to form 9-hydroperoxy-9-phenylxanthene **22**. Alternatively, radical **30** can undergo hydrogen-atom abstraction to form 9-phenylxanthene **24**. Benzophenone-sensitized (Glover, 1984) as well as unsensitized (Taljaard, 1986) irradiation of 9-phenylxanthene in benzene produced 9-hydroperoxy-9-phenylxanthene. The hydroperoxide was proposed to be generated via initial formation of the 9-phenylxanthyl radical and subsequent trapping by O_2 generating the 9-phenylxanthene-9-peroxyl radical (Glover, 1985).

Once formed, the 9-phenylxanthene-9-peroxyl radical **32** can couple with a 9-phenylxanthyl radical **30** to form bis(9-phenylxanthen-9-yl) peroxide **23**, accounting for the remaining observed photoproducts.

Scheme 7

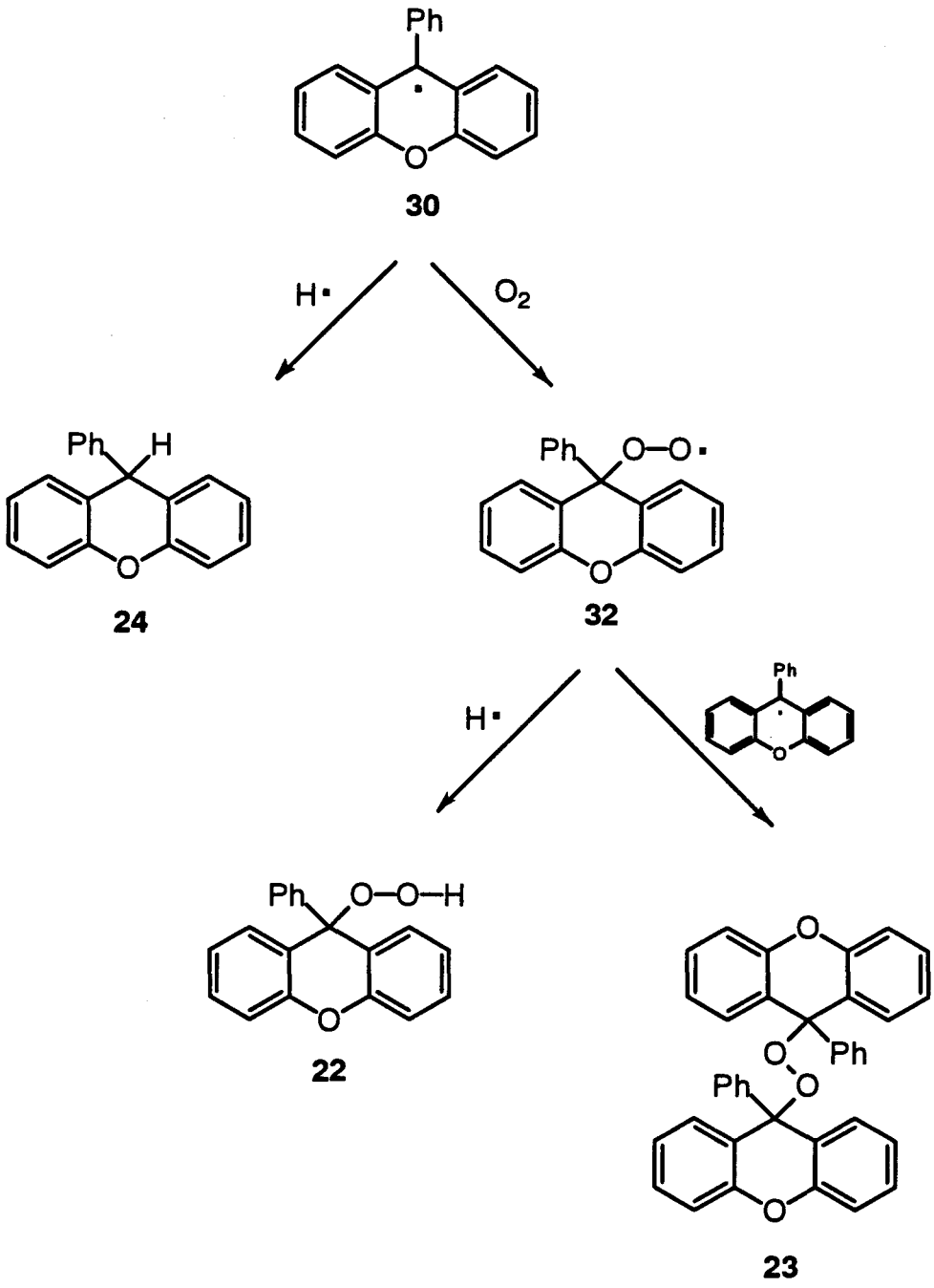

The photoproducts **22-27** formed via our proposed mechanism indicate that both

proton and hydrogen-atom sources are necessary. The ether radical cation **31** can act as a source of both, in a cascade process with a proposed mechanism shown in Scheme 8. The ether radical cation **31** is an excellent proton source yielding radical **33**. Subsequently, radical **33** is an excellent hydrogen-atom donor to form alkene **34**.

Scheme 8

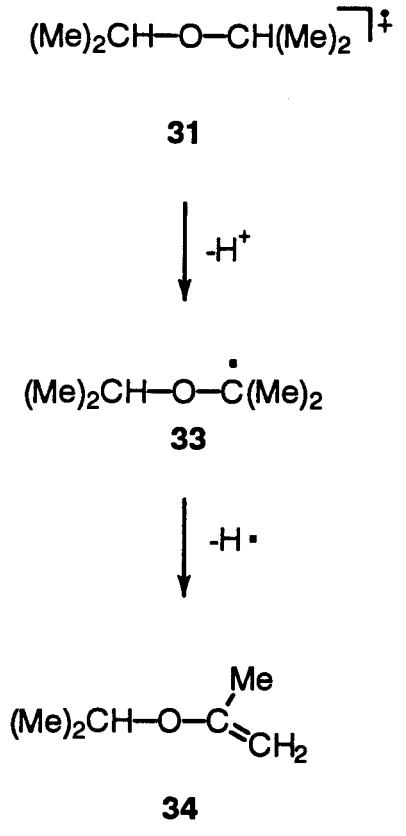

It might be expected that the relative amounts of the oxygen trapping products 9-hydroperoxy-9-phenylxanthene **22**, 2-(*o*-hydroxyphenoxy)benzophenone **25** and xanthone **26** should increase compared to the amount of hydrogen-atom abstraction

product 9-phenylxanthene **24** if photolysis solutions are purged with oxygen. Conversely, the relative amounts of hydrogen-atom abstraction product **24** should increase, compared to the amounts of hydroperoxide **22**, 2-(*o*-hydroxyphenoxy)benzophenone **25** and xanthone **26** produced if photolysis solutions are purged with argon. Contrary to this hypothesis, solutions purged with O_2 or argon show no difference in the photoproducts produced or their relative amounts.

A rate constant of 3.42×10^9 M^{-1} s^{-1} has been obtained for the reaction of the benzyl radical with O_2 in acetonitrile (Maillard, 1983). This $k_q(O_2)$ value is several orders of magnitude larger than the rate constant of 3.13×10^5 M^{-1} s^{-1} obtained for the reaction of the benzyl radical with the very efficient hydrogen-atom donor, PhSH, in hexane or cyclohexane (Franz, 1986). We can use these $k_q(O_2)$ and $k_q(H\bullet)$ values obtained for the benzyl radical as a model to explain the data obtained for our structurally similar 9-phenylxanthyl radical **30**. Since $k_q(O_2) >> k_q(H\bullet)$, the 9-phenylxanthyl radical **30** can be trapped by small amounts of adventitious oxygen in the argon purged photolysis solution to form the hydroperoxide **22** and subsequent rearrangement products 2-(*o*-hydroxyphenoxy)benzophenone **25** and xanthone **26** much faster than radical **30** can abstract a hydrogen to form 9-phenylxanthene **24**. Therefore, lack of an increase in the amount of 9-phenylxanthene **24** compared to 9-hydroperoxy-9-phenylxanthene **22** with argon purging is rationalized based on the $k_q(O_2)$ and $k_q(H\bullet)$ values.

Photophysical Properties of the Aryl Substituted Cations

The observed substituent effects on the photophysical properties of the 9-arylxanthyl cations **20a-f** indicate that an increase in the electron donating ability of the 9-aryl substituent results in a decrease in fluorescence lifetimes and quantum yields and an increase in the non-radiative rate constants. A study of 9-arylfluorenyl anions by Tolbert and co-workers (1992) show that both *meta*-withdrawing and *para*-donating substituents result in shorter fluorescence lifetimes and lower fluorescence quantum yields. These substituent effects on the photophysical properties of the fluorenyl anions were rationalized using the energy gap law, relating the nonradiative decay rates to the energy difference between the first excited state and ground state, ΔE. ΔE was chosen to be the difference between the lowest vibronic levels of the ground and excited states, $E_{0,0}$, estimated from the energy of lowest wavelength emission maximum, due to the presence of well-resolved vibronic structure. A plot of $\ln(k_{nr})$ versus ΔE gave very good correlation, providing a rationalization of the photophysical properties by intrinsic properties. This approach can not be applied to the 9-arylxanthyl cations **20a-f**, as they exhibit no substituent effect on either the absorption or emission spectra.

Another possibility which may account for the observed photophysical properties of the 9-arylxanthyl cations is a substituent effect on the rates of intersystem crossing of the cation from the singlet excited state to the triplet state. The triplet excited state of the 9-phenylxanthyl and 9-(4-fluorophenyl)xanthyl cations have been

characterized using transient absorption techniques (Johnston, 1993). The 9-(4-methoxyphenyl)xanthyl cation exhibits behavior different from that of the parent and *p*-F substituted cations. The *p*-OMe substituted cation exhibits a short fluorescence lifetime, and no phosphorescence could be detected at room temperature. A large rate constant for intersystem crossing thus was ruled out to account for the short fluorescence lifetime. Instead, a rapid intramolecular charge transfer quenching mechanism was proposed as a possible deactivational mode, consistent with the previous observation of efficient quenching of the 9-phenylxanthyl cation by anisole ($k_q = 4.9 \times 10^9\ M^{-1}\ s^{-1}$) (Azarani, 1991). The *p*-OMe substituted xanthyl cation exhibits an absorption spectum different than each of the other 9-arylxanthyl cations. In contrast to **20a-f** which exhibit an absorption band centered at about 450 nm, the longest wavelength absorption band for the *p*-OMe substituted cation is shifted to 500 nm. Xanthyl cations **20a-f** give absorption spectra which are virtually superimposable, ruling out intramolecular charge transfer as an explanation for the short lifetimes and low fluorescence quantum yield for the stronger electron-donating substituted 9-arylxanthyl cations. A substituent effect on the rate constant for intersystem crossing may account for the substituent dependence on the fluorescence lifetimes and other photophysical parameters for **20a-f**. However, it can not account for the observed substituent effect on the quenching of the singlet excited 9-arylxanthyl cations by water, alcohols and ethers, in which the magnitude of the quenching rate constants increases as the electron donating ability of 9-aryl substituent increases.

The 9-arylxanthyl cations **20a-f** exhibit a dramatic substituent effect on the fluorescence quantum yields, lifetimes and excited-state quenching rate constants but no substituent effect on the absorption or emission spectra. We speculate that the 9-arylxanthyl fluorescent species may be different than the species which is quenched, with a possible mechanism shown in Scheme 9.

Scheme 9

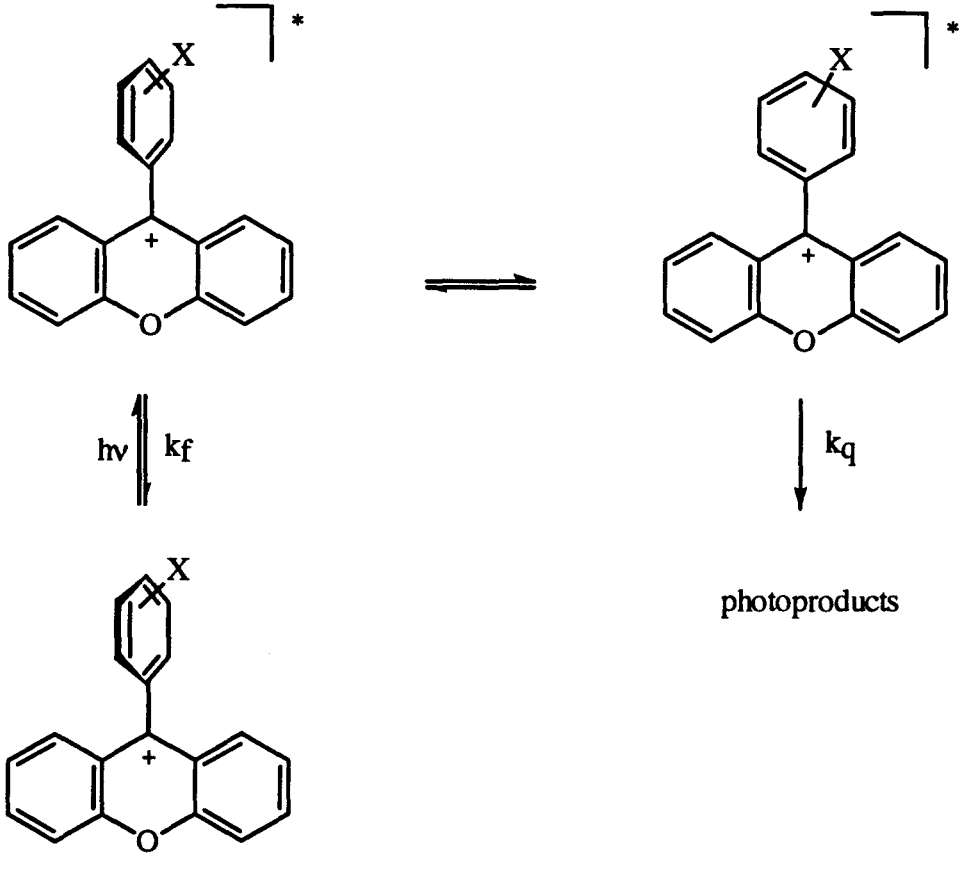

A structure in which the 9-aryl ring is twisted out of planarity (relative to the xanthyl backbone) may exhibit less conjugative effects from the 9-aryl ring on the cation, thus

not effecting the position of the absorption and fluorescence maxima. This twisted cation may be in equilibrium with a (partially) planar species where the substituents may exert a greater conjugative effect during the quenching. Substituent effects are observed on the quenching rate constants, fluorescence lifetimes and quantum yields for the 9-arylxanthyl cations, in support of the mechanism outlined in Scheme 9.

In contrast to the substantial substituent effect seen in the photophysical properties of the xanthyl cations **20a-f**, there is little or no substituent effect exhibited on the photophysical properties of the 9-arylthioxanthyl cations **21a-e**. One explaination for the absence of a substituent effect is the sulfur atom in the thioxanthyl backbone causing an enhanced intersystem crossing of the singlet excited cation to the triplet state, an influence which might overwhelm any effects due to the 9-aryl substituent.

Another possibility to explain the lack of substituent effect on the thioxanthyl cations is that structural changes due to the presence of the sulfur atom could result in a greater twisting of the 9-aryl ring out of planarity (relative to the xanthyl backbone), decreasing the conjugative interactions from the 9-aryl ring. To investigate this possibility, geometry optimization calculations were carried out on the 9-phenylxanthyl and 9-phenylthioxanthyl cations at the AM1 level. The minimized structures show that the 9-phenyl ring is twisted 59° out of planarity (where a 90° degree twist represents the structure with the 9-phenyl ring perpendicular to the xanthyl portion of the molecule). The 9-phenyl ring in the thioxanthyl cation has a

twist angle of 68°. Thus, less conjugative interactions are suggested in the thioxanthyl system, in accord with our experimental results.

CHAPTER IV

CONCLUSIONS

9-Arylxanthyl and 9-arylthioxanthyl tetrafluoroborate salts have been synthesized and prove to be excellent substrates for the study of carbocation photochemistry and photophysics. The fluorescence intensity of the 9-arylxanthyl cations in acetonitrile decreased upon addition of water, alcohols and ethers. Relative fluorescence quantum yields were measured for these cations and plotted versus the quencher concentration. Stern-Volmer analyses gave excited-state bimolecular rate constants. A substantial substituent dependence is observed in each case, with the larger rate constants associated with the electron-donating substituted cations.

The substituent effect was further examined through Hammett analyses. Excited-state Hammett plots, were constructed and resulted in negative ρ values in every case. This negative ρ value is opposite in sign to the ρ value obtained for the nucleophilic reaction of the ground-state 9-arylxanthyl cations with water.

The relative order for quenching of the 9-arylxanthyl cations by water and the alcohols is different compared to the ground-state quenching order for similarly reactive cations with H_2O and alcohols. The relative quenching order of the ground-state cations by the alcohols is strictly steric dependent. This is in contrast to the excited-state quenching order for the excited-state cations which is not based solely on steric considerations. Since both the relative reactivity order and the substituent

dependence are different between the excited-state and ground-state, a mechanism other than nucleophilic attack is suggested. The possibility of an excited-state electron transfer mechanism was considered and eliminated through application of the Rehm-Weller equation using the reduction potentials of the 9-arylxanthyl cations and the excited-state quenching rate constants.

To further study the excited-state quenching mechanism, photoproducts for the reaction of the 9-phenylxanthyl cation with *i*-Pr_2O were isolated. Unique photoproducts were isolated and identified that were not produced in the corresponding "dark" reaction. The photoproducts formed suggest the intermediacy of the 9-phenylxanthyl radical. Because an electron-transfer mechanism was ruled out, we propose that the excited-state mechanism proceeds via nucleophilic attack of the ether on the 9-phenylxanthyl cation to form an oxonium ion intermediate. Homolytic cleavage generates the resonance-stabilized 9-phenylxanthyl radical and the corresponding ether radical cation.

The effect of the heteroatom in the xanthyl backbone on the cation was also investigated. The fluorescence intensity of the 9-arylthioxanthyl cations in acetonitrile decreased upon addition of water and alcohols. Relative fluorescence quantum yields were measured for these cations and plotted versus the quencher concentration. Stern-Volmer analyses gave excited-state bimolecular rate constants. In contrast to the 9-arylxanthyl cations, there is no substituent effect observed for quenching of the 9-arylthioxanthyl cations by H_2O and MeOH. The excited-state quenching of two 9-

arylthioxanthyl cations by the alcohol series was also investigated. The same relative quenching order for quenching of the 9-arylxanthyl cations was observed for quenching of the 9-arylthioxanthyl cations.

Photophysical properties of the 9-arylxanthyl and 9-arylthioxanthyl cations were investigated. For the xanthyl series, there is a substantial substituent dependence observed in the lifetimes, fluorescence quantum yields, total decay rate constants and non-radiative rate constants. In contrast, no substituent effect was observed on the same photophysical properties in the 9-arylthioxanthyl series. The calculated fluorescence rate constants for the xanthyl and thioxanthyl cations show only a modest substituent effect. Additionally, there is no substituent dependence observed on the position of the absorbance or fluorescence maxima for either the 9-arylxanthyl or 9-arylthio-xanthyl cations.

In order to account for the substituent dependence observed on the τ_f^o, Φ_f and k_q values but no substituent effect observed on the absorption or emission spectra, we speculate that the 9-arylxanthyl fluorescent species may be different than the species being quenched. This may be due to the twisting of the 9-aryl ring out of planarity. A stucture in which the 9-aryl ring is twisted out of planarity may exhibit less conjugative effects from the 9-aryl ring on the cation.

Another possibility to explain the lack of substituent effect observed on the thioxanthyl cations is that structural changes, due to the presence of the sulfur atom, may result in a greater twisting of the 9-aryl ring out of planarity. Again, this twisting

out of planarity would decrease the conjugative interactions from the 9-aryl ring on the cation.

CHAPTER V

EXPERIMENTAL

Instrumentation

Melting points were taken on a Mel-Temp melting point apparatus and are uncorrected. UV and visible absorption spectra were measured on a Hewlett Packard 8452A Diode Array spectrophotometer. Fluorescence measurements were obtained on a Photon Technology International LS-100 spectrophotometer. NMR spectra were obtained on a Varian VXR300 instrument operating at 300Hz for ^{1}H and 75Hz for ^{13}C. ^{1}H NMR signals are reported in parts per million (δ) from TMS as an internal standard. ^{13}C NMR chemical shifts (δ) were reported in reference to the 77.0 ppm NMR peak for $CDCl_3$. GC analyses were conducted on a Hewlett-Packard 5890 Series II gas chromatograph equipped with an FID detector and a 25 m x 0.2 mm x 0.33 μm film thickness HP-1 polymethylsiloxane capillary column operated at 200 °C for 0 minutes and raised at 3 °C/min to 225 °C, and held there for 10 minutes. Injector and detector temperatures were held at 250 °C. HPLC analyses were obtained with a Beckman Model 334 Liquid Chromatograph equipped with a Beckman Model 210 injector under isocratic conditions with a flow rate of 1 mL/min using a Beckman ODS column (Ultrasphere, 5 μm packing, 4.6 mm x 25 cm) using 1:1 2% aqueous TEA:acetonitrile. A Beckman Model 153 variable wavelength detector was used for detection, monitored at 254 nm.

Fluorescence Measurements

Fluorescence quantum yields for both the 9-arylxanthyl **20a-f** and 9-arylthioxanthyl **21a-e** cations in dry acetonitrile were measured versus quinine sulfate monohydrate in 0.1 N H_2SO_4 (Φ_f=0.52) (Weber, 1957). Fluorescence lifetimes of **20a-e** and **21a-e** were measured in dry acetonitrile using a nanosecond flash lamp filled with nitrogen. Excitation of **20a-e** and **21a-e** was at 381 nm (N_2), and emission monitored at 540 nm for the xanthyl cations **20a-e** and 573 nm for the thioxanthyl cations **21a-e**, with a 350 nm cut-off filter placed before the emission monochromator to eliminate excitation and Raman scattering. All lifetimes measured were independent of cation concentration below $5.0x10^{-5}$M. The fluorescence lifetime of **20f** was estimated according to the method used by Boyd (1991) for weakly fluorescent compounds. The lifetime of **20f** was assumed to be proportional to its maximum fluorescence intensity and equal to the same proportion of **20e**. By measuring the fluorescence intensity of both compounds and the lifetime of **20e**, the lifetime of **20f** was calculated. An internal check of this method estimated the lifetime of **20c** to be 12.6 ns, relative to **20b**, and consistent with the measured value of **20c**. Steady state fluorescence emission was measured using a pulsed Xe lamp apparatus and the 350 nm cut-off filter previously described. Stern-Volmer quenching of the 9-arylxanthyl and 9-arylthioxanthyl cations in dry acetonitrile was conducted at a cation concentration of $5.0x10^{-5}$M. Quencher solutions in acetonitrile were prepared below the concentration that might permit ground state quenching to occur.

Solvents

All ^{1}H and ^{13}C NMR spectra were taken in $CDCl_3$ solvent obtained from Aldrich Chemical Company, unless otherwise specified. Anhydrous tetrahydrofuran used in Grignard syntheses was dried over calcium hydride and then freshly distilled. Arylbromides were obtained from Aldrich and distilled prior to use. Spectroscopic grade acetonitrile used in UV, steady state and fluorescence lifetime measurements was obtained from Mallinckrodt. Residual water was removed by passing the acetonitrile through a column of neutral aluminum oxide obtained from Aldrich. Propionic anhydride and fluoroboric acid used in the syntheses of xanthylium tetrafluoroborate salts were obtained from Aldrich and used as received. Alcoholic quenchers were obtained from Fisher and Aldrich and used without further purification. Water used as quencher was doubly distilled. Diethyl ether, isopropyl ether, *tert*-butyl methyl ether and *tert*-butyl ethyl ether (>99%) used as quenchers were obtained from Aldrich and distilled from sodium metal prior to use. Tetrahydrofuran (>99%) used as a quencher was obtained from Aldrich and distilled from CaH_2 prior to use. Isopropyl ether used in irradiation experiments was distilled from CaH_2 prior to use.

9-Phenylxanthen-9-ol (18a)

9-Phenylxanthen-9-ol was obtained from the Aldrich Chemical Company as an off-white solid. Recrystallization from 95% ethanol yielded white crystals, mp 158-161°C

(lit. mp 158.5-159 °C (Bunzly, 1904)).

Synthesis of 9-Arylxanthen-9-ols

A Grignard reagent was prepared from the appropriate arylbromide (5.8 mmol) and magnesium turnings (5.8 mmol) in anhydrous tetrahydrofuran (30mL). Recrystallized xanthone (5.0 mmol) was added and the mixture heated at reflux temperature until no more alcohol was being produced, determined by thin layer chromatography (1-4 hours). The mixture was quenched by the addition of aqueous ammonium chloride. The organic layer was washed with water and dried over anhydrous magnesium sulfate. After filtration, the solvent was removed by rotary evaporation yielding a yellow solid. The solid was identified as two components by thin layer chromatography, where methylene chloride was used as the eluant. One component corresponded to unreacted xanthone and was removed by column chromatography. The desired alcohol was obtained as an off-white solid. Recrystallization from 95% ethanol yielded a white solid.

9-(4'-Fluorophenyl)xanthen-9-ol (18b)

Yield 0.71g (49%); mp 152-154 °C; ^{1}H NMR 2.77 (s, 1H), 7.10-7.59 (m, 12H); ^{13}C NMR δ 163.18, 159.92, 149.62, 143.87, 143.83 129.22, 128.87, 128.00, 127.89, 126.95, 123.63, 116.50, 114.90, 114.61, 70.12; UV at 244 nm (ε =13,600), 290 nm (ε=4,300).

9-(3'-Fluorophenyl)xanthen-9-ol (18c)

Yield 0.21g (18%); mp 95-96 °C; ^{1}H NMR δ 2.77 (s, 1H), 7.10-7.96 (m, 12H); ^{13}C NMR δ 154.69, 151.17, 129.34, 129.28, 129.20, 129.18, 129.08, 128.86, 123.67, 123.44, 123.28, 122.51, 122.47, 116.54, 116.32, 113.41, 113.37, 113.09, 58.92; UV at 244 nm (ε =12,300), 290 nm (ε=5,100).

9-(4'-Methylphenyl)xanthen-9-ol (18d)

Yield 0.99g (69%); mp 146-148 °C (lit. mp 150 °C (Gomberg, 1909), lit. mp 141-142 °C (Gaffney, 1991)); ^{1}H NMR δ 2.28(s, 3H), 2.66 (s, 1H), 7.00-7.36 (m, 12H); UV at 226 nm (ε =28,000), 244 nm (ε=15,000), 290 nm (ε=4,900).

9-(3'-Methylphenyl)xanthen-9-ol (18e)

Yield 0.34g (24%); mp 144-146 °C (lit. mp 149 °C (Schonberg, 1947)); ^{1}H NMR δ 2.39 (s, 3H), 2.76 (s, 1H), 7.09-7.46 (m, 12H); UV at 244 nm (ε =13,000), 290 nm (ε=5,600).

9-(3'-Methoxyphenyl)xanthen-9-ol (18f)

Yield 0.57g (38%); mp 120-123 °C (lit. mp 112-113 °C (Hori, 1973)); ^{1}H NMR δ 3.81 (s, 3H), 2.85 (br, 1H), 6.73-7.45 (m, 12H); UV at 244 nm (ε =13,000), 282 nm (ε=5,900).

Synthesis of 9-Arylxanthylium Tetrafluoroborate Salts

The tetrafluoroborate salts were prepared following the method of Dauben, *et al.* (1960). The corresponding 9-arylxanthen-9-ol (1.7 mmol) was dissolved in propionic anhydride (34.9 mmol) at room temperature or slightly higher, where heat was provided by a warm water bath. This temperature was maintained as fluoroboric acid (3.8 mmol) was added to immediately yield a yellow solution. The xanthylium tetrafluoroborate salt was allowed to crystallize, whereafter, cold dry ethyl ether (5mL) was added to the solution and the supernatant discarded. This washing procedure was repeated five times to remove residual starting material. The precipitate was suction filtered and washed with cold, dry ethyl ether (10mL) to yield a bright yellow solid in every case except the *m*-OCH_3 cation salt which was dark orange.

9-Phenylxanthylium Tetrafluoroborate (20a)

Yield 0.46g (76%); mp 228 °C dec; ^{1}H NMR δ 7.75-8.52 (m, 13H); ^{13}C NMR δ 156.60, 143.80, 132.26, 131.72, 130.81, 130.57, 129.13, 123.93, 123.51, 120.18, 116.37; UV at 260 nm (ε=38,700), 372 nm (ε=29,400), and 446 nm (ε=4,900).

9-(4'-Fluorophenyl)xanthylium Tetrafluoroborate (20b)

Yield 0.14g (78%); mp 216°C dec; ^{1}H NMR δ 7.44-8.50 (m, 12H); ^{13}C NMR δ 159.28, 158.76, 143.83, 133.38, 133.26, 131.68, 129.28, 128.93, 128.05, 124.20, 123.89, 120.20, 117.05, 116.75, 116.56; UV at 260 nm (ε=42,300), 374 nm

(ε=36,200), and 450 nm (ε=5,600).

9-(3'-Fluorophenyl)xanthylium Tetrafluoroborate (20c)

Yield 0.06g (86%); mp 200 °C dec; ^{1}H NMR δ 7.04-8.49 (m, 12H); ^{13}C NMR (Acetone-d_6) δ 164.99, 161.74, 159.83, 145.79, 132.60, 130.60, 129.76, 128.67, 128.57, 127.41, 125.15, 124.29, 123.19, 120.77, 119.91, 119.63, 118.50, 118.18, 116.96; UV at 260 nm (ε=37,500), 376 nm (ε=27,500), and 448 nm (ε=3,900).

9-(4'-Methylphenyl)xanthylium Tetrafluoroborate (20d)

Yield 0.06g (100%); mp 200 °C dec; ^{1}H NMR δ 2.57 (s, 3H), 7.56-8.50 (m, 12H); ^{13}C NMR δ 158.53, 143.83, 143.76, 132.04, 131.96, 131.16, 130.02, 129.16, 128.07, 123.83, 120.22, 21.78; UV at 260 nm (ε=31,000), 370 nm (ε=25,000), and 454 nm (ε=6,300).

9-(3'-Methylphenyl)xanthylium Tetrafluoroborate (20e)

Yield 0.06g (43%), mp 185 °C dec; ^{1}H NMR δ 2.59 (s, 3H), 7.57-8.54 (m, 12H); ^{13}C NMR δ 158.61, 143.86, 139.40, 133.16, 131.84, 131.32, 130.95, 130.82, 129.15, 129.03, 127.65, 123.90, 120.22, 21.48; UV at 260 nm (ε=31,000), 370 nm (ε=25,000), and 454 nm (ε=6,300).

9-(3'-Methoxyphenyl)xanthylium Tetrafluoroborate (20f)

Yield 0.09g (50%); mp 204 °C dec; ^{1}H NMR δ 3.97 (s, 3H), 7.27-8.58 (m, 12H); ^{13}C NMR δ 159.89, 158.63, 143.78, 131.85, 130.23, 129.09, 128.92, 124.06, 123.55, 122.55, 120.11, 118.36, 115.72, 55.93; UV at 260 nm (ε=34,000), 372 nm (ε=29,000), and 452 nm (ε=4,400).

Synthesis of 9-Arylthioxanthen-9-ols

A Grignard reagent was prepared from the appropriate arylmagnesium bromide (8.7 mmol) and recrystallized thioxanthone (4.4 mmol) in anhydrous tetrahydrofuran. The reaction mixture was heated at reflux temperature for 1 h. Aqueous workup followed by purification with silica gel chromatography using methylene chloride as eluant, and subsequent recrystallization from 95% ethanol gave the pure 9-arylthioxanthenols as white solids.

9-Phenylthioxanthen-9-ol (19a)

Yield 0.50 g (39%); mp 103-107 °C (lit. mp 106 °C (Gomberg, 1910)); ^{1}H NMR δ 2.76 (s, 1H), 7.00-8.05 (m, 13H); UV at 200 nm (ε=50,900), 216 nm (ε=29,700), 268 nm (ε=11,000).

9-(4'-Fluorophenyl)thioxanthen-9-ol (19b)

Yield 23 mg (17%); mp 140-142 °C (lit. mp 141-142 °C (Ahn, 1982)); ^{1}H NMR δ 2.79 (s, 1H), 6.86-8.08 (m, 12H); UV at 200 nm (ε=48,500), 216 nm (ε=30,000), 266

nm (ε=13,000).

9-(3'-Fluorophenyl)thioxanthen-9-ol (19c)

Yield 53 mg (2.2%); mp 123-125 °C ^{1}H NMR δ 2.78 (s, 1H), 6.74-8.02 (m, 12H); ^{13}C NMR δ 164.09, 160.83, 146.21, 146.12, 139.29, 131.29, 129.49, 129.38, 127.55, 127.29, 126.60, 126.40, 126.11, 122.49, 114.78, 114.48, 114.20, 113.90, 73.37; UV at 200 nm (ε=44,600), 216 nm (ε=28,200), 266 nm (ε=12,000).

9-(4'-Methylphenyl)thioxanthen-9-ol (19d)

Yield 46 mg (7%); mp 161-163 °C (lit. mp 164-165 °C (Nagao, 1987)); ^{1}H NMR δ 2.29 (s, 3H), 2.81 (s, 1H), 6.88-8.11 (m, 12H); UV at 200 nm (ε=47,800), 216 nm (ε=26,600), 266 nm (ε=9,400).

9-(3'-Methylphenyl)thioxanthen-9-ol (19e)

Yield oil, 56 mg (8.4%); ^{1}H NMR δ 2.19 (s, 3H), 2.74 (s, 1H), 6.71-8.02 (m, 12H); ^{13}C NMR δ 143.38, 140.05, 137.74, 131.58, 128.63, 127.90, 127.56, 127.26, 126.66, 126.48, 126.17, 124.04, 53.32, 21.57.

9-Arylthioxanthylium Tetrafluoroborate Salts

Tetrafluoroborate salts **21a-e** were prepared following the method of Dauben, *et al.* (1960). The corresponding 9-arylthioxanthen-9-ol (0.1 mmol) was dissolved in

propionic anhydride (0.27 mL) at room temperature or slightly higher, where heat was provided by a warm water bath. This temperature was maintained upon the addition of fluoboric acid (19 mg, 0.22 mmol), which immediately gave a red solution. The thioxanthylium tetrafluoroborate salt precipitated and was collected by suction filtration. The salts were washed repeatedly with cold, anhydrous diethyl ether to yield a bright red solid in every case.

9-Phenylthioxanthylium Tetrafluoroborate (21a)

Yield 10 mg (27%); mp 194-196 °C dec; ^{1}H NMR δ 7.00-8.88 (m, 13H); ^{13}C NMR δ 170.72, 146.60, 137.56, 135.40, 134.40, 131.13, 130.98, 130.21, 129.56, 129.07, 128.23; UV at 192 nm (ε=42,000), 218 nm (ε=22,500), 246 nm (ε=14,000), 278 nm (ε=39,700), 384 nm (ε=17,400), and 494 nm (ε=5,600).

9-(4'-Fluorophenyl)thioxanthylium Tetrafluoroborate (21b)

Yield 48 mg (49%); mp 218-220°C dec; ^{1}H NMR δ 6.88-9.09 (m, 12H); ^{13}C NMR δ 141.72, 138.72, 138.53, 133.08, 132.3, 132.15, 130.02, 129.91, 128.16, 127.39, 127.35, 127.25,116.95, 115.16, 114.88; UV at 194 nm (ε=43,400), 220 nm (ε=22,400), 246 nm (ε=12,400), 278 nm (ε=38,900), 384 nm (ε=18,100), and 496 nm (ε=4,800).

9-(3'-Fluorophenyl)thioxanthylium Tetrafluoroborate (21c)

Yield 9.9 mg (17%); mp 208-210 °C dec; ^{1}H NMR δ 7.28-8.88 (m, 12H); ^{13}C NMR

δ 164.07, 160.74, 148.79, 137.37, 136.17, 136.07, 134.87, 131.16, 131.03, 130.92, 129.97, 128.20, 126.63, 125.54, 125.49, 118.10, 117.82, 117.04, 116.72; UV at 192 nm (ε=43,400), 220 nm (ε=18,500), 246 nm (ε=10,000), 280 nm (ε=40,200), 386 nm (ε=12,400), and 494 nm (ε=3,800).

9-(4'-Methylphenyl)thioxanthylium Tetrafluoroborate (21d)

Yield 11 mg (49%); mp 134-136 °C dec; ^{1}H NMR δ 2.63 (s, 3H), 7.30-8.86 (m, 12H); ^{13}C NMR δ 141.72, 138.72, 138.53, 133.08, 132.30, 132.15, 130.02, 129.91, 128.16, 127.39, 127.35, 127.25, 116.95, 115.16, 114.88; UV at 200 nm (ε=49,800), 180 nm (ε=25,400), 246 nm (ε=11,800), 282 nm (ε=38,900), 382 nm (ε=11,800), and 496 nm (ε=5,200).

9-(3'-Methylphenyl)thioxanthylium Tetrafluoroborate (21e)

Yield 0.10 g (12%), mp 173-175 °C dec; ^{1}H NMR δ 2.57 (s, 3H), 7.29-8.88 (m, 12H); ^{13}C NMR δ 171.02, 148.54, 139.15, 137.48, 135.47, 134.37, 131.70, 131.02, 130.18, 129.95, 128.89, 128.23, 126.75, 21.50; UV at 198 nm (ε=43,600), 218 nm (ε=23,200), 248 nm (ε=10,600), 282 nm (ε=39,000), 378 nm (ε=10,200), and 494 nm (ε=3,900).

Preparative Irradiations (GC Analysis)

Irradiations were performed in a Rayonet reactor equipped with fifteen 350-nm lamps (RPR 3500). A merry-go-round apparatus was used to insure even irradiation of

multiple samples. After irradiation, the samples were rotary evaporated to dryness. To each sample, acetonitrile (0.5 mL) and MeOH (2 drops) were added to quench any unreacted cation, followed by GC analysis.

Irradiation of 9-Phenylxanthen-9-ol (18a) in the Absence and Presence of *i*-Pr_2O

A solution of 9-phenylxanthen-9-ol in acetonitrile (0.001 M) was purged with argon for 30 minutes. The sample was divided and diisopropyl ether (1 M) was added to one of these alcohol solutions and both were irradiated for 10 minutes in quartz tubes. Identical "dark" irradiations were performed simultaneously by wrapping tubes in aluminum foil.

Irradiation of Xanthone (24) in the Absence and Presence of *i*-Pr_2O

A solution of xanthone in acetonitrile (0.001 M) was purged with argon for 30 minutes. The sample was divided and diisopropyl ether (1 M) was added to one of the xanthone solutions and both were irradiated for 10 minutes in quartz tubes. Identical "dark" irradiations were performed simultaneously.

Irradiation of 9-Phenylxanthylium Tetrafluoroborate (20a)

A solution of 9-phenylxanthylium tetrafluoroborate in acetonitrile (0.0024 M) was purged with argon for 30 minutes. The sample was placed in a quartz vessel equipped with a cold finger apparatus and irradiated for 10 minutes. Identical "dark"

irradiations were performed simultaneously.

Irradiation of 9-Phenylxanthylium Tetrafluoroborate (20a) in the Presence of *i*-Pr_2O A solution of 9-phenylxanthylium tetrafluoroborate in acetonitrile (0.0024 M) was purged with argon for 30 minutes. The sample was placed in a quartz vessel equipped with a cold finger apparatus along with diisopropyl ether (25 mL) and irradiated for 10 minutes. The products of this irradiation were separated by column chromatography and identified by spectroscopic methods. Identical "dark" irradiations were performed simultaneously.

2-(o-Hydroxyphenoxy)benzophenone (25)

Prepared as described in the literature (Quint, 1931): yield 0.011 g (66%); mp 196-198 °C (lit. mp 104 °C (Quint, 1931) and 103-104 °C (Glover, 1984)); ^{1}H NMR δ 6.88-800 (m, 13H), 8.16 (s,1H); ^{13}C NMR δ 196.88, 156.65, 149.29, 142.98, 136.77, 133.86, 132.68, 130.56, 128.78, 128.55, 126.32, 122.56, 122.32, 119.62, 117.61; UV at 204 nm (ε=48,000), 252 nm (ε=9,900), and 276 nm (ε=7,9400).

9-Phenylxanthene (24)

Prepared as described in the literature (Ullmann, 1904): yield 0.12g (13%); mp 137-139 °C (lit. mp 145 °C (Ullmann, 1904) and 148-150 °C (Glover, 1984)); ^{1}H NMR δ 5.28 (s, 1H), 7.00-7.30 (m, 13H); UV at 202 nm (ε=44,000), 248 nm (ε=8,300), and

282 nm (ε=3,300).

9-Hydroperoxy-9-phenylxanthene (22)

Prepared as described in the literature(Glover, 1984): yield 0.39 g (30%); double mp 126-127 and 225-226 °C (lit. double mp 134 and 208 °C (Glover, 1984)); ^{1}H NMR δ 7.10-7.40 (m, 13H), 7.43 (s, 1H, OOH); UV at 204 nm (ε=46,000), 244 nm (ε=16,000), and 292 nm (ε=5,600).

Di-(9-phenylxanthen-9-yl) Peroxide (23)

Prepared as described in the literature (Glover, 1984): yield 18 mg (77%); mp 214-215 °C turns brown and 222-223 liquid °C dec. (lit. mp 212-214 °C (Glover, 1984), 232 °C (Wan, 1993), 215-219 °C (Gomberg, 1909) and 230 °C (Schönberg, 1945)); ^{1}H NMR δ 6.72-7.30 (m, 26H).

9-Methoxy-9-phenylxanthene (28)

Prepared as described in the literature (Llama, 1989): yield 12 mg (47%); mp 90-92 °C (lit. mp 142-144 °C (Llama, 1989)); ^{1}H NMR δ 2.95 (s, 3H), 7.05-7.41 (m, 13H); ^{13}C NMR δ 151.54, 148.97, 129.53, 129.00, 127.78, 126.50, 126.44, 123.42, 123.04, 116.18, 75.91, 51.03; UV at 202 nm (ε=44,000), 244 nm (ε=14,000), and 290 nm (ε=5,300).

Quantitative Irradiations (HPLC Analysis)

Irradiations were performed in a Rayonet reactor equipped with fifteen 350-nm lamps (RPR 3500). Irradiations took place at 4 °C. A merry-go-round apparatus was used to insure even irradiation of multiple samples. Irradiations were done to quantify the amount of photoproducts present in the reaction mixture. Photoproduct **22** was not stable for GC analysis and therefore analyzed by HPLC. Standard solutions of each photoproduct were prepared to determine the yields of the photoproducts for the irradiation. The irradiated samples and the standard solutions were analyzed by HPLC. The integrated areas for the standards containing a known amount of photoproduct were compared to the integrated areas of the photoproducts.

Irradiation of 9-Phenylxanthylium Tetrafluoroborate (20a)

A solution of 9-phenylxanthylium tetrafluoroborate in acetonitrile (.001 M) was purged with O_2 for 30 minutes. To 4 small quartz tubes, 8 mL of the cation solution was added. The total time of irradiation varied, with one tube removed from the merry-go-round apparatus every ten minutes. After irradiation, the samples were rotary evaporated to dryness. To each sample, 0.8 mL of acetonitrile and 0.6 mL of methanol were added, followed by HPLC analysis.

Irradiation of 9-Phenylxanthylium Tetrafluoroborate (20a) in the Presence of *i*-Pr_2O

A solution of 9-phenylxanthylium tetrafluoroborate in acetonitrile (.001 M) was purged

with O_2 for 30 minutes. To 4 small quartz tubes, 8 mL of the cation solution was added along with 1.13 mL of *i*-Pr_2O. The total time of irradiation varied, with one tube removed from the merry-go-round apparatus every ten minutes. After irradiation, the samples were rotary evaporated to dryness. To each sample, 0.8 mL of acetonitrile and 0.6 mL of methanol were added, followed by HPLC analysis.

Irradiation of 9-Phenylxanthylium Tetrafluoroborate (20a) in the Presence of *i*-Pr_2O

A solution of 9-phenylxanthylium tetrafluoroborate in acetonitrile (.001 M) was purged with argon for 30 minutes. To 4 small quartz tubes, 8 mL of the cation solution was added along with 1.13 mL of *i*-Pr_2O. The total time of irradiation varied, with one tube removed from the merry-go-round apparatus every ten minutes. After irradiation, the samples were rotary evaporated to dryness. To each sample, 0.8 mL of acetonitrile and 0.6 mL of methanol were added, followed by HPLC analysis.

Irradiation of 9-Hydroperoxy-9-phenylxanthene (22)

A solution of 9-hydroperoxy-9-phenylxanthene in acetonitrile (.001 M) was purged with O_2 for 30 minutes. To 4 small quartz tubes, 8 mL of the hydroperoxide solution was added. The total time of irradiation varied, with one tube removed from the merry-go-round apparatus every five minutes. After irradiation, the samples were rotary evaporated to dryness. To each sample, 0.8 mL of acetonitrile and 0.6 mL of methanol were added, followed by HPLC analysis.

Irradiation of 9-Hydroperoxy-9-phenylxanthene (22) in the Presence of Acid

A solution of 9-hydroperoxy-9-phenylxanthene in acetonitrile (.001 M) was purged with O_2 for 30 minutes. To 4 small quartz tubes, 8 mL of the hydroperoxide solution was added along with 72 μL of a 1.87% (w/w) H_2SO_4 solution. The total time of irradiation varied, with one tube removed from the merry-go-round apparatus every five minutes. After irradiation, the samples were rotary evaporated to dryness. To each sample, 0.8 mL of acetonitrile and 0.6 mL of methanol were added, followed by HPLC analysis.

SPECTRA

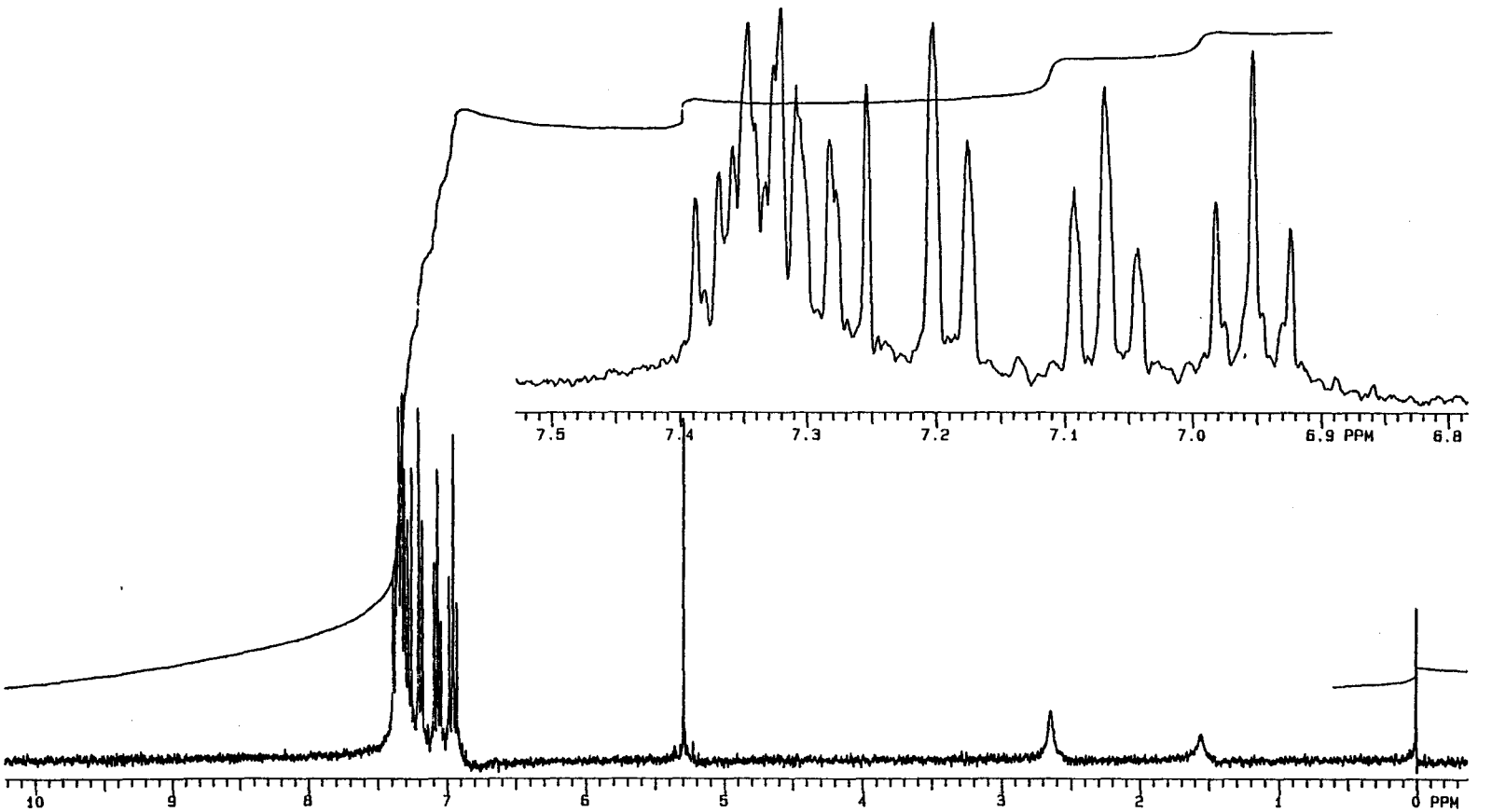

^{1}H NMR of 9-(4-fluorophenyl)xanthen-9-ol, **(18b)**

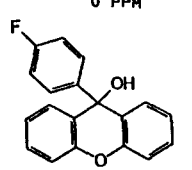

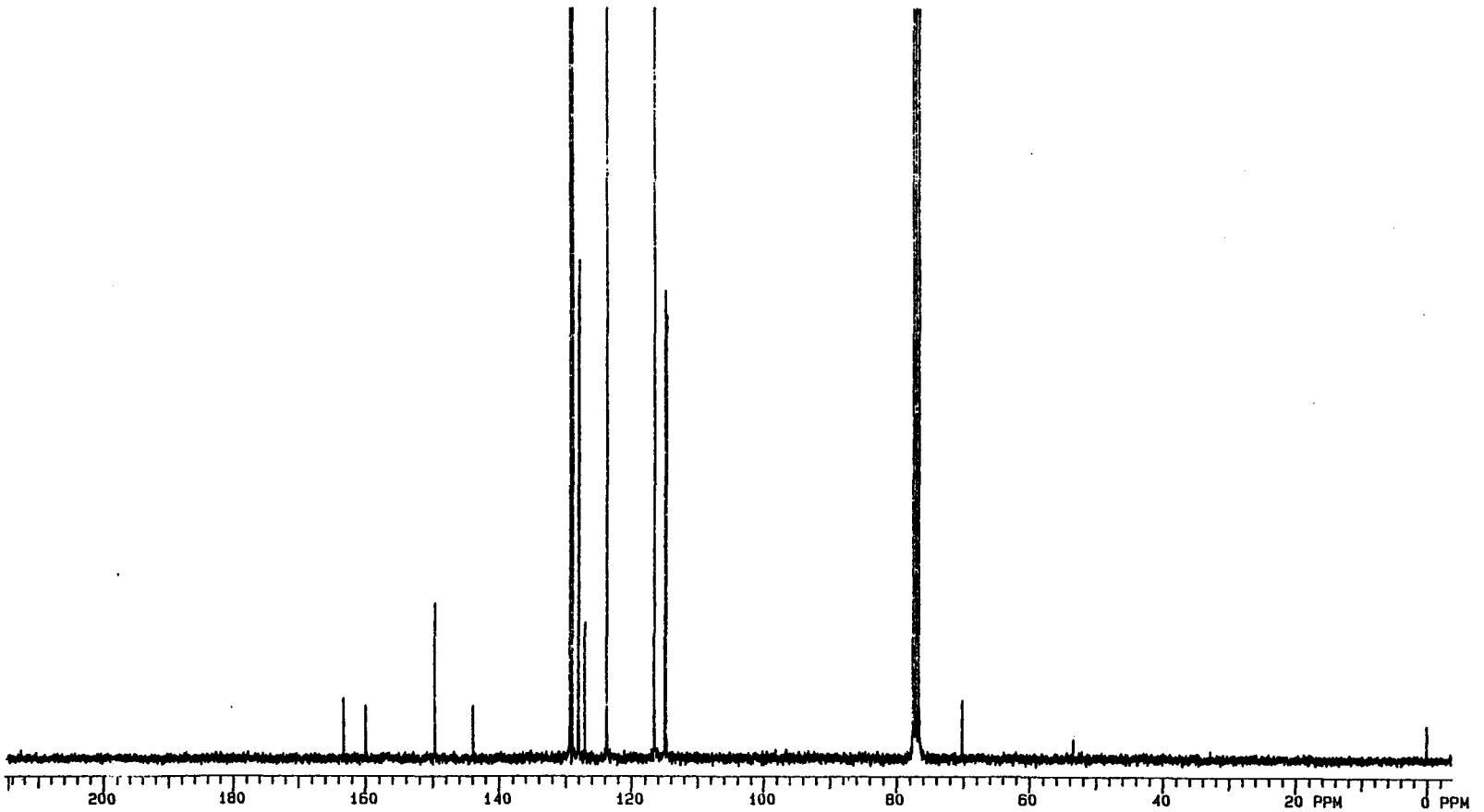

^{13}C NMR of 9-(4-fluorophenyl)xanthen-9-ol, (**18b**)

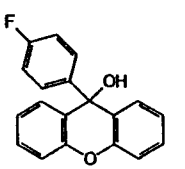

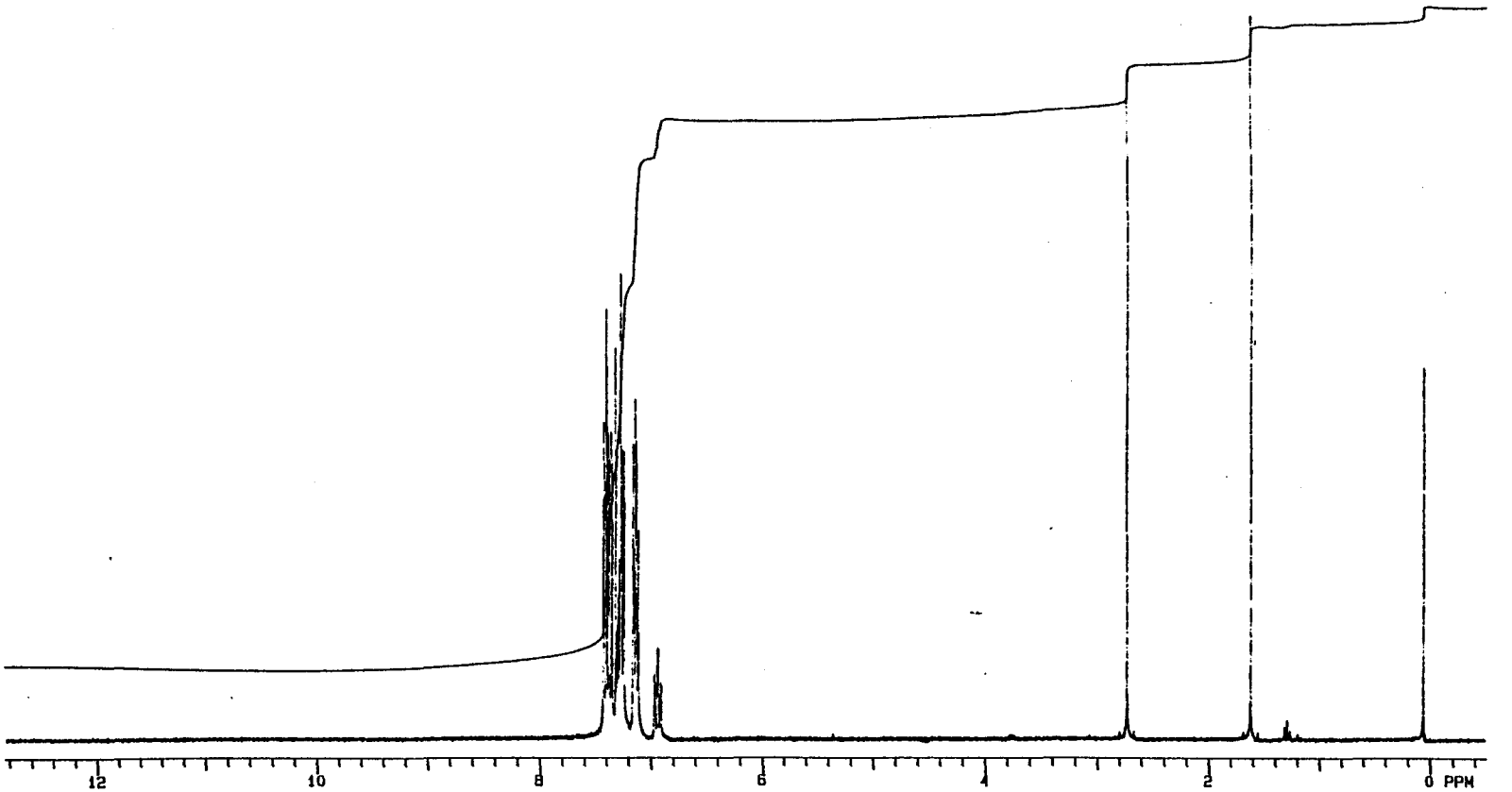

^{1}H NMR of 9-(3-fluorophenyl)xanthen-9-ol, (18c)

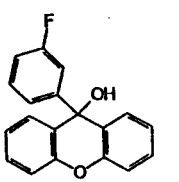

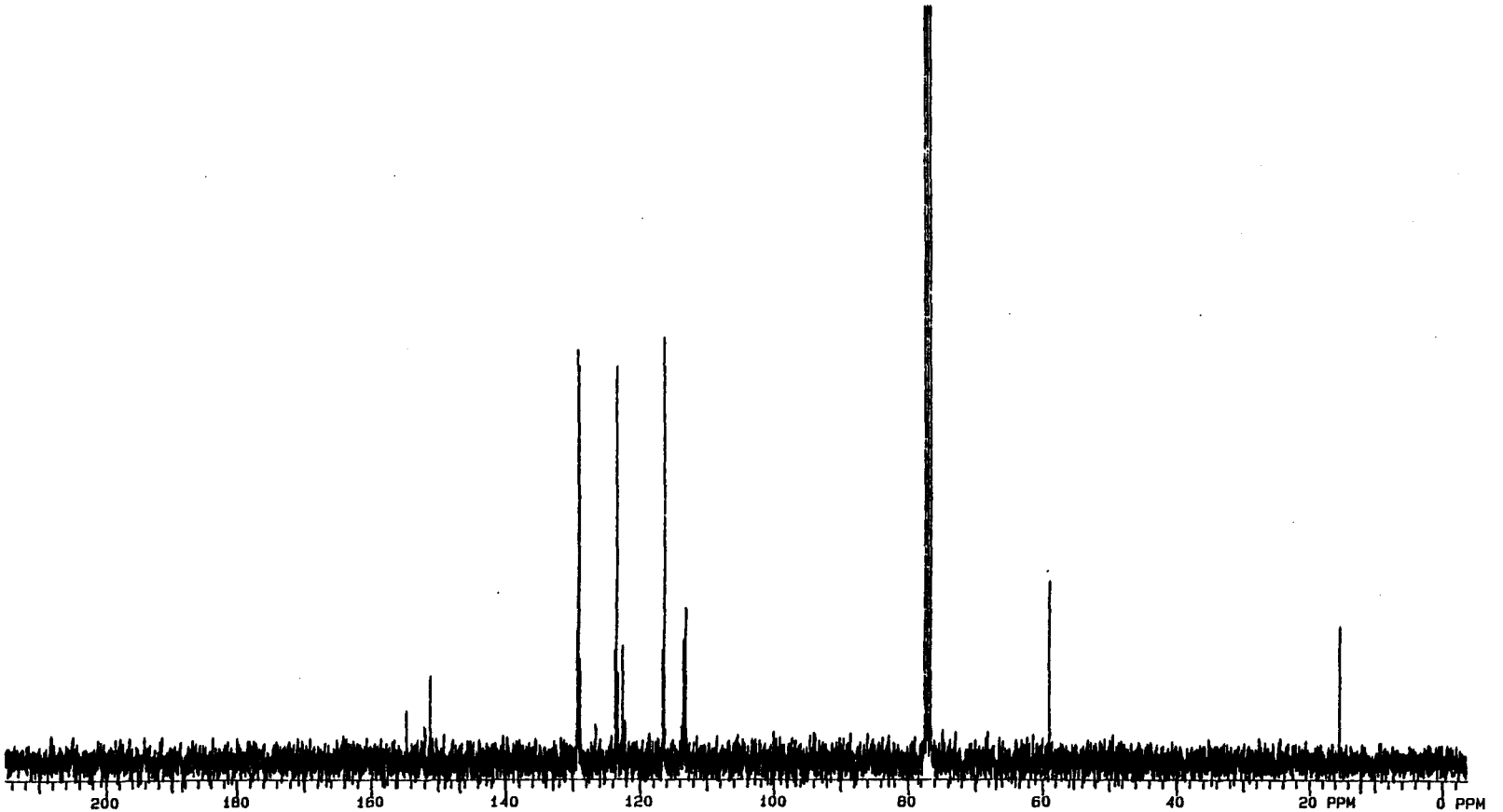

^{13}C NMR of 9-(3-fluorophenyl)xanthen-9-ol, (18c)

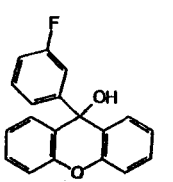

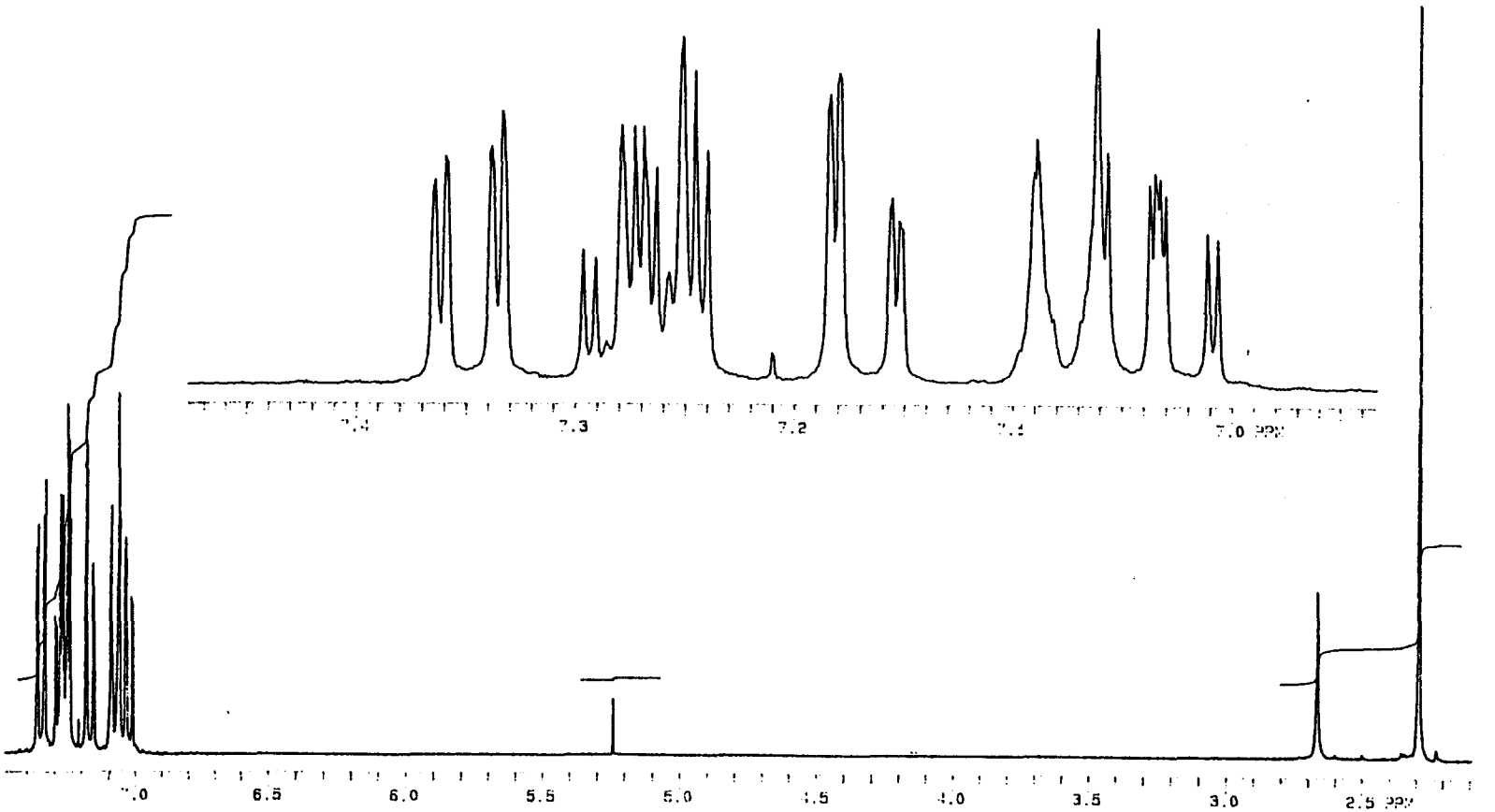

^{1}H NMR of 9-(4-methylphenyl)xanthen-9-ol, (18d)

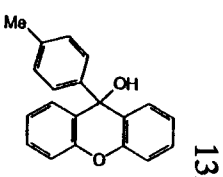

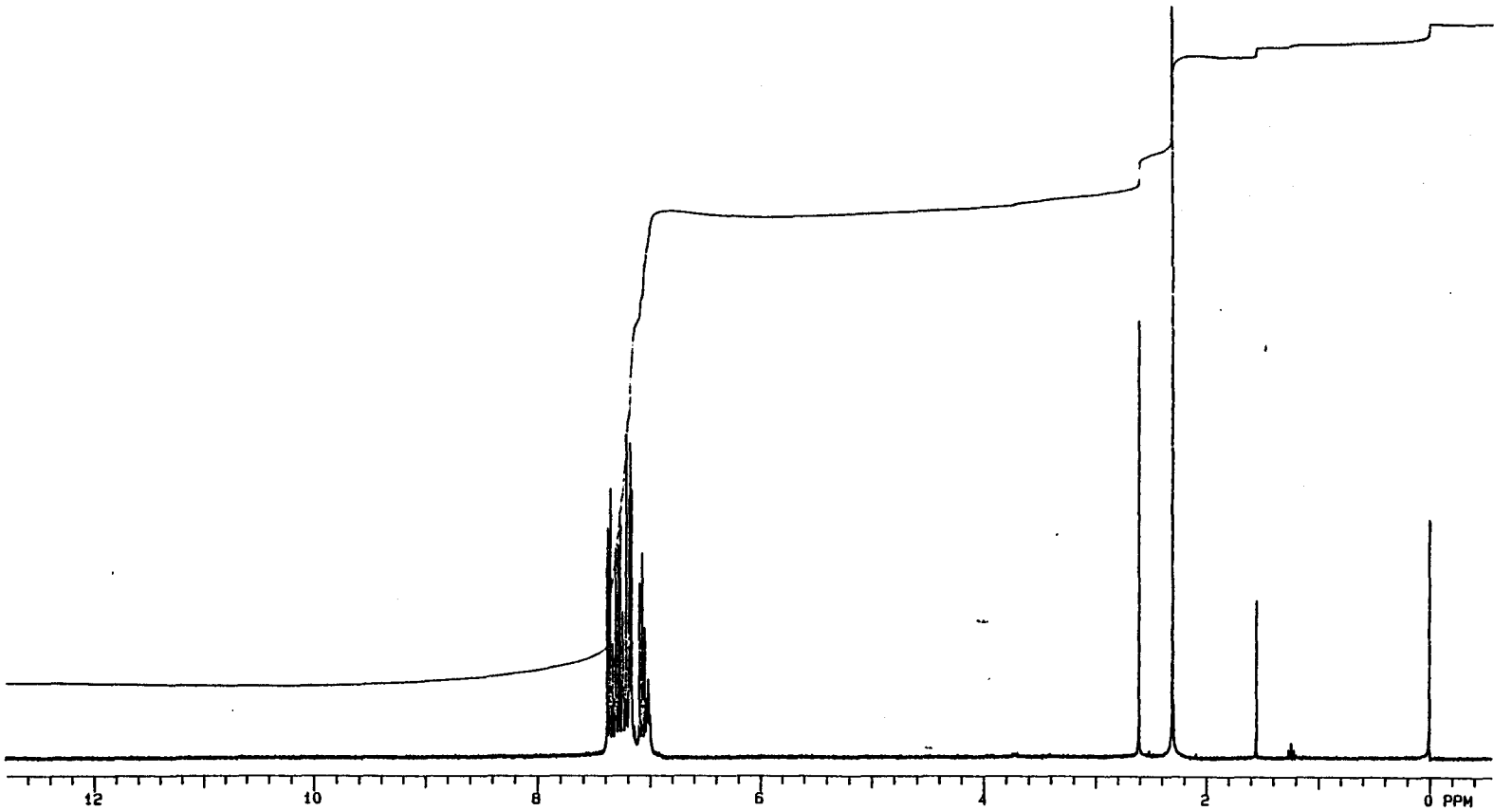

^{1}H NMR of 9-(3-methylphenyl)xanthen-9-ol, (18e)

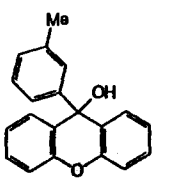

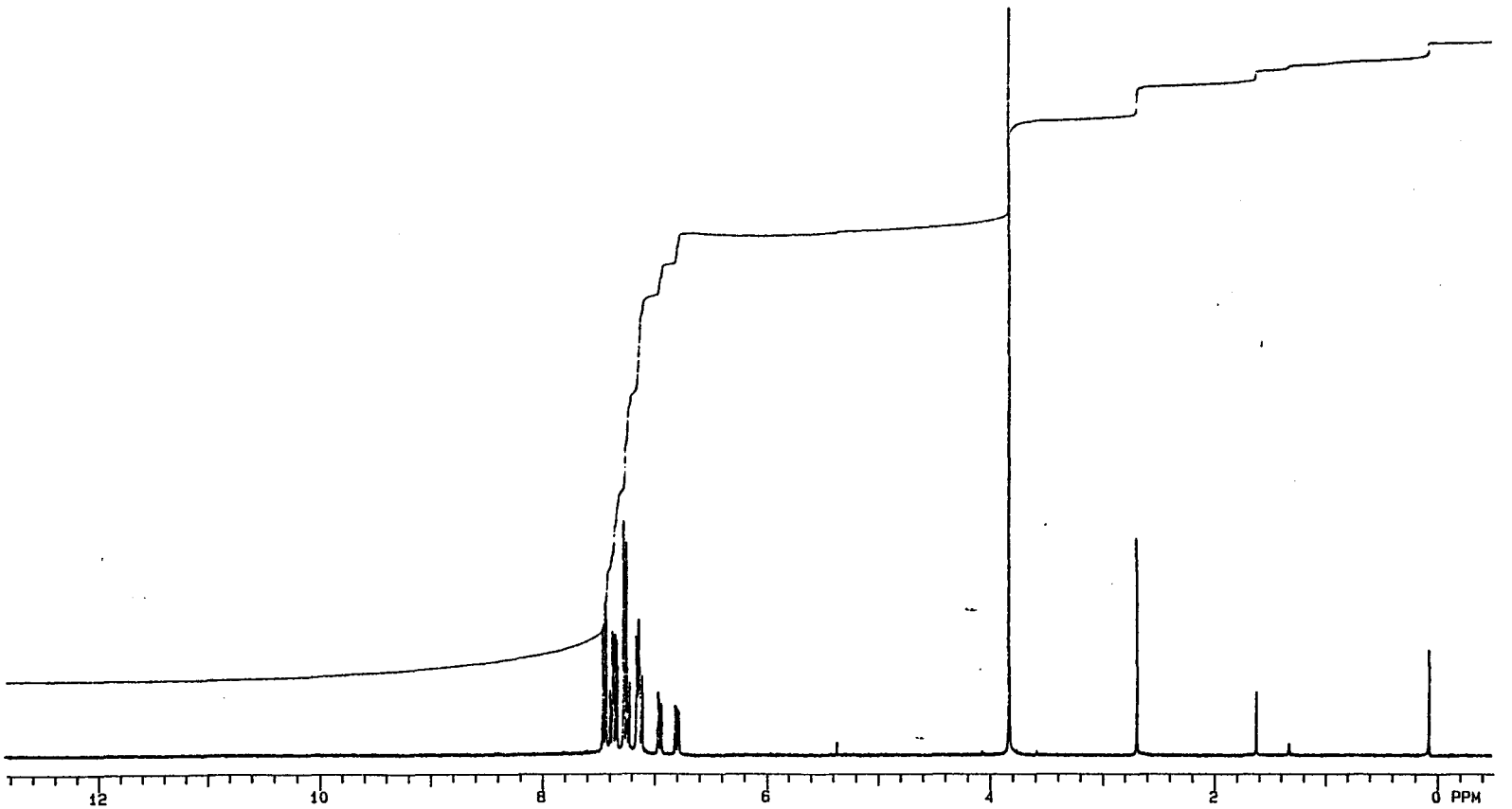

^{1}H NMR of 9-(3-methoxyphenyl)xanthen-9-ol, (18f)

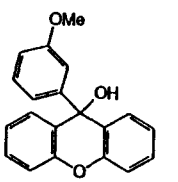

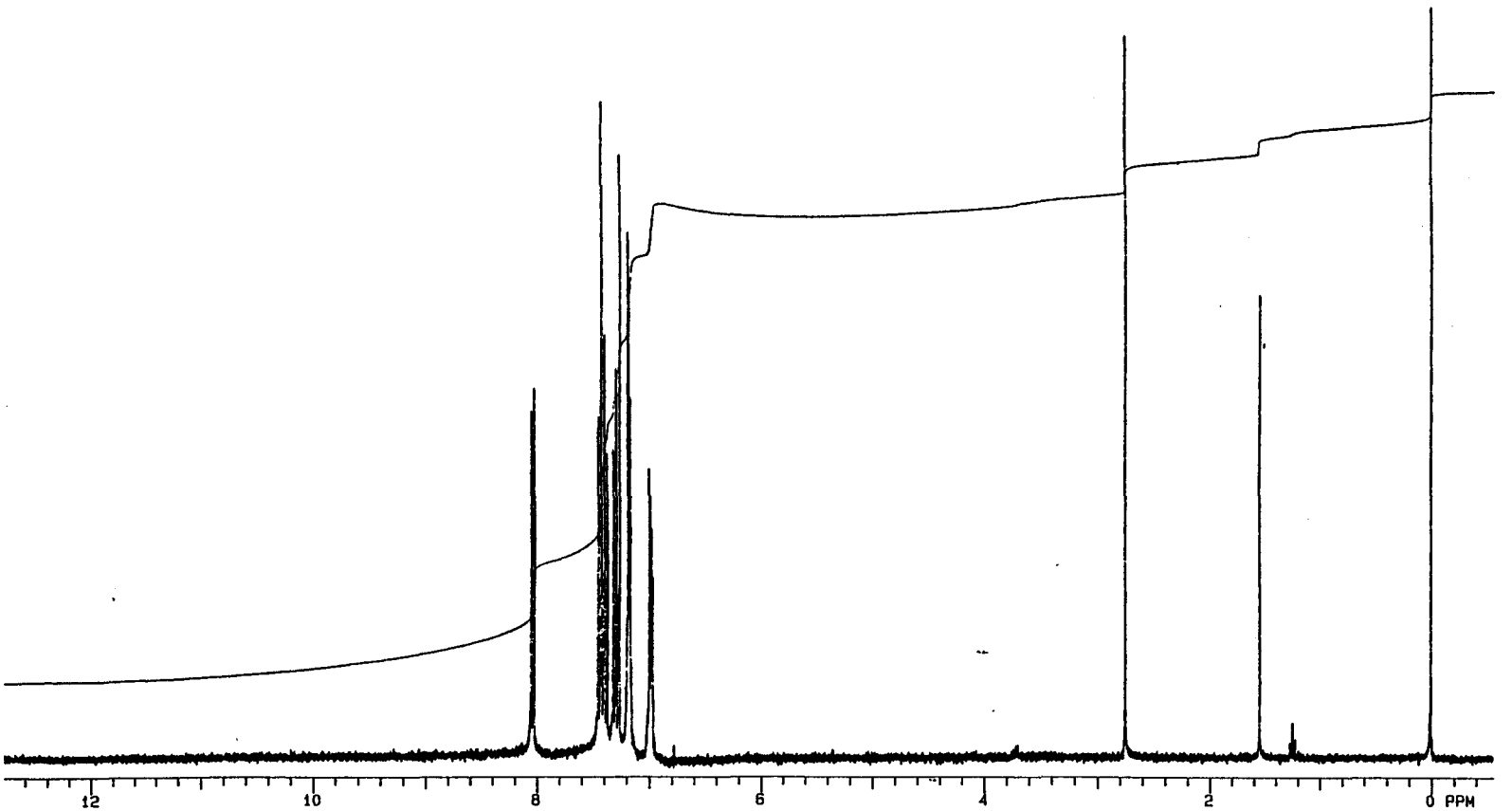

^{1}H NMR of 9-phenylthioxanthen-9-ol, (19a)

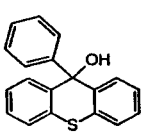

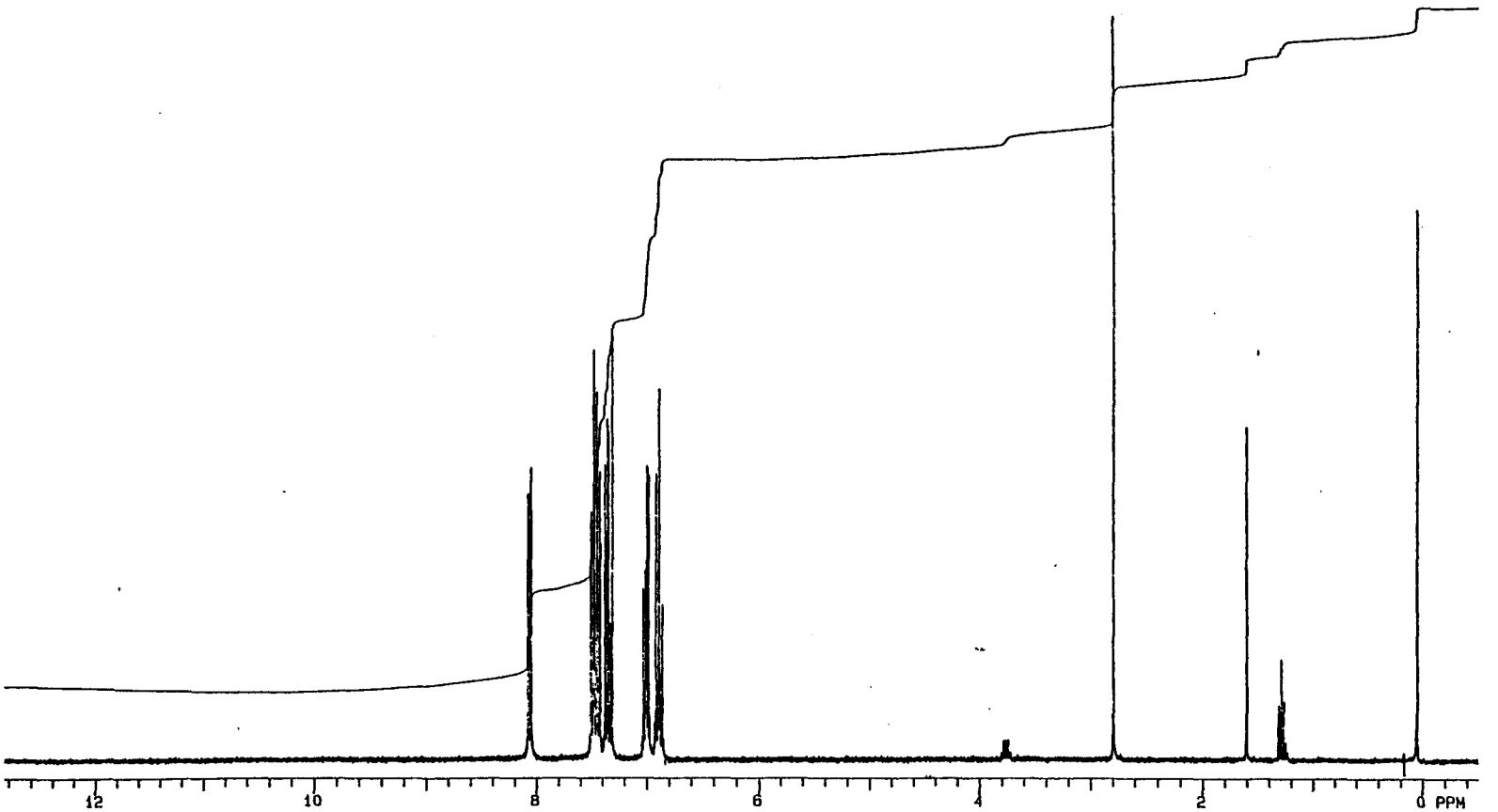

^{1}H NMR of 9-(4-fluorophenyl)thioxanthen-9-ol, (19b)

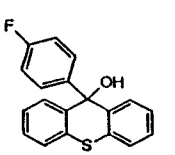

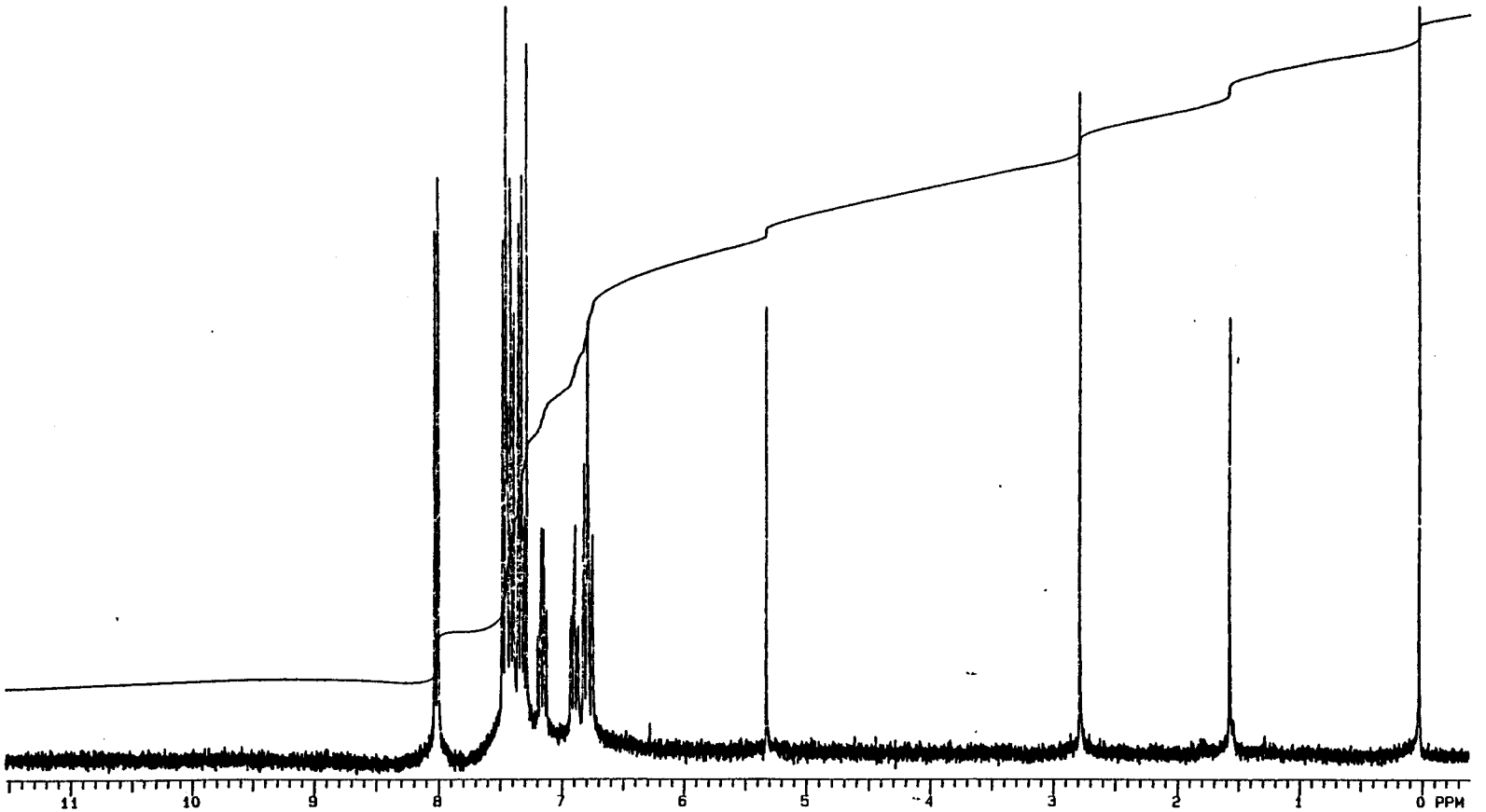

^{1}H NMR of 9-(3-fluorophenyl)thioxanthen-9-ol, **(19c)**

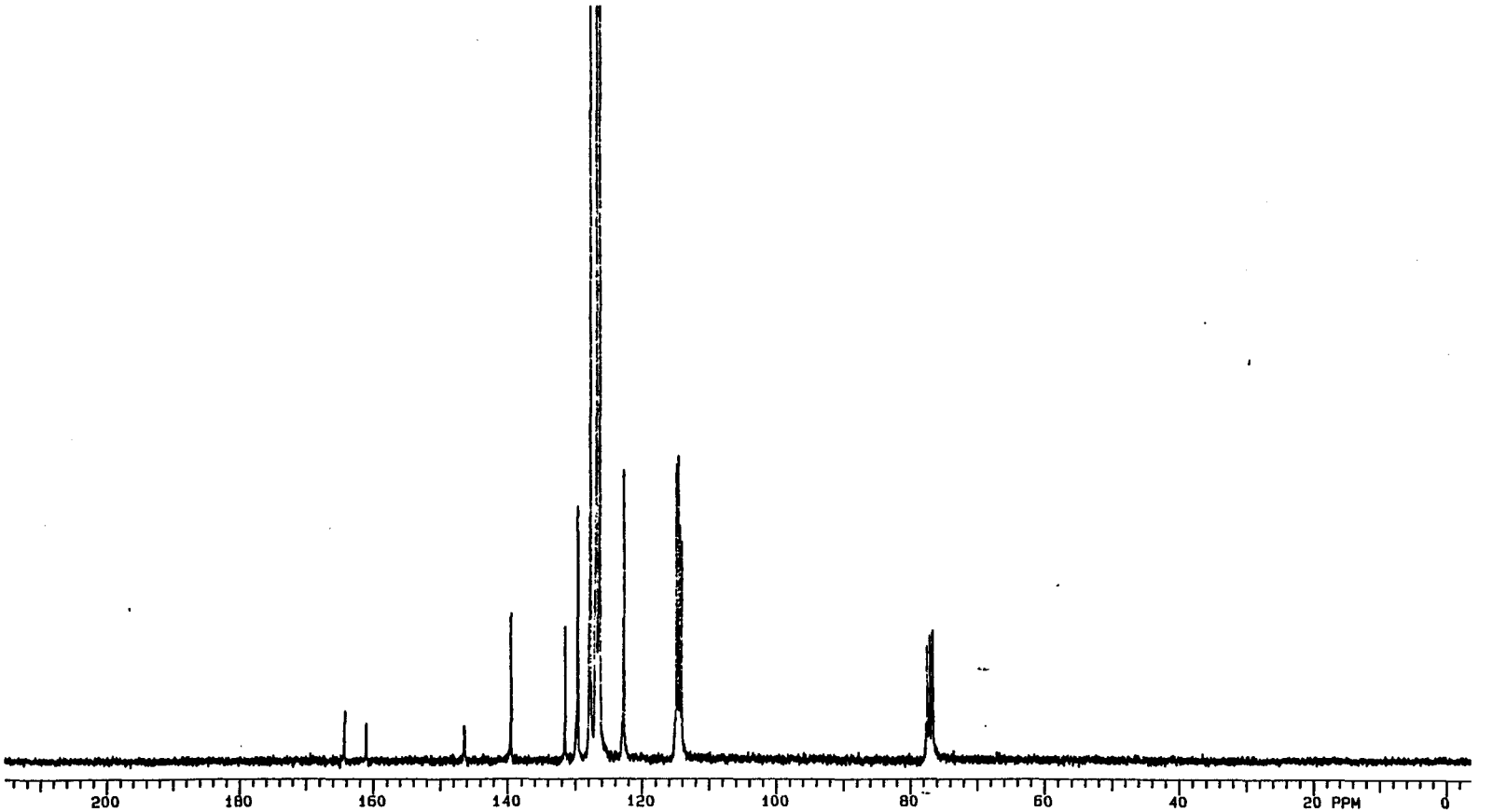

^{13}C NMR of 9-(3-fluorophenyl)thioxanthen-9-ol, (19c)

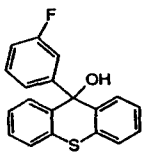

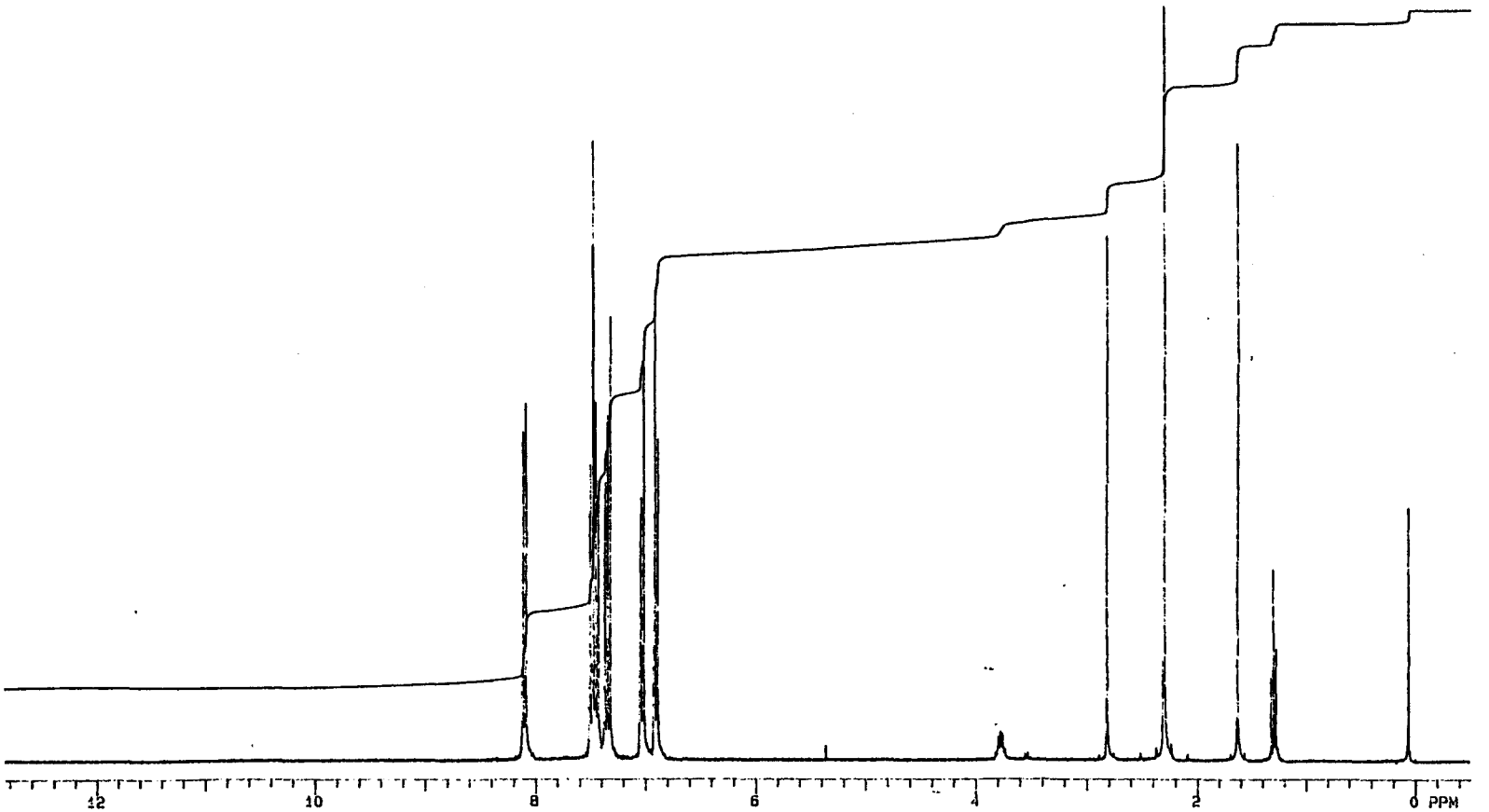

^{1}H NMR of 9-(4-methylphenyl)thioxanthen-9-ol, **(19d)**

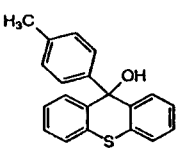

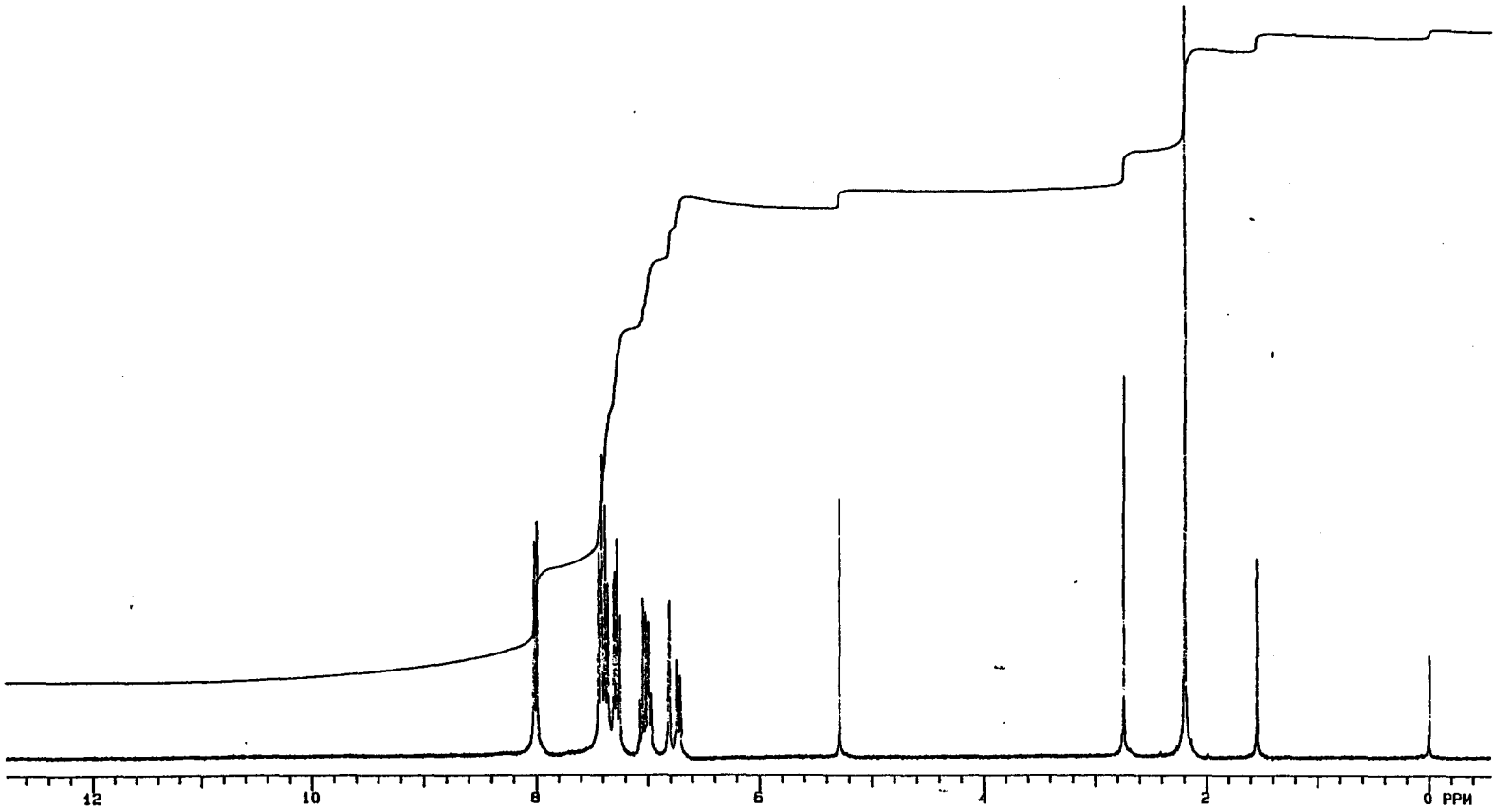

^{1}H NMR of 9-(3-methylphenyl)thioxanthen-9-ol, (19e)

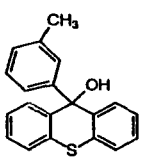

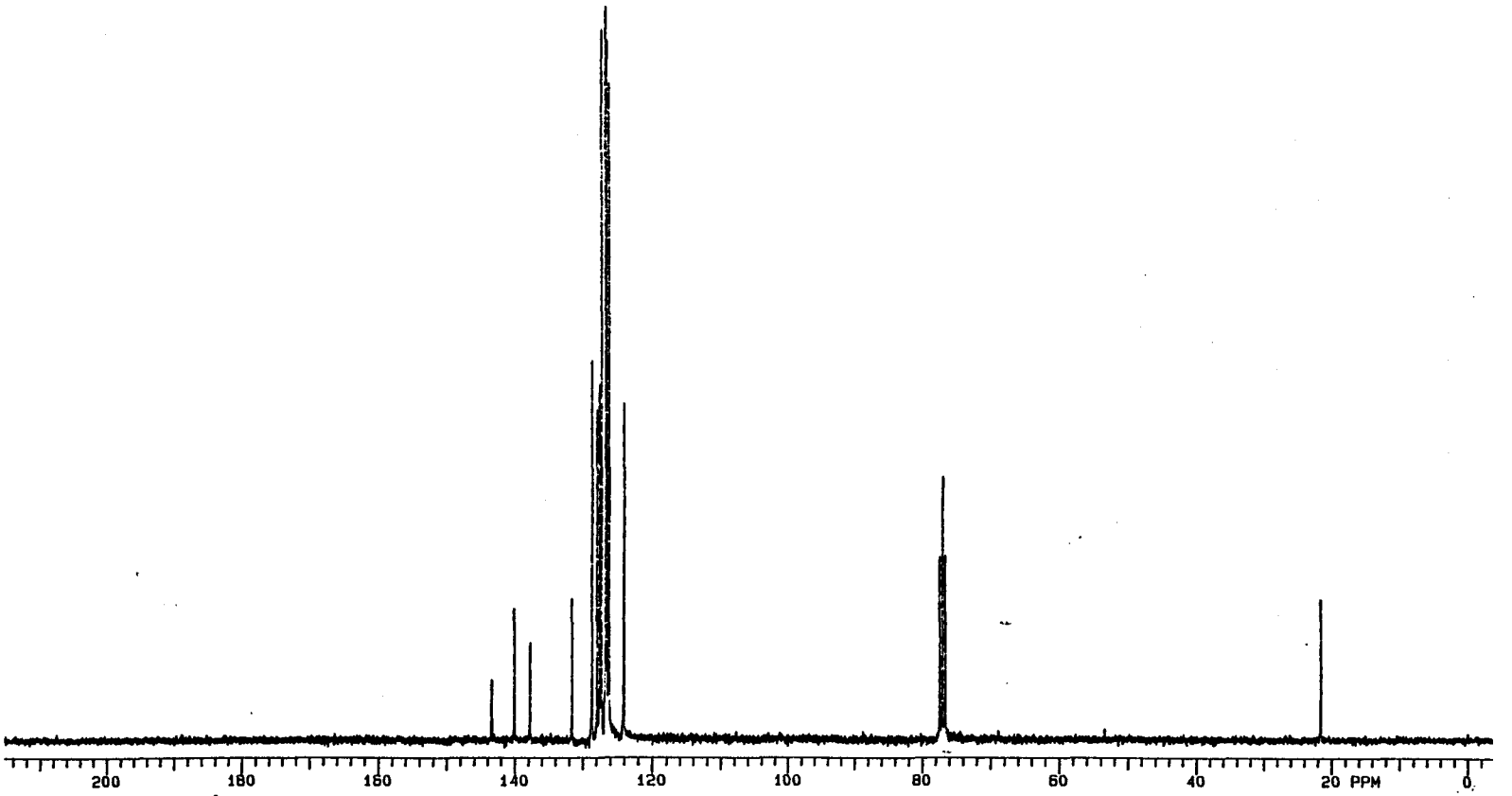

^{13}C NMR of 9-(3-methylphenyl)thioxanthen-9-ol, (19e)

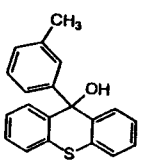

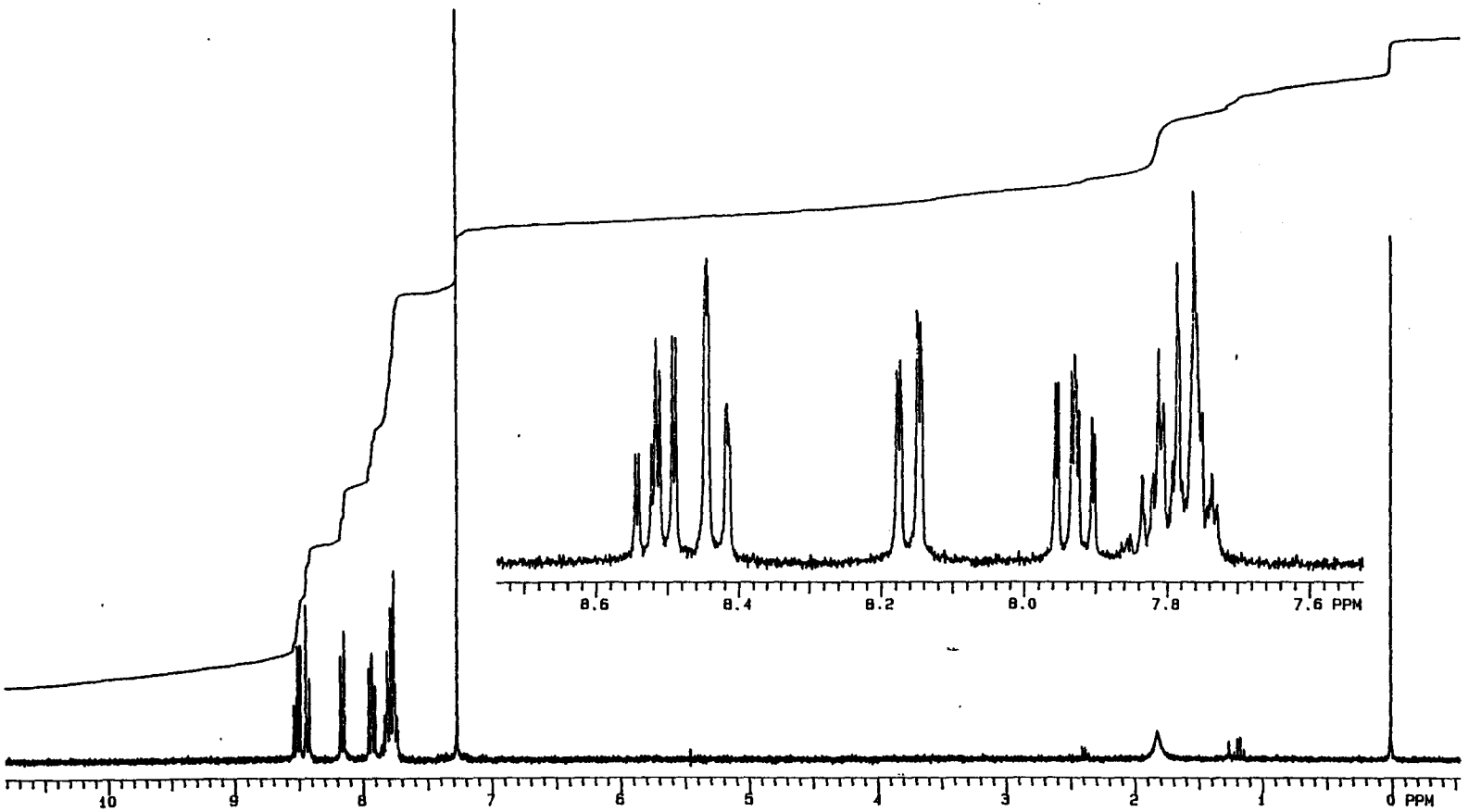

^{1}H NMR of 9-phenylxanthylium tetrafluoroborate, (**20a**)

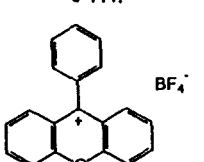

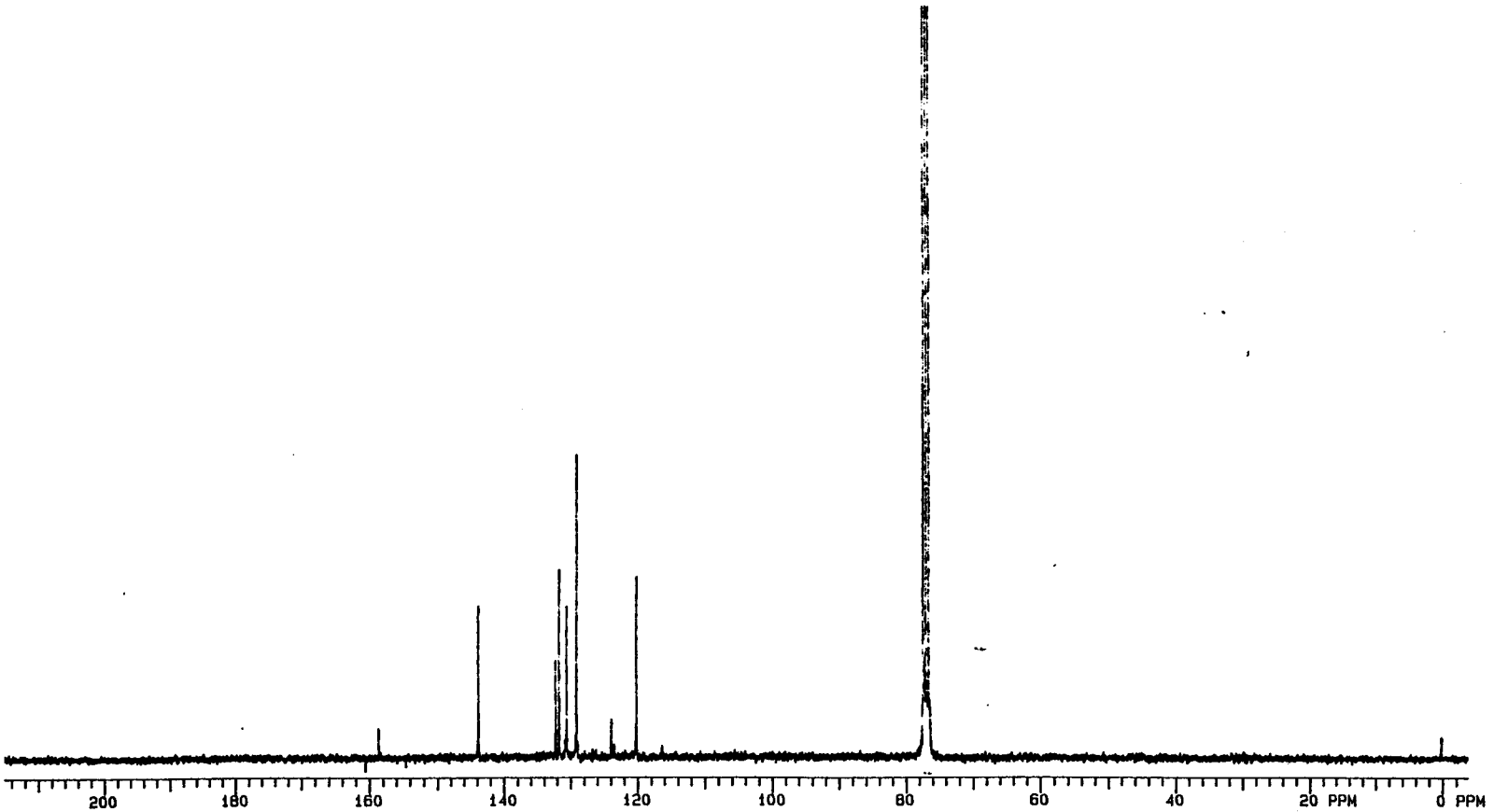

^{13}C NMR of 9-phenylxanthylium tetrafluoroborate, (20a)

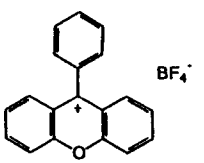

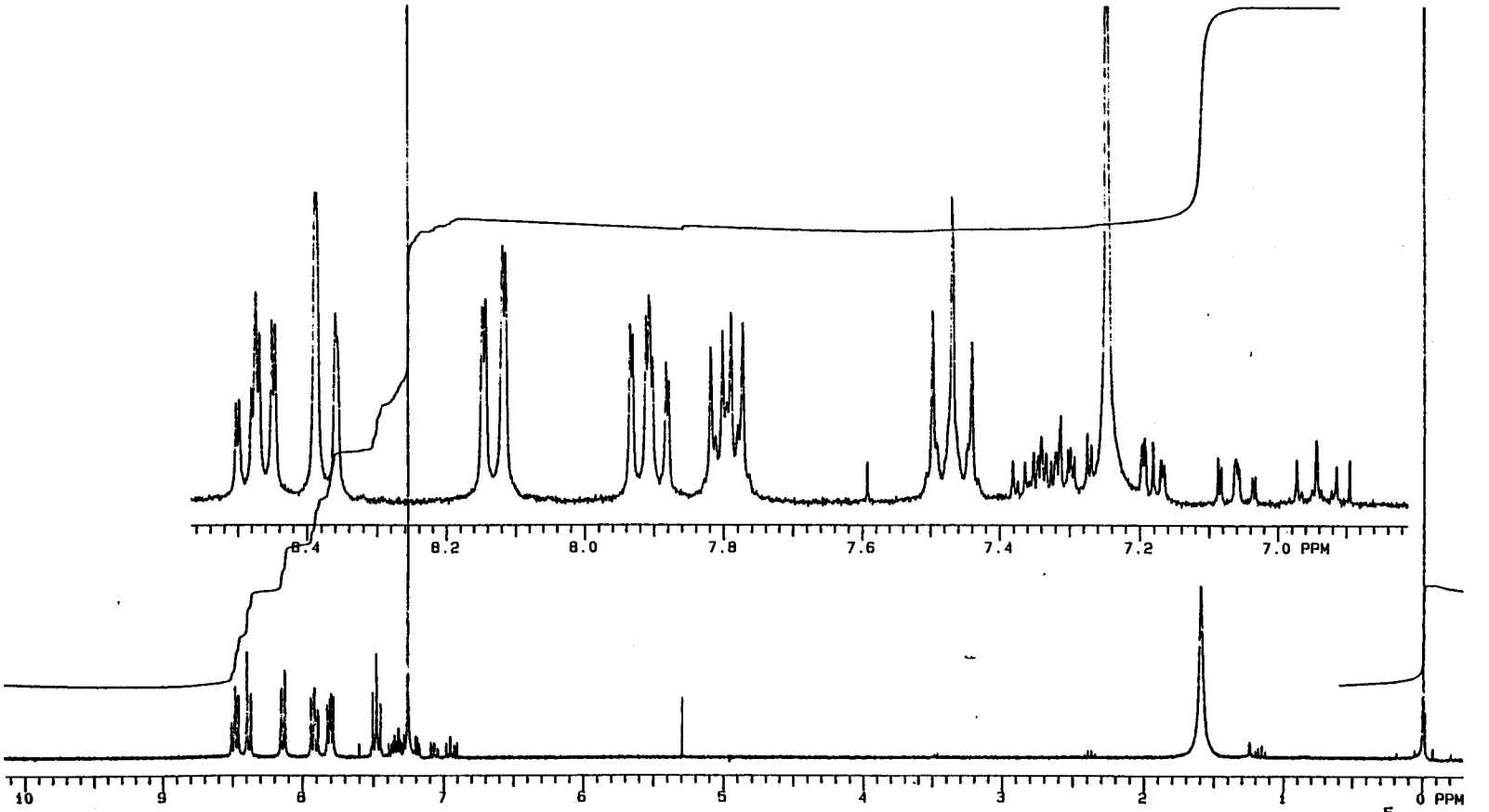

^{1}H NMR of 9-(4-fluorophenyl)xanthylium tetrafluoroborate, (20b)

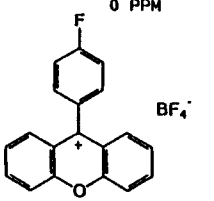

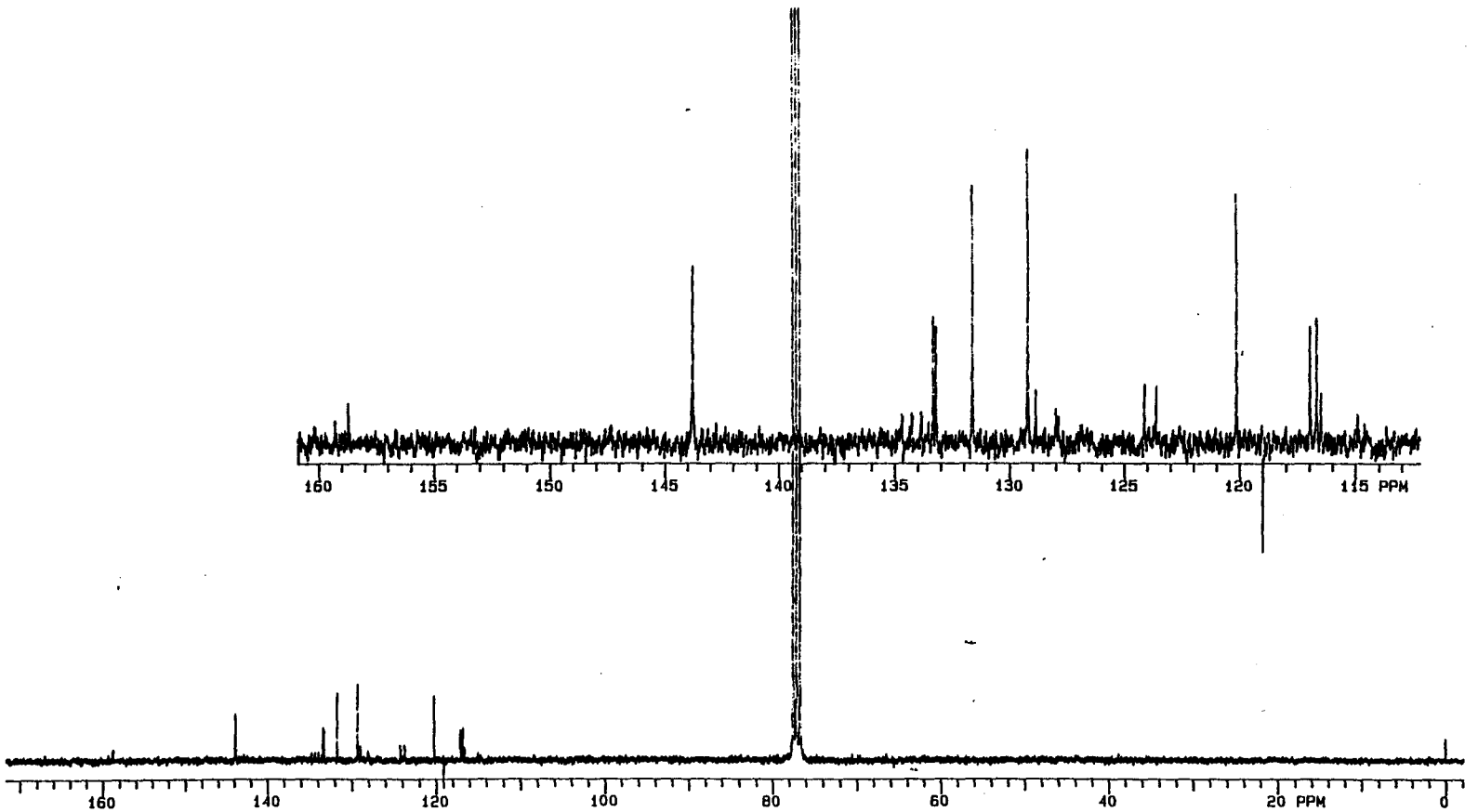

^{13}C NMR of 9-(4-fluorophenyl)xanthylium tetrafluoroborate, (20b)

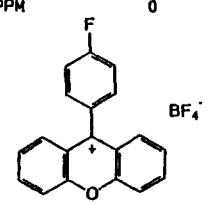

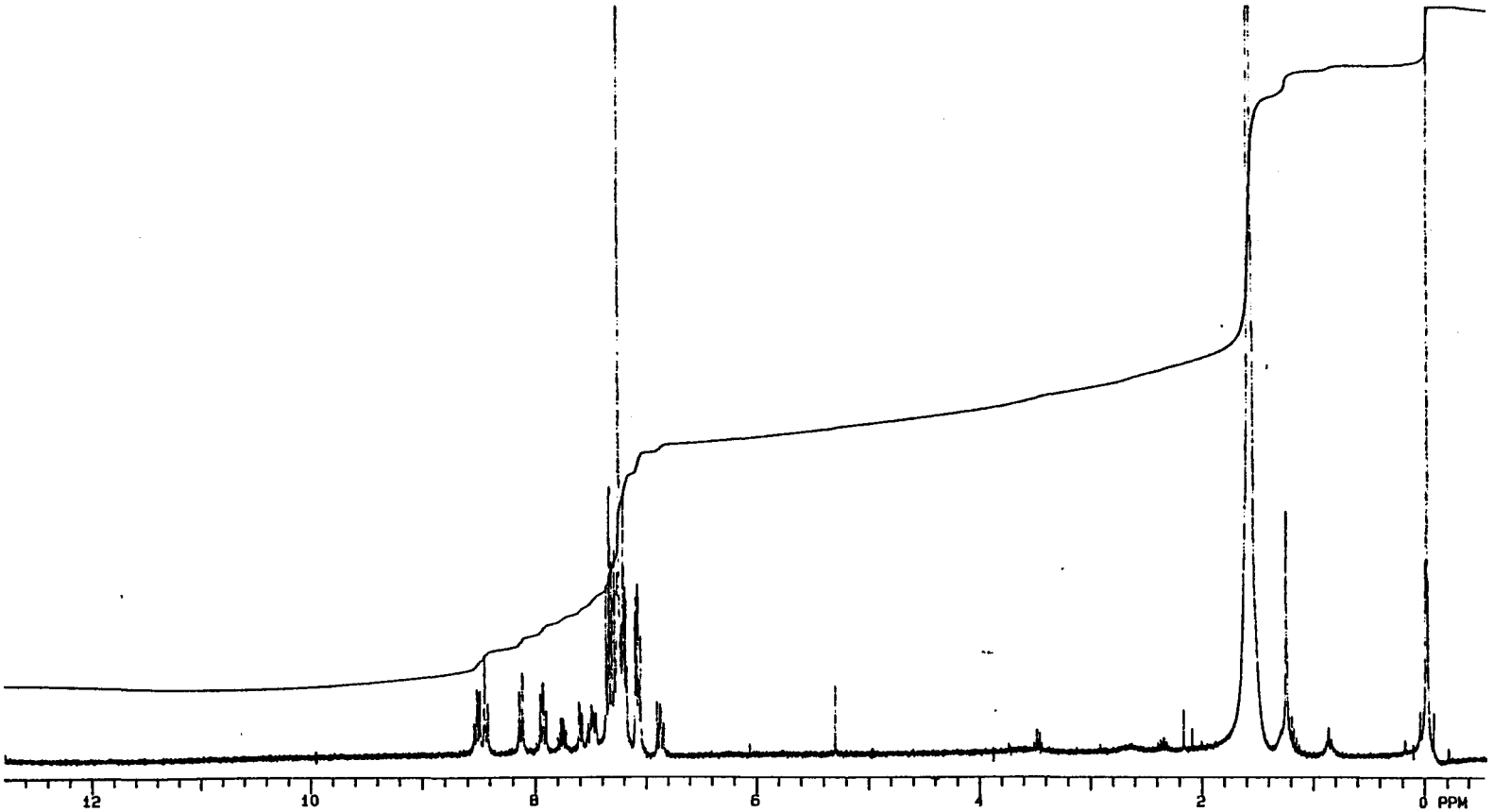

^{1}H NMR of 9-(3-fluorophenyl)xanthylium tetrafluoroborate, (20c)

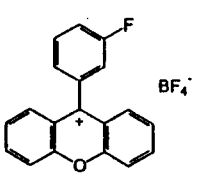

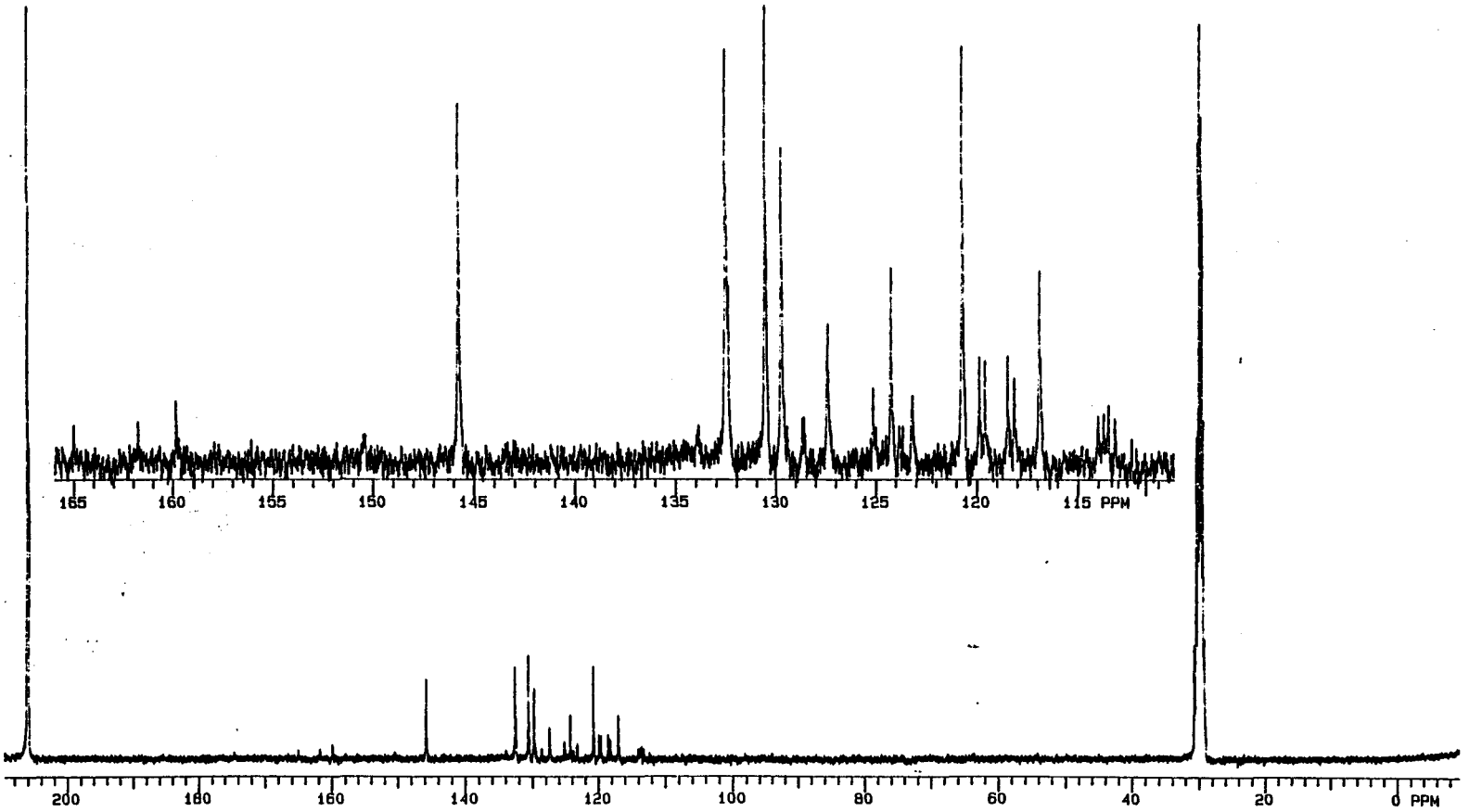

^{13}C NMR of 9-(3-fluorophenyl)xanthylium tetrafluoroborate, (20c)

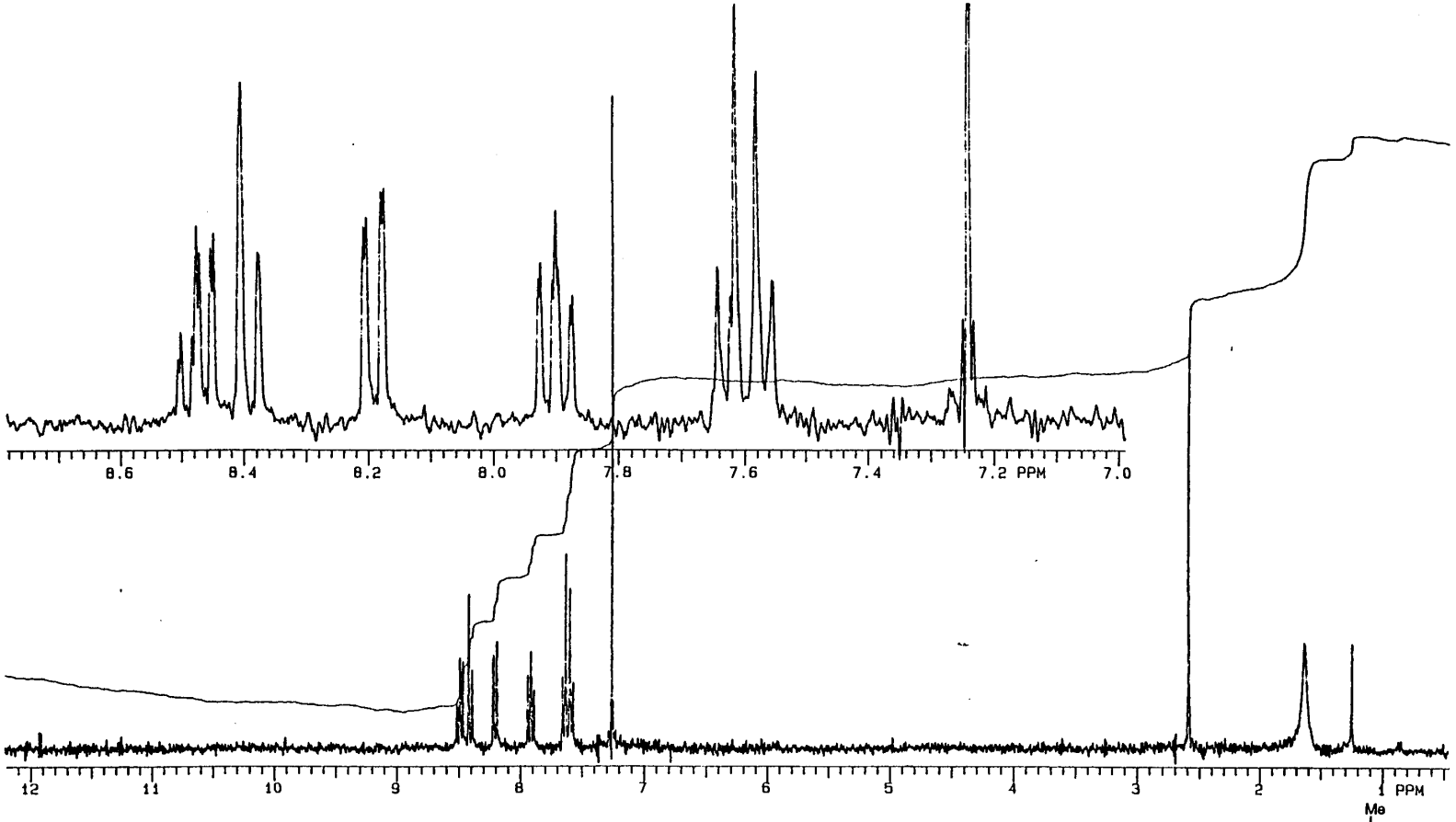

^{1}H NMR of 9-(4-methylphenyl)xanthylium tetrafluoroborate, **(20d)**

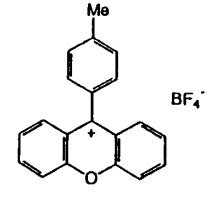

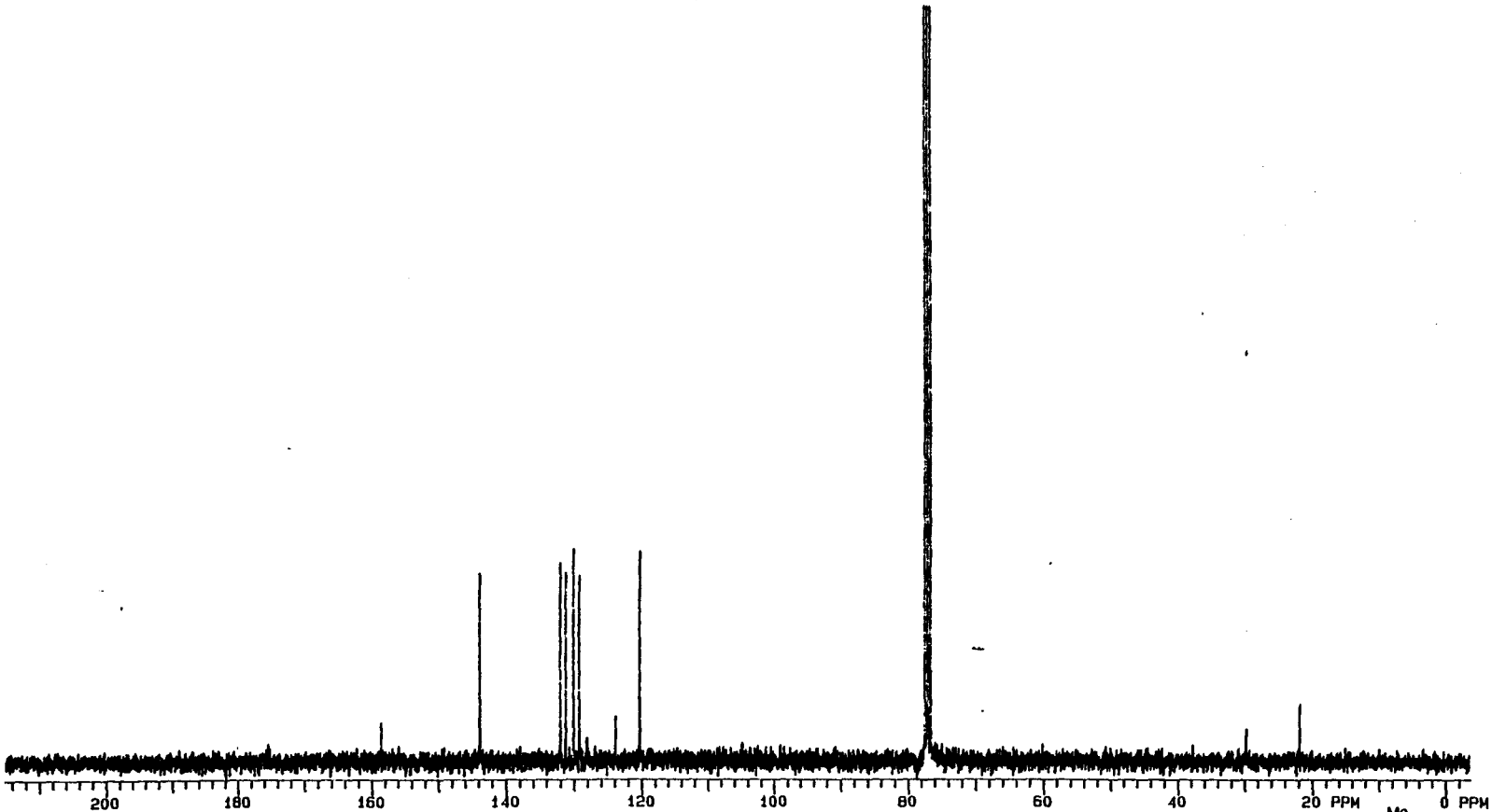

^{13}C NMR of 9-(4-methylphenyl)xanthylium tetrafluoroborate, (20d)

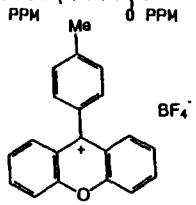

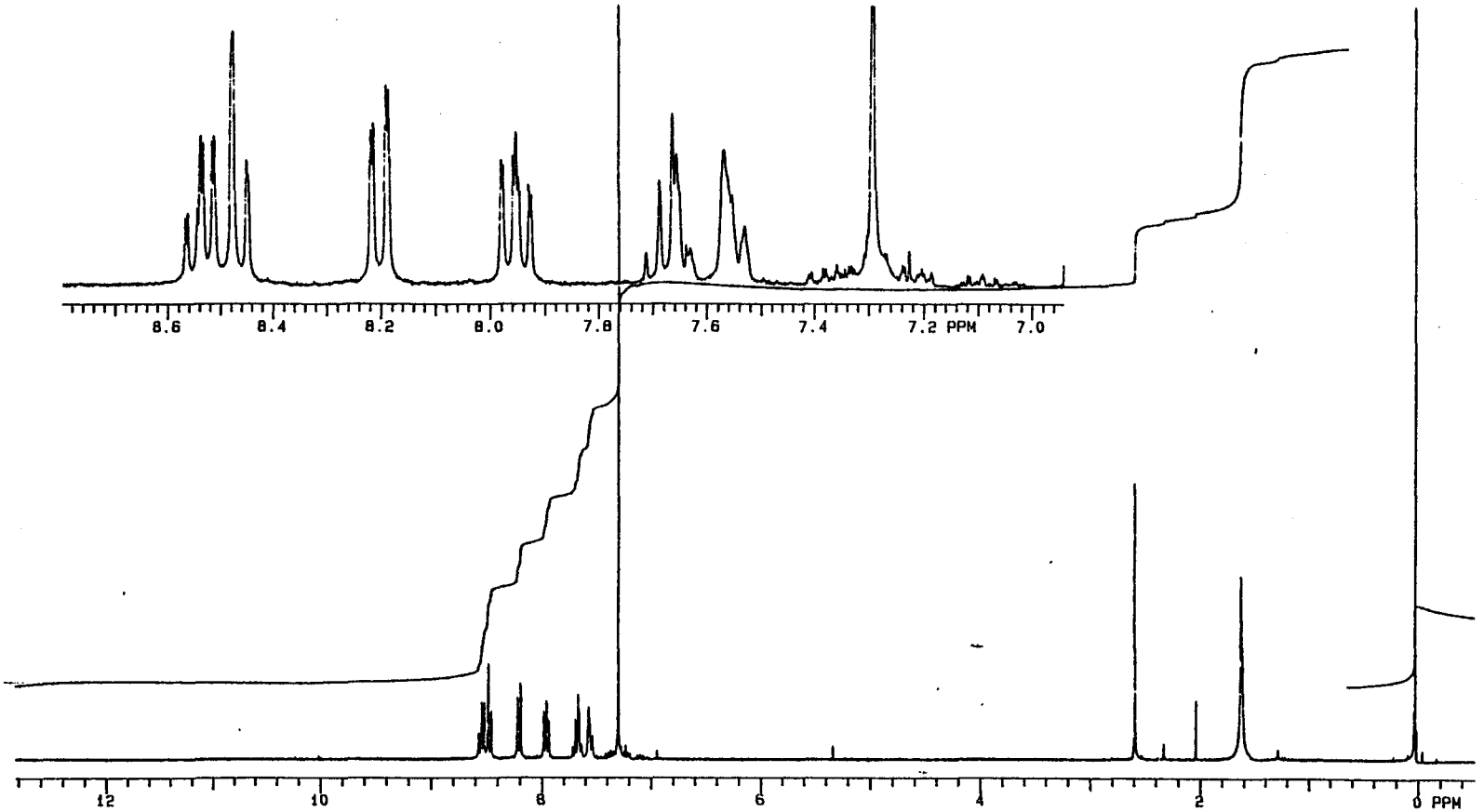

^{1}H NMR of 9-(3-methylphenyl)xanthylium tetrafluoroborate, (20e)

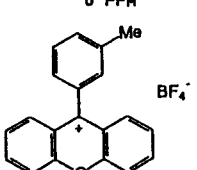

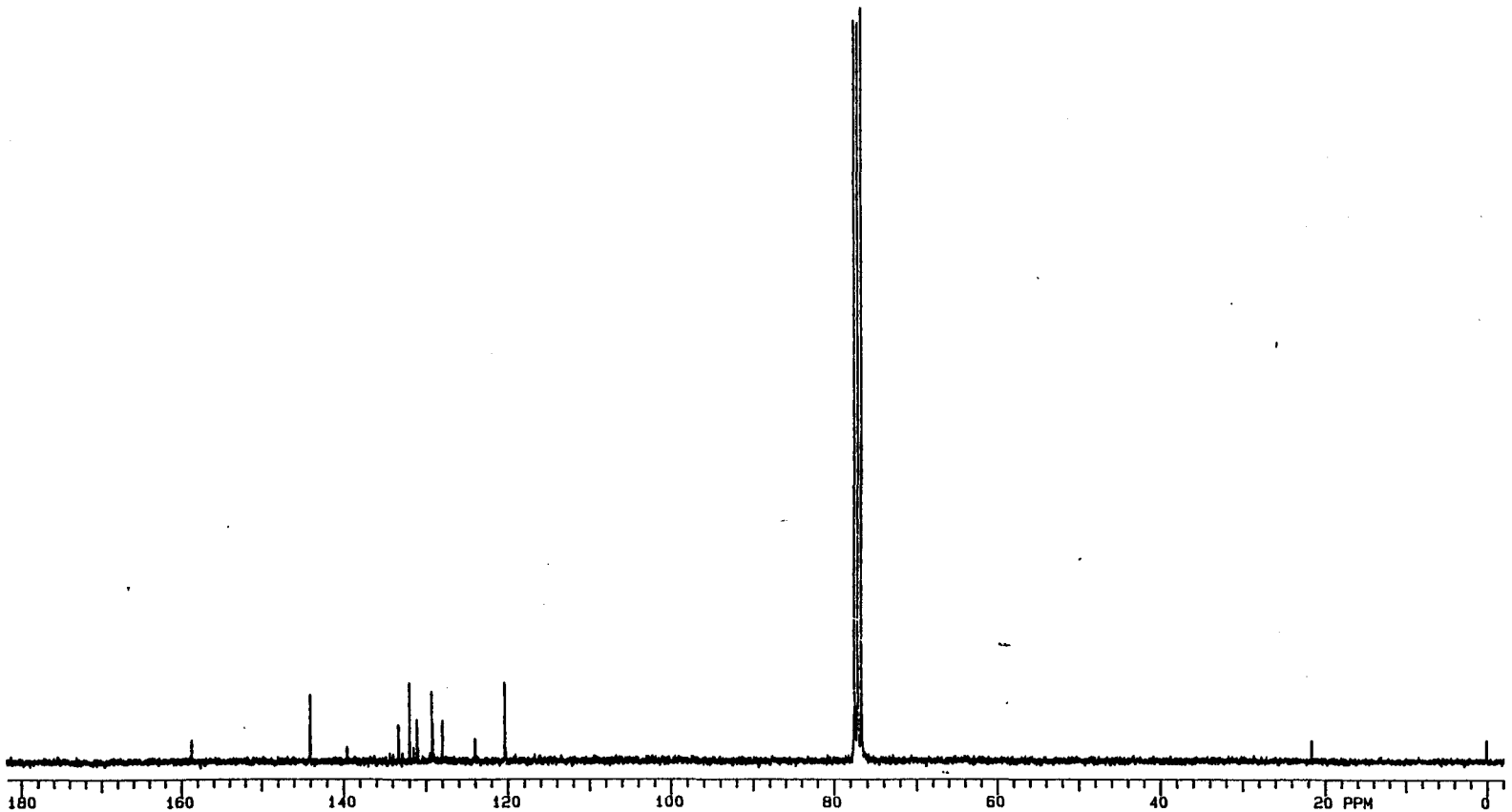

^{13}C NMR of 9-(3-methylphenyl)xanthylium tetrafluoroborate, (20e)

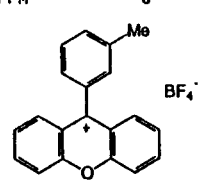

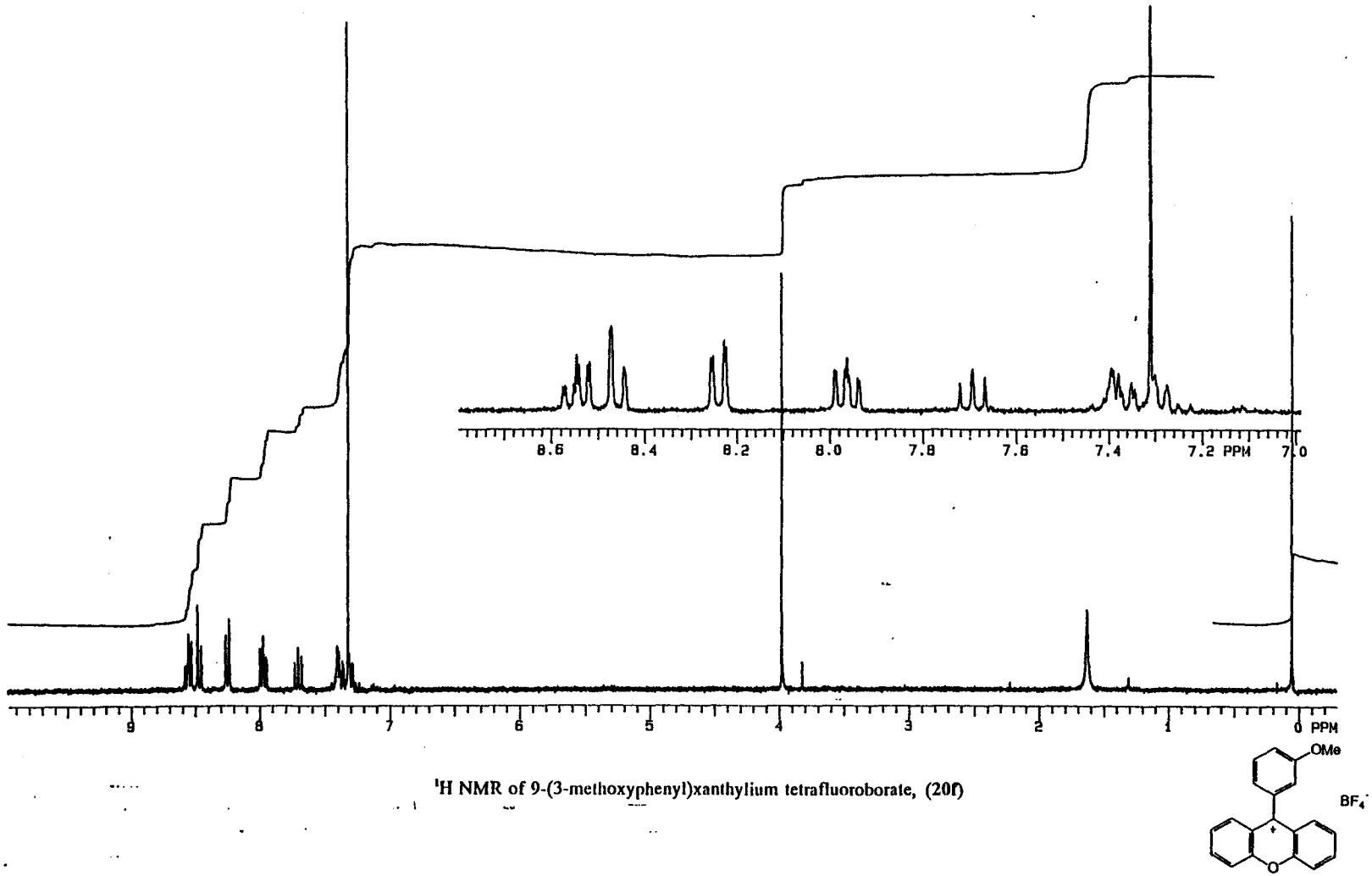

^{1}H NMR of 9-(3-methoxyphenyl)xanthylium tetrafluoroborate, (20f)

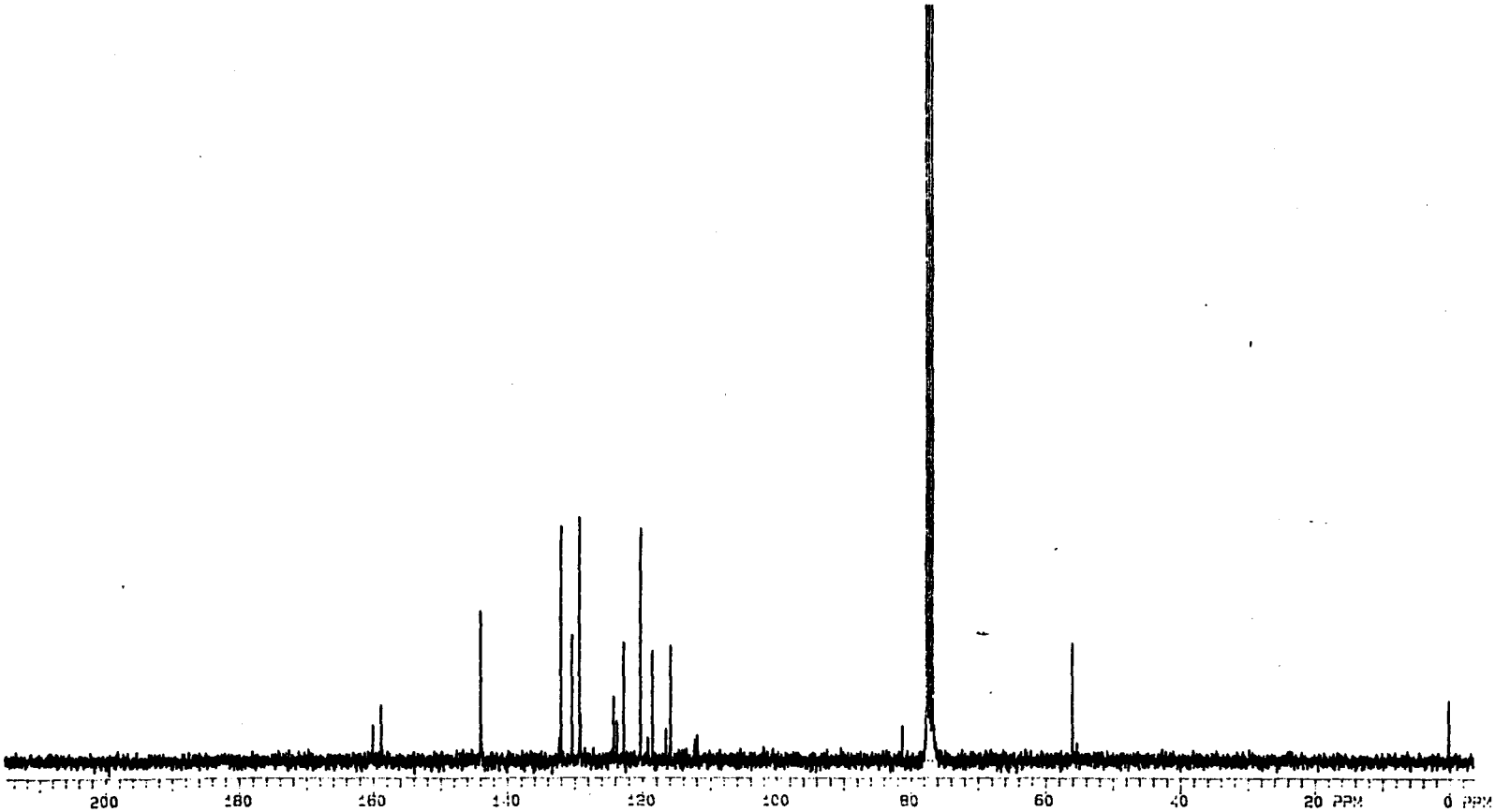

^{13}C NMR of 9-(3-methoxyphenyl)xanthylium tetrafluoroborate, (20f)

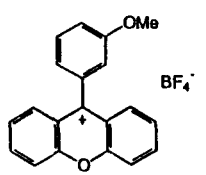

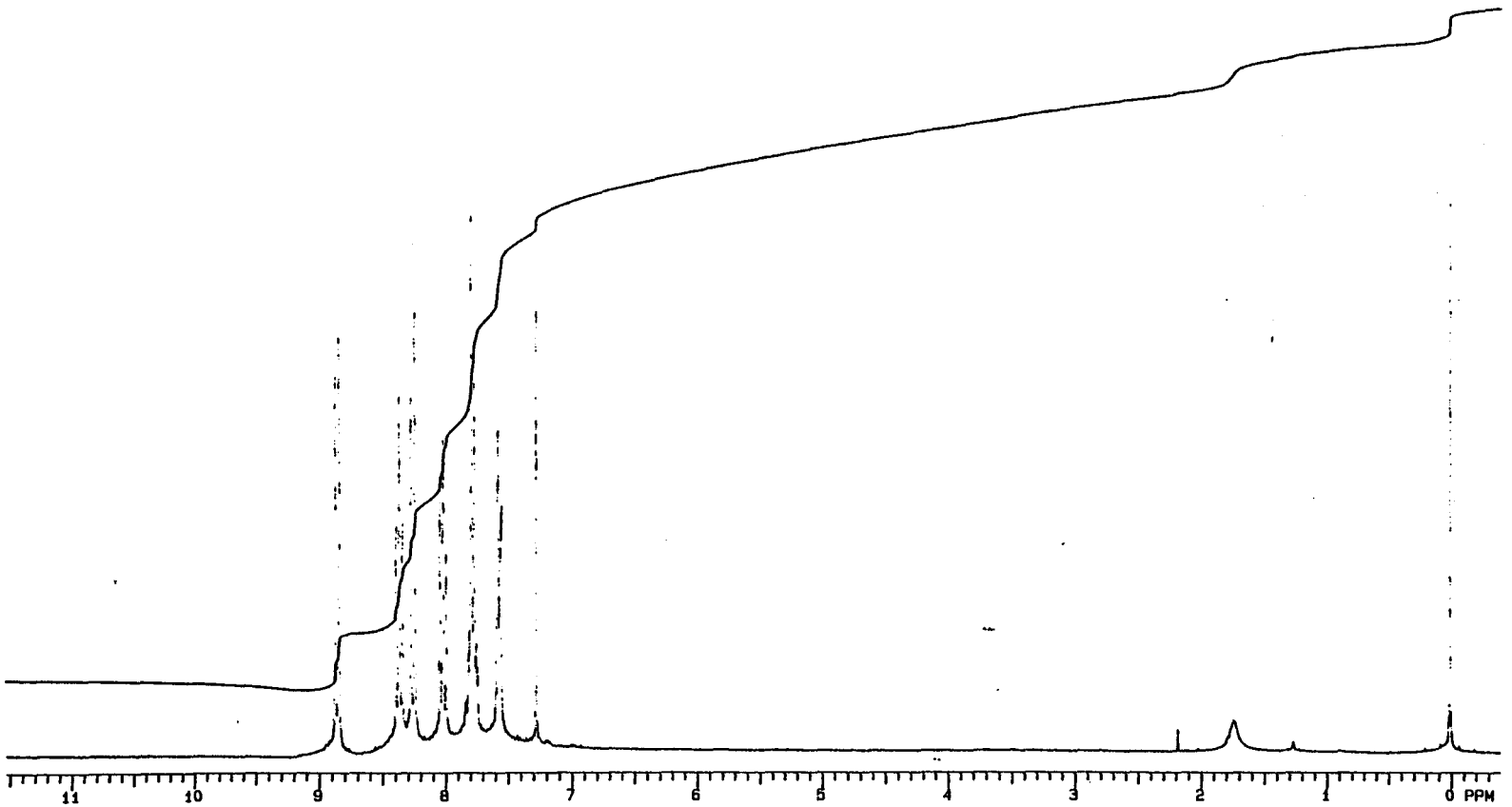

^{1}H NMR of 9-phenylthioxanthylium tetrafluoroborate, (21a)

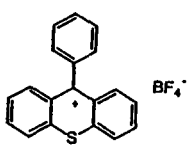

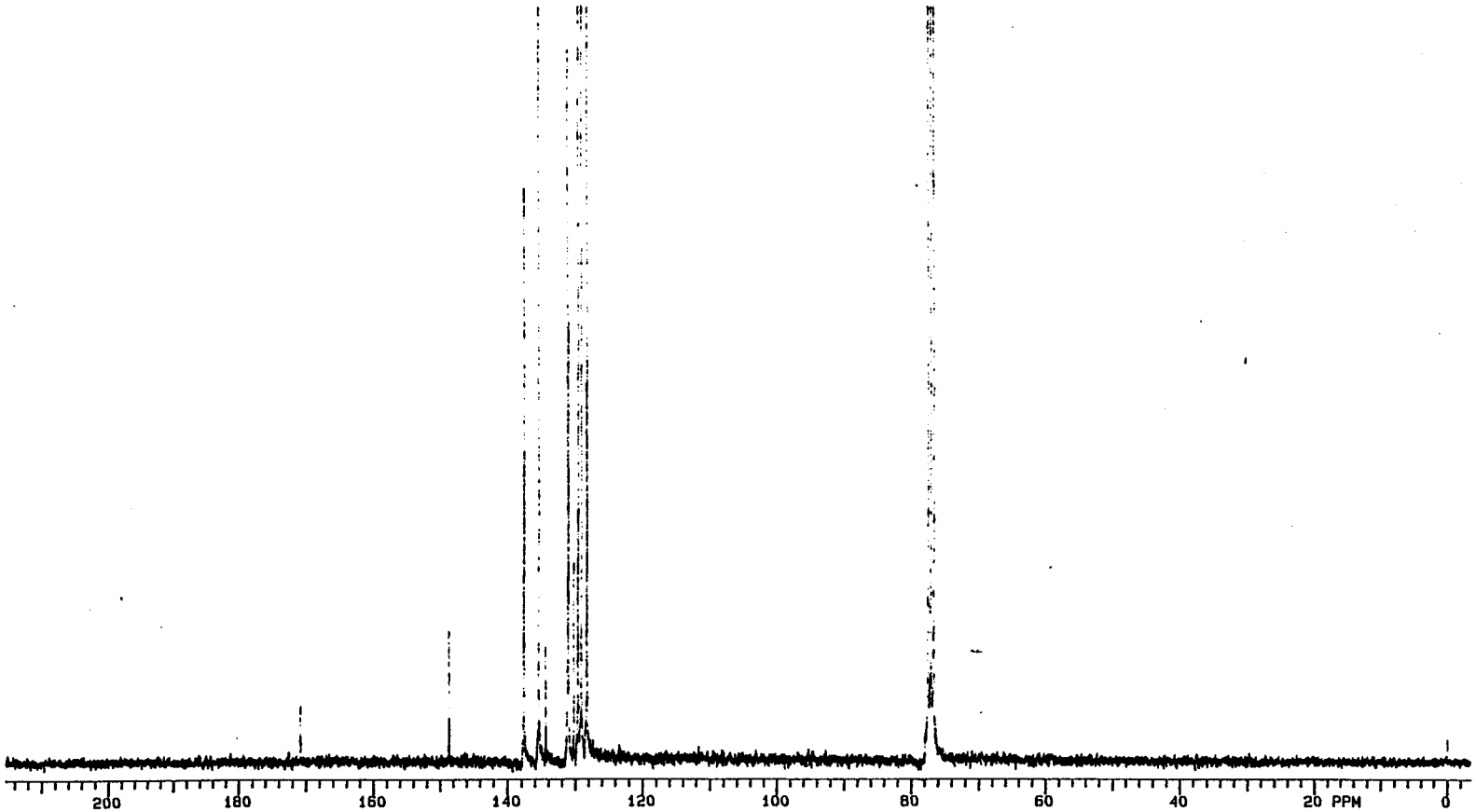

^{13}C NMR of 9-phenylthioxanthylium tetrafluoroborate, (21a)

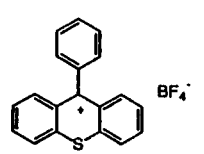

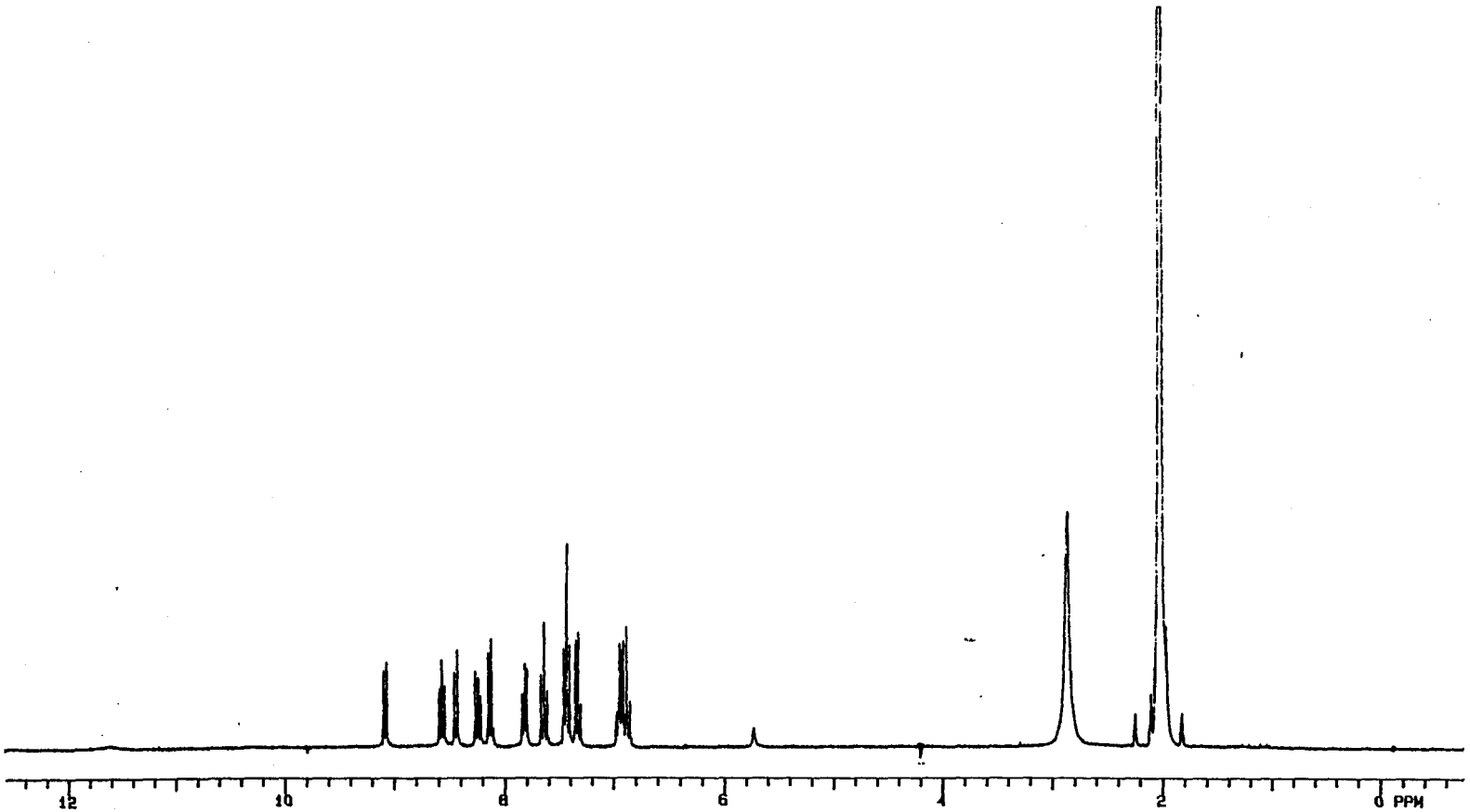

^{1}H NMR of 9-(4-fluorophenyl)thioxanthylium tetrafluoroborate, (21b)

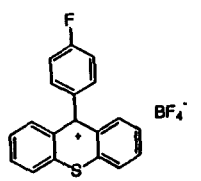

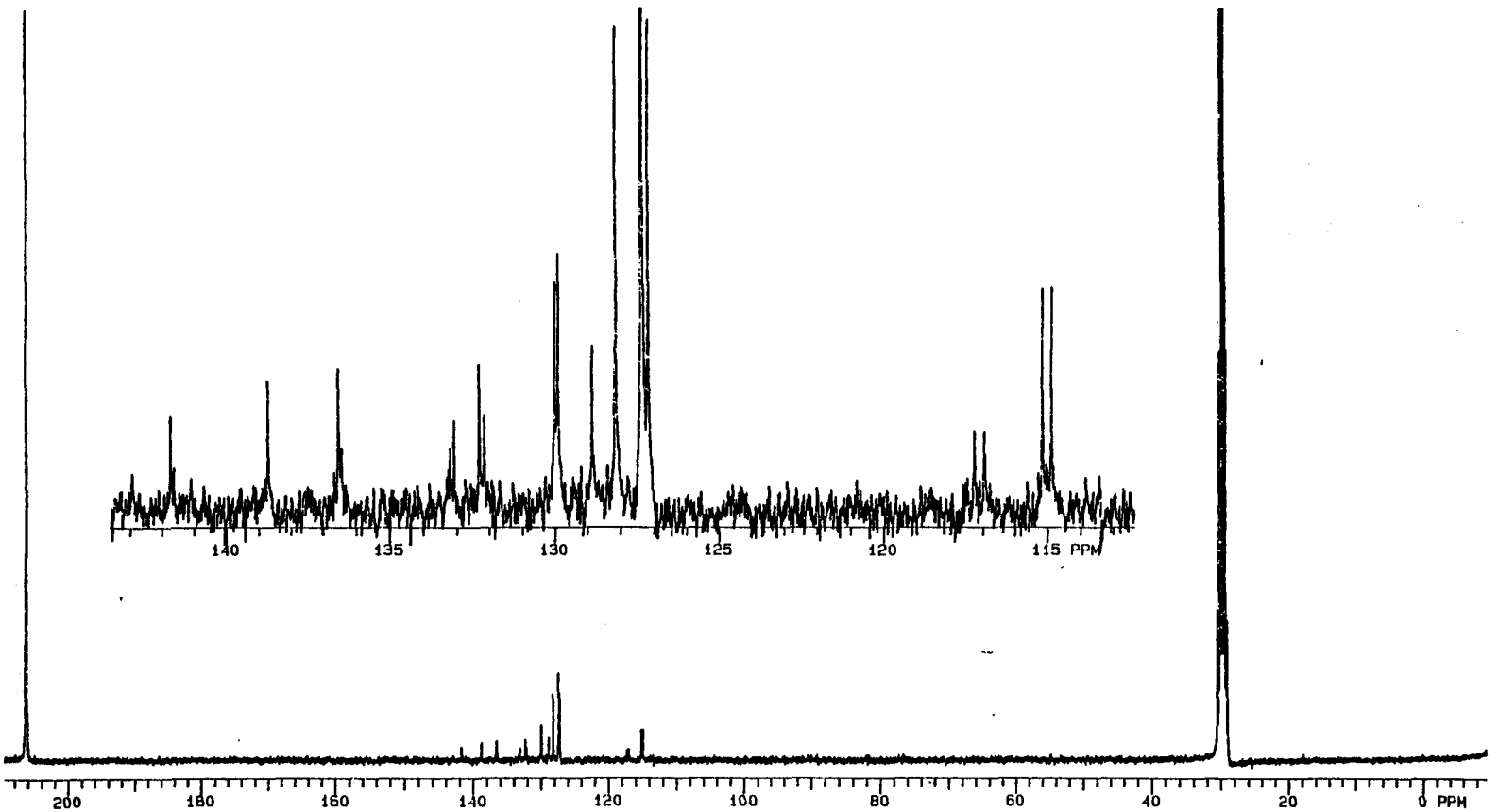

^{13}C NMR of 9-(4-fluorophenyl)thioxanthylium tetrafluoroborate, (21b)

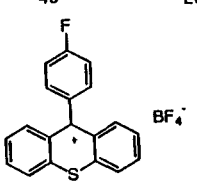

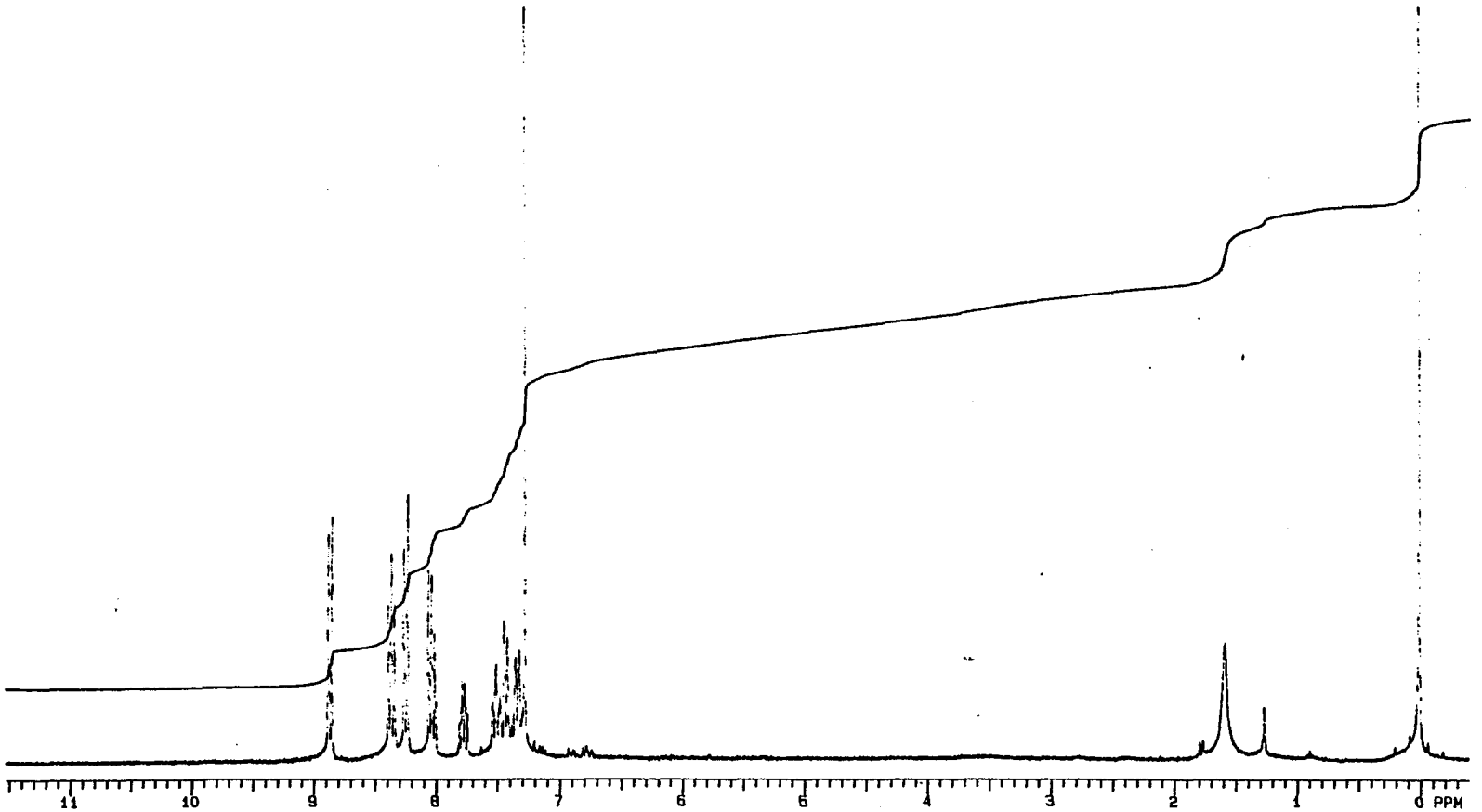

^{1}H NMR of 9-(3-fluorophenyl)thioxanthylium tetrafluoroborate, (21c)

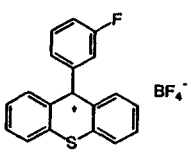

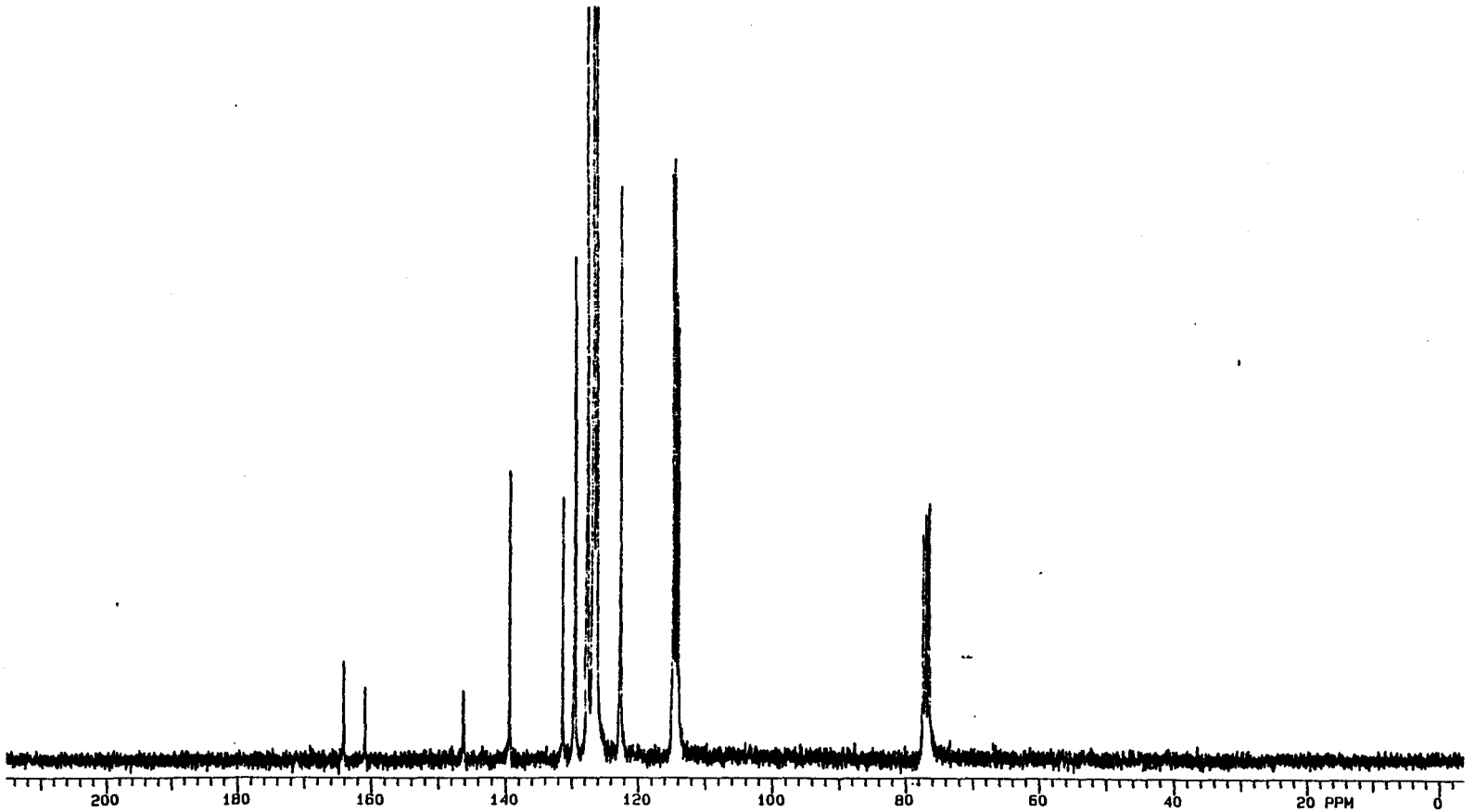

^{13}C NMR of 9-(3-fluorophenyl)thioxanthylium tetrafluoroborate, (21c)

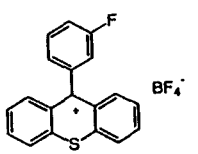

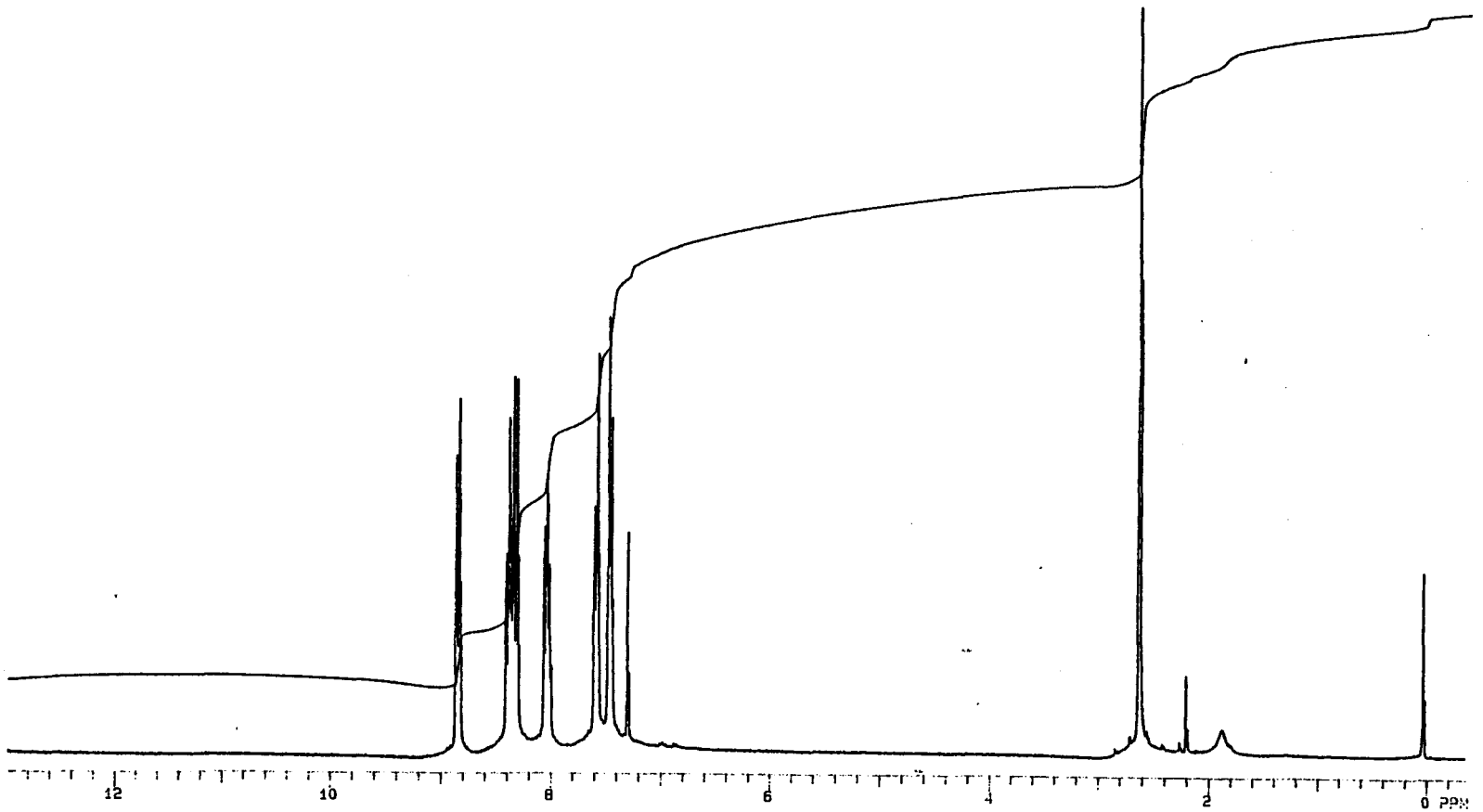

^{1}H NMR of 9-(4-methylphenyl)thioxanthylium tetrafluoroborate, (**21*d***)

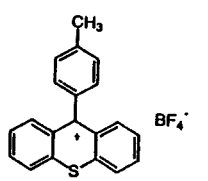

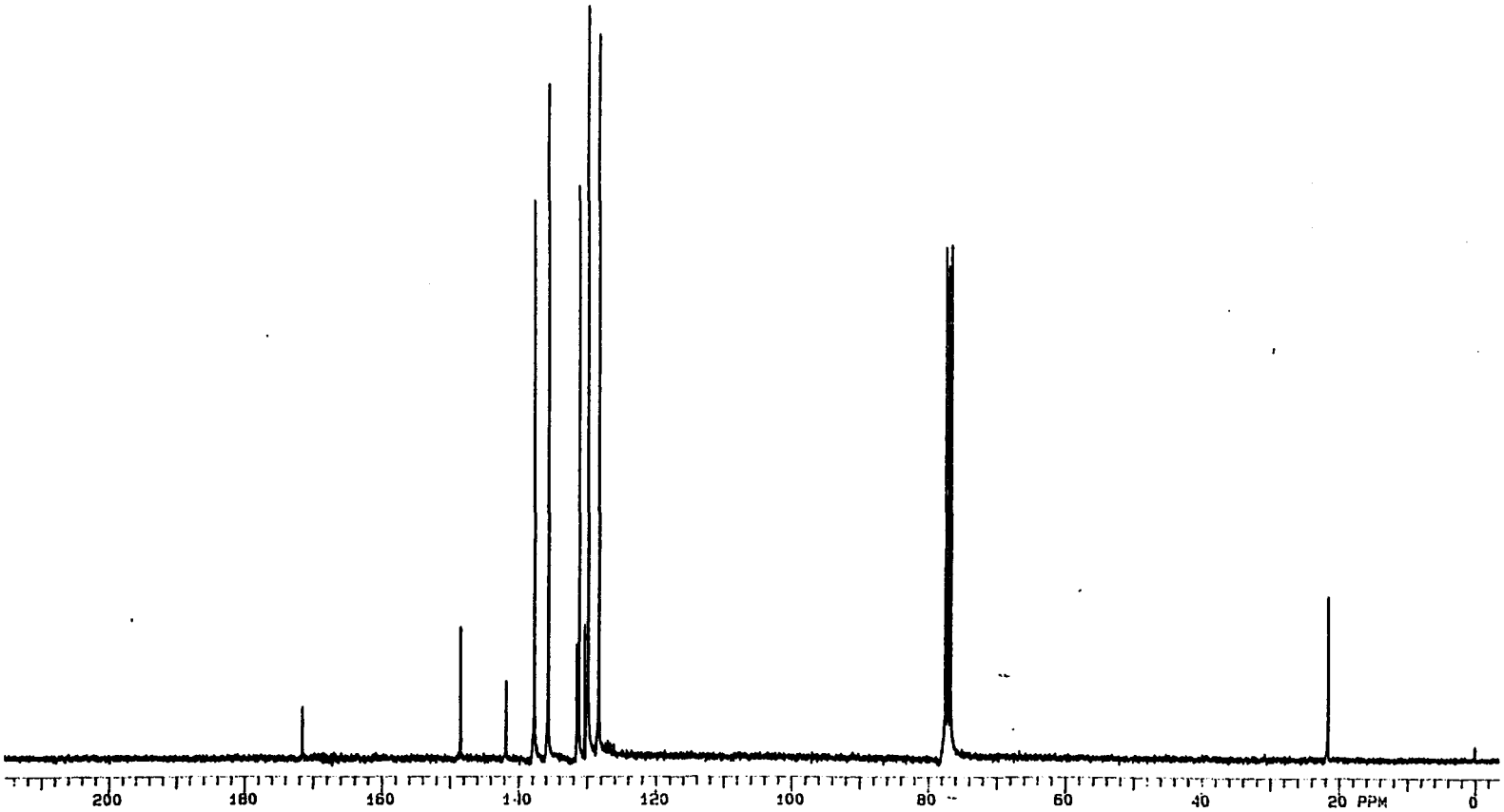

^{13}C NMR of 9-(4-methylphenyl)thioxanthylium tetrafluoroborate, (21d)

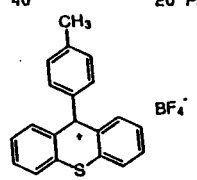

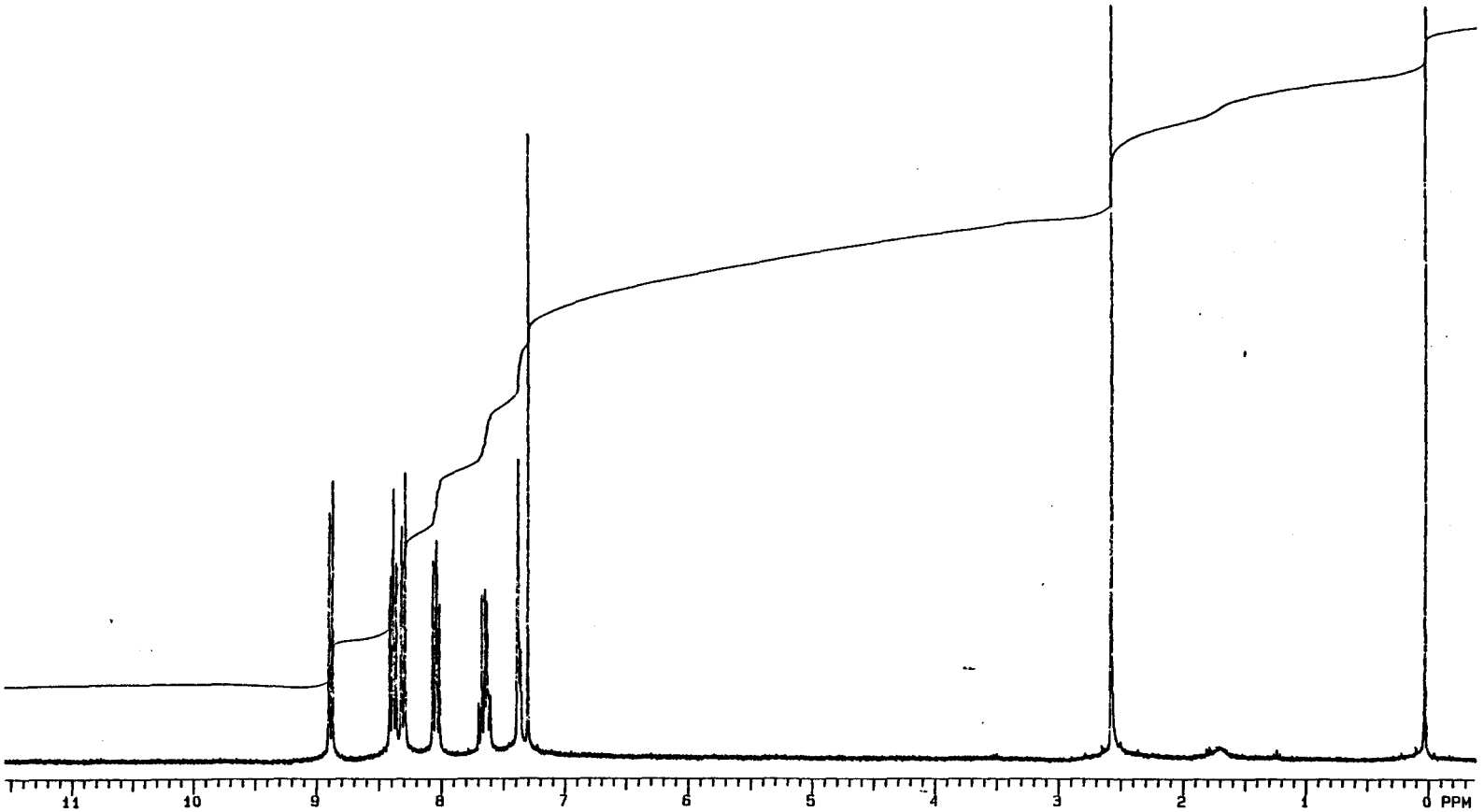

^{1}H NMR of 9-(3-methylphenyl)thioxanthylium tetrafluoroborate, (21e)

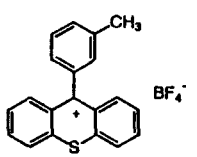

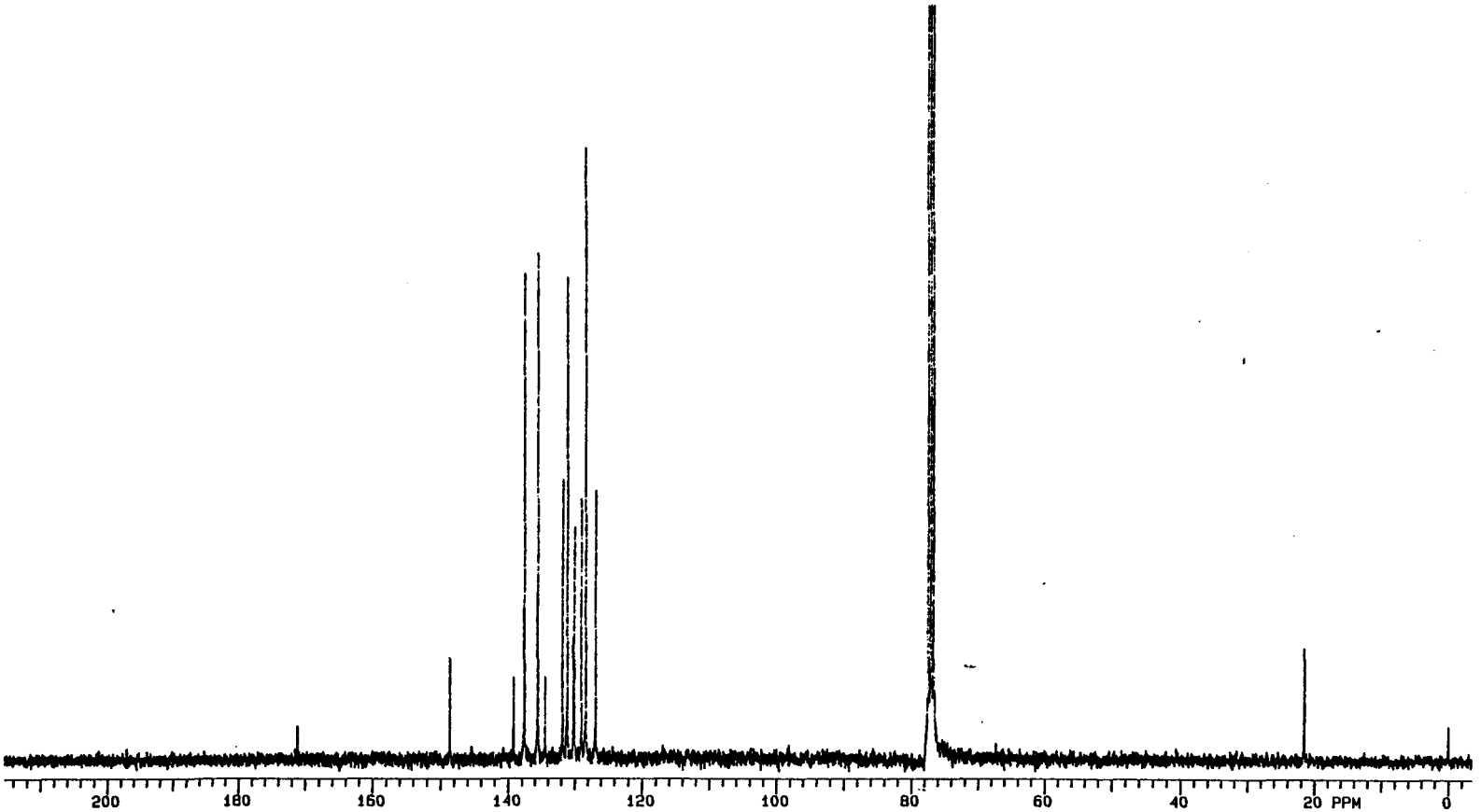

^{13}C NMR of 9-(3-methylphenyl)thioxanthylium tetrafluoroborate, (21e)

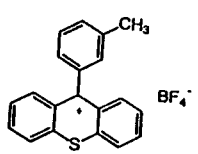

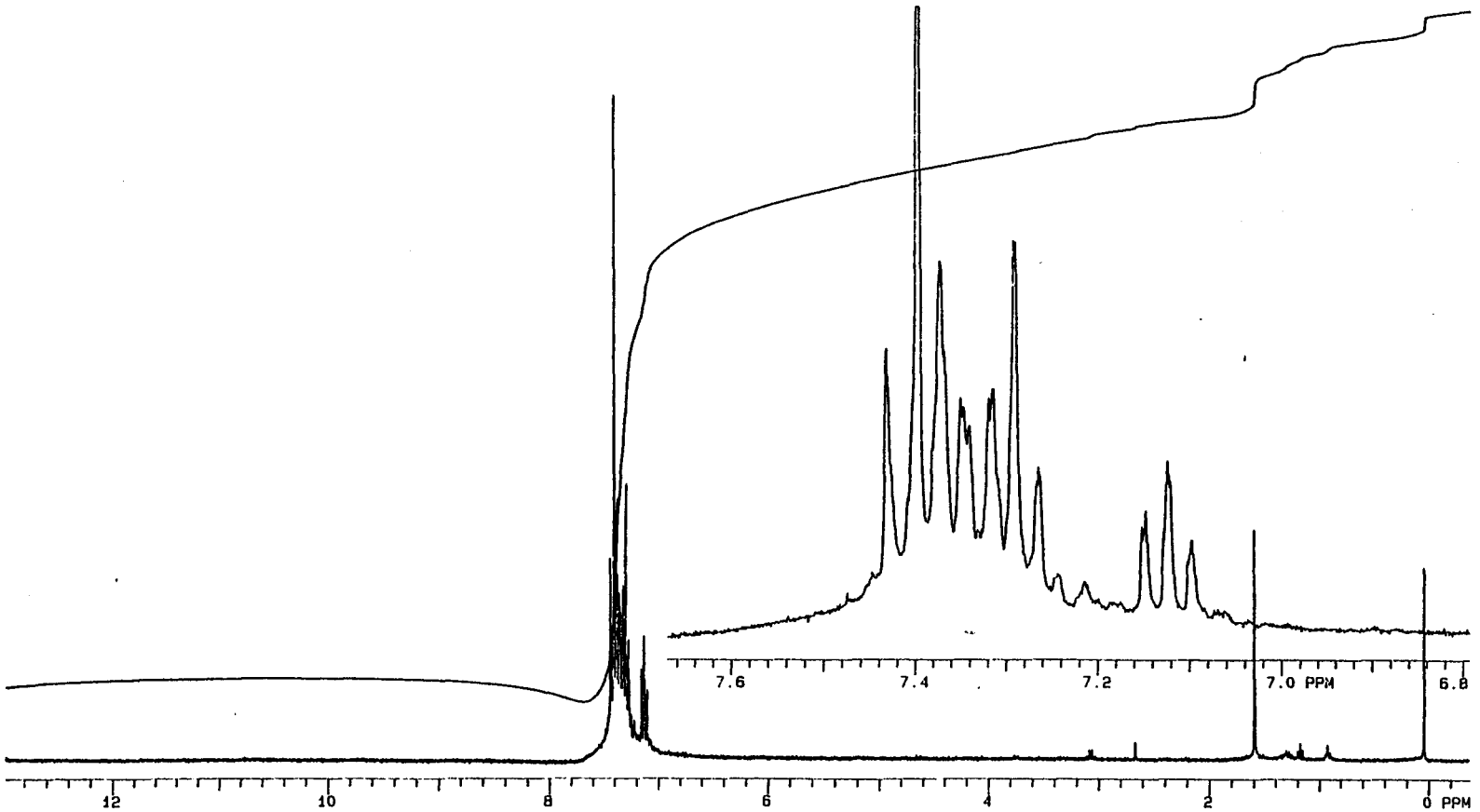

^{1}H NMR of 9-hydroperoxy-9-phenylxanthene, (22)

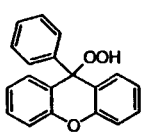

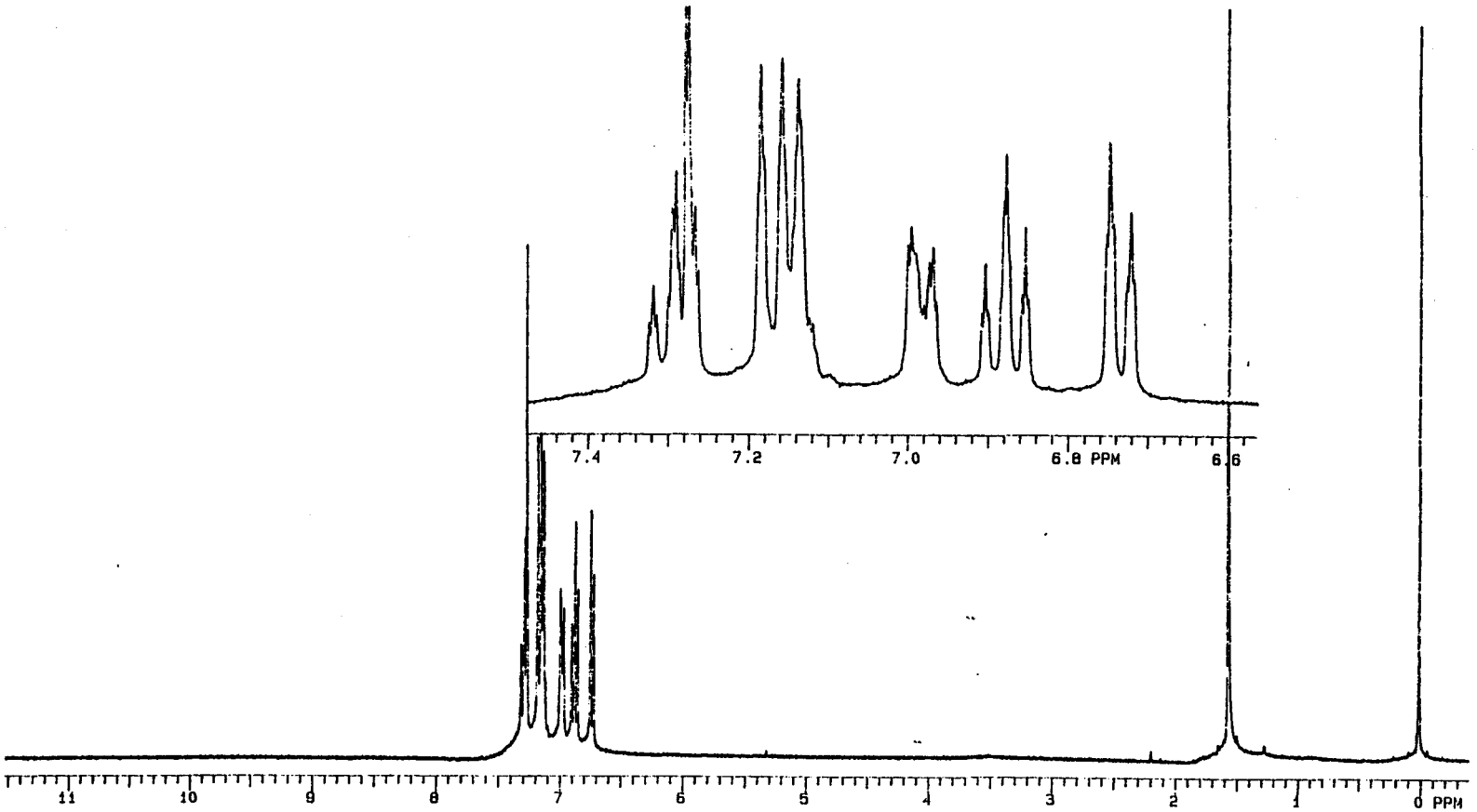

^{1}H NMR of di-(9-phenylxanthen-9-yl) peroxide, (23)

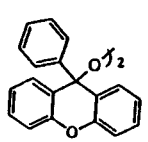

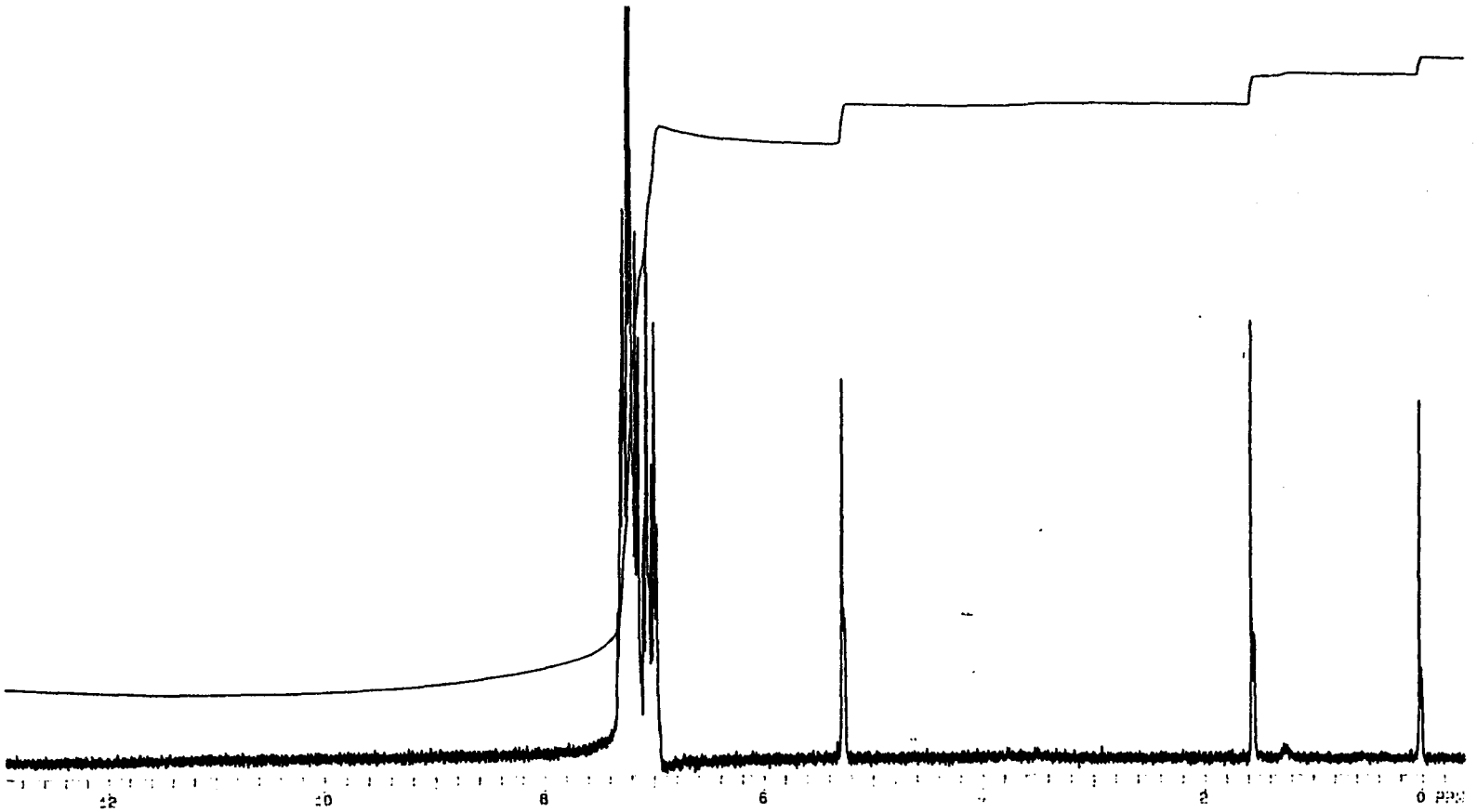

^{1}H NMR of 9-phenylxanthene, (24)

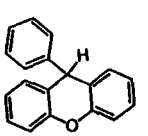

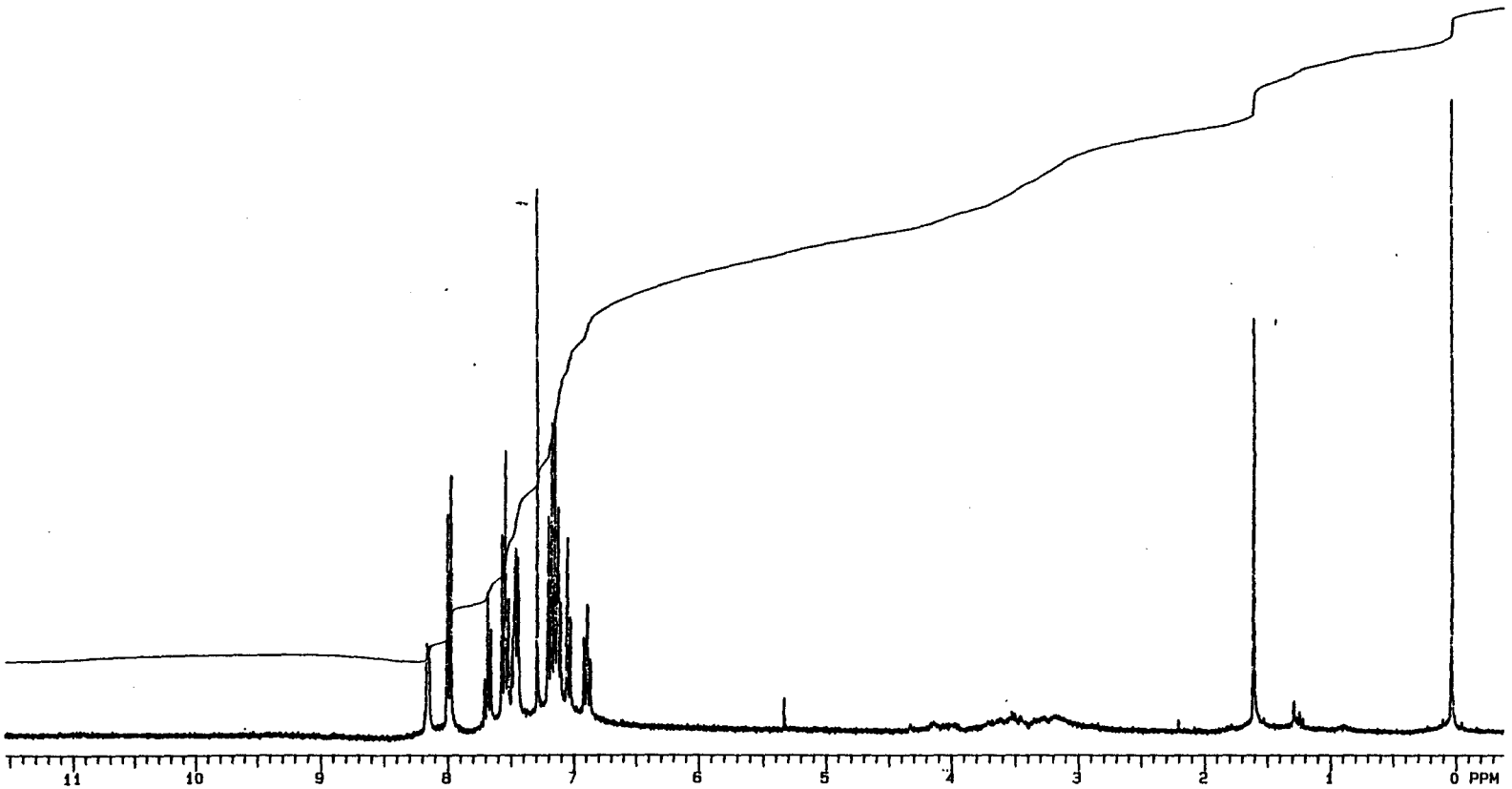

^{1}H NMR of 2-(*o*-hydroxyphenoxy)benzophenone, (25)

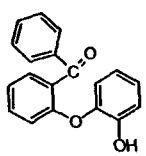

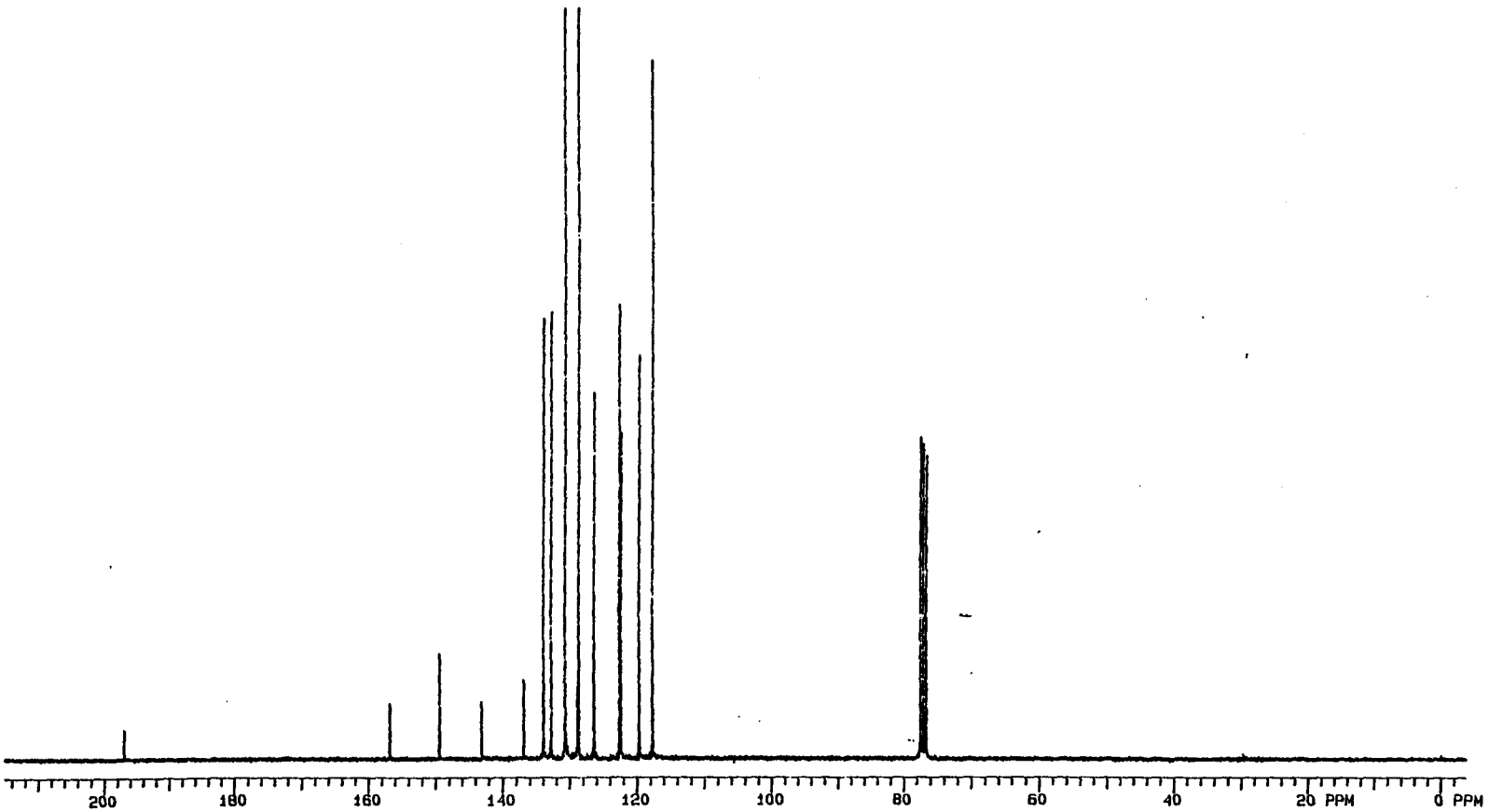

^{13}C NMR of 2-(*o*-hydroxyphenoxy)benzophenone, (**25**)

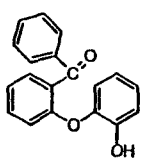

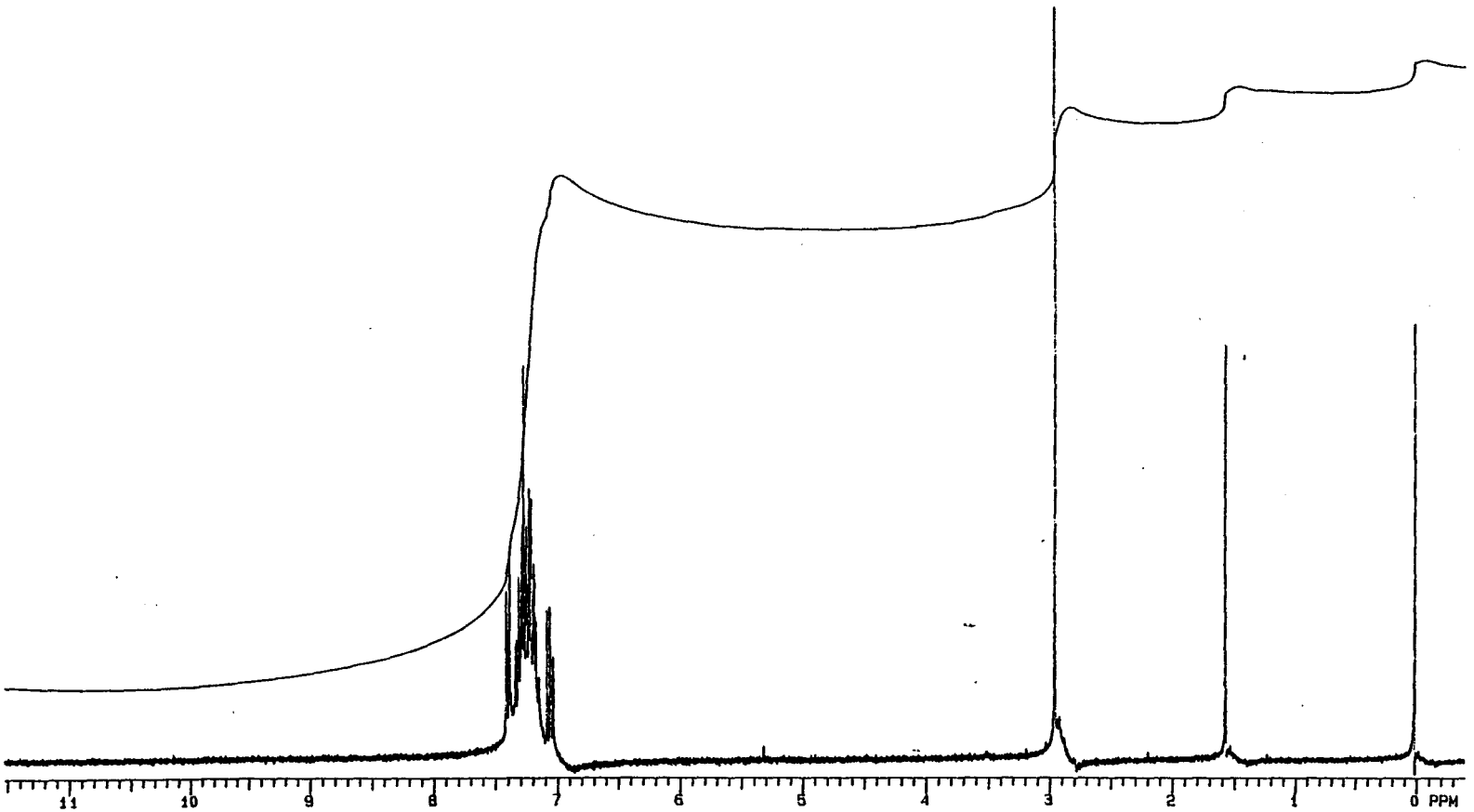

^{1}H NMR of 9-methoxy-9-phenylxanthene, (28)

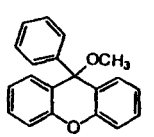

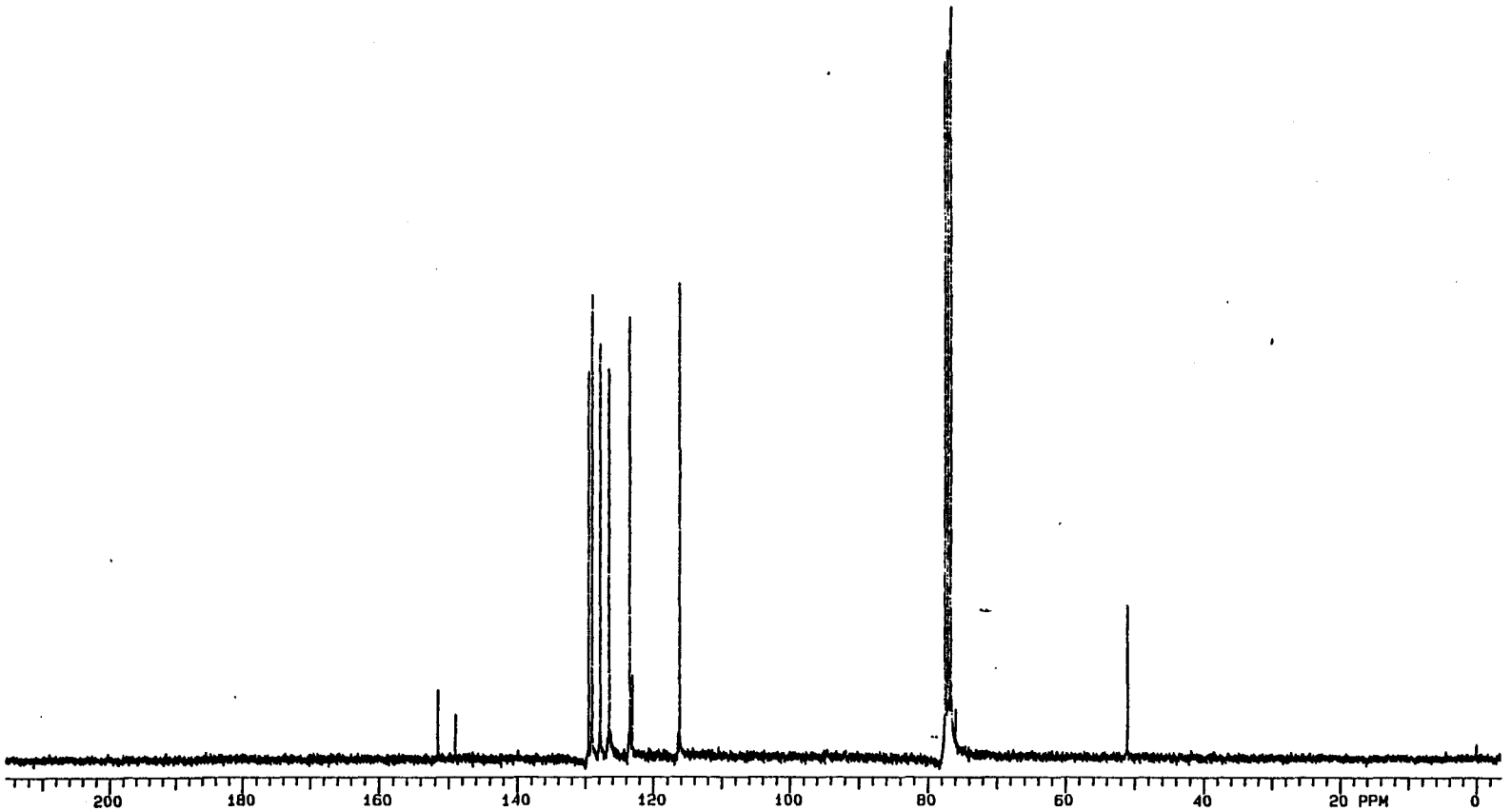

^{13}C NMR of 9-methoxy-9-phenylxanthene, (28)

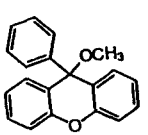

REFERENCES

Ahn, Y.-S.; Shin, J.-H. Low Temperature NMR Study on *p*-Fluorophenyl-thioxanthylium Ions. *Korean Chem. Soc.* **1982**, *26*, 165.

Al-Ekabi, H.; Kawata, H.; de Mayo, P. Photoinduced Electron Transfer to a Carbenium Ion. *J. Org. Chem.* **1988**, *53*, 1471.

Allen, D.M.; Owen, E.D. Photolysis of Triphenylmethyl Cations in Sulphuric Acid. *Chem. Comm.*, **1971**, 848.

Arnett, E.M.; Flowers, R.A. II; Meekhof, A.E.; Miller, L. Energies of Formation for Conjugate Xanthyl Carbenium Ions, Carbanions, and Radicals by Hydride, Proton, and Electron Transfer in Solution and Their Reactions to Give Symmetrical Bixanthyls. *J. Am. Chem. Soc.* **1993**, *115*, 12603.

Azarani, A.; Berinstain, B.; Johnston, L.J.; Kazanis, S. Electron Transfer Reactions Between Excited Diarylmethyl and Triarylmethyl Carbocations and Aromatic Donors. *J. Photochem. Photobiol. A: Chem.* **1991**, *57*, 175.

Bartl, J.; Steenken, S.; Mayr, H. Kinetics of the Reactions of Laser-Flash Photolytically Generated Carbenium Ions with Alkyl and Silyl Enol Ethers. Comparison with the Reactivity toward Alkenes, Allysilanes and Alcohols. *J. Am. Chem. Soc.* **1991**, *113*, 7710.

Berger, R.M.; Weir, D. Stable Cation Formation and Luminescence on Inorganic Oxide Surfaces: 9-Phenylxanthenyl Cation. *Chem. Phys. Lett.* **1990**, *169*, 213.

Bethell, D.; Clare, P.N. Photo-oxidation of Triarylmethanes sensitized by Carbonium Ions. *J. Chem. Soc. Perkin II.* **1972**, 1464.

Boyd, M.K.; Lai, H.Y.; Yates, K. Water Quenching Behavior of Excited 9-Xanthylium Cations in Aqueous Sulfuric Acid Solutions. *J. Am. Chem. Soc.* **1991**, *113*, 7294.

Bunzly, H.; Decker, H. Ueber Xanthonium- und Thioxanthonium Verbindungen. *Ber.* **1904**, *37*, 2931.

Cabell-Whiting, P.W.; Hogeveen, H. The Photochemistry of Carbonium Ions. *Adv. Phys. Org. Chem.* **1973**, *10*, 129.

Childs, R.F.; Shaw, G.B. The Photochemistry of Carbenium Ions and Related Species. *Org. Photochem.* **1991**, *11*, 111.

Childs, R.F.; Taguchi, V. The Photoisomerization of Some Tropylium Cations and Protonated Tropone. *Chem. Comm.* **1970**, 695.

Das, P.K. Transient Carbocations and Carbanions Generated by Laser Flash Photolysis and Pulse Radiolysis. *Chem. Rev.* **1993**, *93*, 119.

Dauben, H.J.; Honnen, L.R.; Harmon, K.U. Improved Preparation of Triphenylmethyl Perchlorate and Fluoroborate for Use in Hydride Ion Exchange Reactions. *J. Org. Chem.* **1960**, *25*, 1442.

Dinnocenzo, J.P.; Todd, W.P.; Simpson, T.R.; Gould, I.R. Nucleophilic Cleavage of One-Electron σ Bonds: Stereochemistry and Cleavage Rates. *J. Am. Chem. Soc.* **1990**, *112*, 2462.

Gaffney, P.R.; Changsheng, L.; Rao, M.V.; Reese, C.B.; Ward, J.C. Some Substituted 9-Phenylxanthen-9-yl Protecting Groups. *J. Chem. Soc., Perkin Trans. 1* **1991**, *6*, 1355.

Fleming, I. *Frontier Orbitals and Organic Chemical Reactions*, Wiley: New York, NY, 1976.

Flowers, R.A. II, Personal Communication, 1993.

Franz, J.A.; Naushadali, S.K.; Alnajjar, M.S. Absolute Rate Constants for Hydrogen Atom Abstraction by Benzyl Radical from Thiophenol, Tributylstannane, Tributylstannane-*d*, and Dicyclohexylphosphine and for the Cyclization of the 2-Allylbenzyl Radical. *J. Org. Chem.* **1986**, *51*, 19.

Glover, S.A.; Goosen, A.; McCleland, C.W.; Taljaard, B.; Vogel, F. R. Stable Hydroperoxide Synthesis. *S. Afr. J. Chem.* **1984**, *37(4)*, 164.

Glover, S.A.; Goosen, A.; McCleland, C.W.; Taljaard, B.; Vogel, F. R. Benzophenone-sensitized Photo-oxidation of 9-Phenylxanthene Analogues. *S. Afr. J. Chem.* **1985**, *38(4)*, 203.

Gomberg, V.M.; Cone, L.H. II. Thioxanthonderivate. *Justus Liebigs Ann. Chem.*

1910, *376*, 201.

Gomberg, M.; Cone, L. Phenylxanthenolperoxyd. *Justus Liebigs Ann. Chem.* **1909**, *370*, 158.

Gomberg, M.; Cone, L. Ueber Triphenylmethyl; XVIII. Mittheilung: Zur Kenntniss Der Chinocarboniumsalze. *Justus Liebigs Ann. Chem.* **1909**, *370*, 142.

Havinga, E.; DeJongh, R.O.; Dorst, W. Photochemical Acceleration of the Hydrolysis of Nitrophenyl Phosphates and Nitrophenyl Sulphates. *Rec. Trav. Chim.* **1956**, *75*, 378.

Hogeveen, H.; Gaasbeek, C.J. Photochemically Induced Conversion of Tropylium Ion Into 7-Norbornadienyl Ion. *Rec. Trav. Chim.* **1970**, *89*, 1079.

Hori, M.; Kataoka, K.; Ohno, K; Toyoda, T. Reactivities of 9-Phenylxanthylium and 9-Phenylthioxanthylium Salts in Electrophilic and Nucleophilic Reactions. I. Nitration. *Chem Pharm. Bull.* **1973**, *21*, 1272.

Johnston, L.J.; Wong, D.F. Electron Transfer Reactions of Triplet 9-Arylxanthenium and 9-Arylthioxanthenium Cations. *J. Phys. Chem.* **1993**, *97*, 1589.

Johnston, L.J.; Wong,, D.F. Characterization of the Triplet Excited State of the Phenylxanthenium Carbocation. *Can. J. Chem.* **1992**, *70*, 280.

Johnston, L.J.; Lobaugh, J.; Wintgens, V. Laser Flash Photolysis Studies of Dibenzosuberenyl Cations and Radical Cations. *J. Phys. Chem.* **1989**, *93*, 7370.

Kobayashi, S.; Zhu, Q.Q.; Schanbel, W. Reactions of Substituted Vinyl Cations in Acetonitrile Solution as Studied by Flash Photolysis. *Z. Naturforsch.* **1987**, *43b*, 825.

Kobayashi, S.; Kitamura, T.; Taniguchi, H.; Schanbel, W. Absorption Spectra of Vinyl Cations. *Chem. Lett.* **1983**, 1117.

Koorts, J.; Taljaard, B.; Goosen, A. 2-(*o*-Hydroxyphenoxy)benzophenones from 9-Aryl-9-hydroperoxyxanthenes: An Experimental and Theoretical Investigation. *S. Afr. J. Chem.* **1987**, 237.

Llama, E. F.; del Campo, C.; Capo, M.; Anadon, M. Synthesis and Antinociceptive Activity of 9-Phenyl-oxy or 9-Acyl-oxy Derivatives of Xanthene, Thioxanthene and Acridine. *Eur. J. Med. Chem.* **1989**, *24*, 391.

Maillard, B.; Ingold, K.U.; Scaiano, J.C. Rate Constants for the Reactions of Free Radicals with Oxygen in Solution. *J. Am. Chem. Soc.* **1983**, *105*, 5095.

McClelland, R.A.; Banait, N.; Steenken, S. Electrophilic Reactions of Xanthylium Carbocations Produced by Flash Photolysis of 9-Xanthenols. *J. Am. Chem. Soc.* **1989**, *111*, 2929.

McEwen, J. and Yates, K. Substituent Effects in the Photohydration of Styrenes and Phenylacetylenes. An Attempt to Establish a $\sigma^{h\nu}$ Scale for Excited-State Reactions. *J. Phys. Org. Chem.* **1991**, *4*, 193.

Minto, R.E. and Das, P.K. A Laser Flash Photolysis Study of Photodehydroxylation Phenomena of 9-Phenylxanthen-9-ol and Photobehavior of Related Intermediates. Enhanced Electrophilicity of 9-Phenylxanthenium Cation Singlet. *J. Am. Chem. Soc.* **1989**, *111*, 8858.

Nagao, Y.; Abe, Y.; Oyama, T.; Abe, Y.; Misono, T. Synthesis of Leuco Triphenylmethane Derivatives and Their UV-VIS Spectra. *Nippon Kagaku Kaishi*, **1987**, *10*, 1839.

Olah, G.A.; Schleyer, P.v.R. *Carbonium Ions*, Vol. I-V; Wiley: New York, NY, 1970.

Owen, E.D.; Allen, D.M. Photolysis of Triphenylmethyl and Related Cations in Sulphuric Acid. *J. Chem. Soc. Perkin II* **1973**, 95.

Quint, F.; Dilthey, W. Zur Kenntnis der Oxydation von Pyreniumsalzen (Über Pyreniumsalze, XIV). *Ber.*, **1931**, *64*, 2082.

Rehm, D.; Weller, A. Kinetics of Fluorescence Quenching by Electron and H-Atom Transfer. *Isr. J. Chem.* **1970**, *8*, 259.

Rehm, D.; Weller, A. Kinetics and Mechanism of Electron Transfer in Fluorescence Quenching in Acetonitrile. *Ber. Bunsen-Ges. Phys. Chem.* **1969**, *73*, 834.

Ritchie, C. D. Problems Involved in Understanding Orders of Nucleophilic Reactivity. *Pure Appl. Chem.* **1978**, *50*, 1281.

Ritchie, C.D. Cation-Anion Combination Reactions. XIII. Correlation of the Reactions of Nucleophiles with Esters. *J. Am. Chem. Soc.* **1975**, *97*, 1170.

Samanta, A.; Gorpidas, K.R.; Das, P.K. Carbocation Fluorescence and Its Efficient

Electron-Transfer Quenching. *J. Phys. Chem.* **1993**, *97*, 1583.

Samanta, A.; Gopidas, K.R.; Das, P.K. Electron Acceptor Behavior of 9-Phenylxanthenium Carbocation Singlet. *Chem. Phys. Lett.* **1990**, *167*, 165.

Schonberg, A.; Mustafa, A. Photochemical Reactions in Sunlight. Part XII. Reactions with Phenanthraquinone, 9-Arylxanthens, and Diphenyl Triketone. *J. Chem. Soc.* **1947**, 997.

Shukla, D.; Wan, P. Adiabatically Photogenerated Thioxanthenium Cations: Probes of Reactivity of Nucleophiles Towards Excited State Carbocations in Aqueous Solution. *J. Photochem. Photobiol. A: Chem.* **1994**, *79*, 55.

Shukla, D.; Wan, P. Product Studies of Electron Transfer from Dimethoxybenzene and Trimethoxybenzene to Photoexcited Xanthenium Cations in S_1 in Aqueous Acid Solution. *J. Photochem. Photobiol. A: Chem.* **1993**, *76*, 47.

Sim, B.A.; Milne, P.H.; Griller, D.; Wayner, D.D.M. Thermodynamic Significance of ρ^+ and ρ^- from Substituent Effects on the Redox Potentials of Arylmethyl Radicals. *J. Am. Chem. Soc.* **1990**, *112*, 6635.

Stern, O.; Volmer, M. The Extinction Period of Fluorescence. *Z. Physik.* **1919**, *20*, 183.

Strickler, S.J.; Berg, R.A. Relationships Between Absorption Intensity and Fluorescence Lifetime of Molecules. *J. Chem. Phys.*; **1962**, *37*, 814.

Taljaard, B. Ph.D. Thesis, University of Port Elizabeth, 1986.

Turro, N.J. *Modern Molecular Photochemistry*, Benjamin/Cummings: Menlo Park CA, 1978.

Ullmann, F. and Engi, E. 9-Phenyl-xanthen. *Ber.*, **1904**, *37*, 237.

Valentino, M.R. and Boyd, M.K. Ether Quenching of Singlet Excited 9-Arylxanthylium Cations. *J. Photochem. Photobiol. A: Chem.* **1995**, *89*, 7.

Valentino, M.R. and Boyd, M.K. Quenching Behavior of Singlet Excited 9-Arylxanthylium Cations. *J. Org. Chem.* **1993**, *58*, 5826.

van Tamelen, E.E.; Cole, Jr.,T.M. Photolysis of Carbocationic Species. Triphenylcarbonium Ion. *J. Am. Chem. Soc.* **1971**, *93*, 6158.

van Tamelen, E.E.; Greeley, R.H.; Schumacher, H. Photolysis of Carbocationic Species. Nonbenzenoid Aromatics. *J. Am. Chem. Soc.* **1971**, *93*, 6151.

van Tamelen, E.E.; Cole, T.M.; Greeley, R.H.; Schumacher, H. Photolysis of Triphenylcarbonium, Tropylium, and Triphenylcyclopropenium Ions. *J. Am. Chem. Soc.* **1968**, *90*, 1372.

Wan, P.; Yates, K.; Boyd, M.K. Adiabatic Photodehydroxylation of 9-Phenylxanthen-9-ol. Observation of Carbocation Fluorescence in Neutral Aqueous Solution. *J. Org. Chem.* **1985**, *50*, 2881.

Weber, G.; Teale, F.W.J. Determination of the Absolute Quantum Yield of Fluorescent Solutions. *Trans. Faraday. Soc.* **1957**, *53*, 646.

Zimmerman, H.E.; Sandel, V.R. Mechanistic Organic Photochemistry. II. Solvolytic Photochemical Reactions. *J. Am. Chem. Soc.* **1963**, *85*, 915.

Zimmerman, H.E.; Somasekhara, S. Mechanistic Organic Photochemistry. III. Excited State Solvolyses. *J. Am. Chem. Soc.* **1963**, *85*, 922.

VITAE

The author, Maria R. Valentino, was born on September 15, 1962 in Evergreen Park, Illinois. In September, 1980 she entered DePaul University and received a B.S. degree in Chemistry in May, 1985. During her last year as an undergraduate at DePaul, she started her master's project under the guidance of Professor Avrom A. Blumberg. She obtained her M.S. degree in Chemistry in May, 1986.

After graduation she obtained employment at Service Coatings, Inc. in Harvey, Illinois as a Research and Development Chemist. After 1.5 years in the coatings industry, Ms. Valentino obtained employment with Nalco Chemical Company as a Development Chemist where she remained for 1 year prior to pursuing her doctoral studies.

In August, 1990 Ms. Valentino enrolled at Loyola University of Chicago full-time, subsequently working under the direction of Professor Mary K. Boyd. While a graduate student at Loyola, Ms. Valentino received two prestigious fellowships, the Loyola University Teaching Fellowship in 1993 and the Arthur J. Schmitt Dissertation Fellowship in 1994.

DISSERTATION APPROVAL SHEET

The dissertation submitted by Maria R. Valentino has been read and approved by the following committee:

Mary K. Boyd, Ph.D., Director
Assistant Professor, Chemistry
Loyola University Chicago

David S. Crumrine, Ph.D.
Associate Professor, Chemistry
Loyola University Chicago

Daniel J. Graham, Ph.D.
Associate Professor, Chemistry
Loyola University Chicago

Patrick M. Henry, Ph.D.
Professor, Chemistry
Loyola University Chicago

The final copies have been examined by the director of the dissertation and the signature which appears below verifies the fact that any necessary changes have been incorporated and that the dissertation is now given final approval by the committee with reference to content and form.

The dissertation is, therefore, accepted in partial fulfillment of the requirements for the degree of Doctor of Philosophy.

11/29/95
Date

Director's Signature